# Studies on the Synthesis and Use of Rare Earth Doped Nanophosphors for Application on Latent Fingerprints

A thesis submitted for the degree of Doctor of Philosophy

by

Alexander Reip

Wolfson Centre for Materials Processing

Brunel University

September 2014

# Acknowledgements

I would firstly like to express my gratitude to my supervisor Professor Jack Silver for all his support, advice and patience during the whole PhD process and to Professor Robert Withnall for all his help with the Raman spectroscopy as well as the interesting side projects I was able to work on including an amazing two weeks at the Royal Collection in Windsor Castle.

I would like to thank all my fellow PhD students in the Wolfson Centre including Inma Andres, Ed Boughton, Myles Worsley and Xiao Yan for their encouragement during my three years researching at the centre and beyond. Also to Dr Fiona Cotterill who helped keep the centre running smoothly and gave me things to do when I most needed distracting.

From the Experimental Techniques Centre I would like the thank Mrs Nita Verma and Dr Alan Reynolds who helped train me up on the SEM and TEM, Dr Jesús Javier Ojeda for his help on using the IR spectrometer and also to Dr Ben Jones for his input with the fingerprint analysis.

I would like to express my deepest appreciation to my wife, Bekki, who provided reassurance and inspiration throughout the many years of work and who kept me going when I was feeling dejected. To my daughter Eris whom even in the short time she has been with me has been magnificent and finally to my parents and brother for their continuous support and assistance.

For Fadhel Khan, James Reeve, Phyllis Reip and Robert Withnall

# Abstract

Nanotechnology has been increasingly employed in forensic science for the detection of latent fingerprints, using multiple techniques from new aluminium nanomaterials for dusting to quantum dot dispersions, to try to increase and enhance areas where prints are likely to be found at scenes of crime. Different substrates use a diverse range of methods to develop prints when they are found and each method has its own drawbacks. It is not viable to use many of these techniques in conditions other than in a laboratory due to the harmful environmental effects they can cause over long term use. With this in mind a new easier to use technique that can be used on any substrate from wood to glass to paper was looked into.

A range of nano-sized rare earth phosphor precursors were synthesised using homogeneous precipitation and solid state methods which were then converted to phosphors by firing at 980$^{o}$C. $Eu^{3+}$ and $Tb^{3+}$ doped $Y_2O_3$, $YVO_4$ and $Y_2O_2S$ were chosen for their luminescent intensity. Analysis of each of the phosphors was carried out using multiple techniques and a single host lattice chosen for continuation.

$Y_2O_3$:$Eu^{3+}$ and $Y_2O_3$:$Tb^{3+}$ were coated using a modified Stöber process to try and decrease the agglomeration of particles as well as allowing for surface modification to take place. Modifications of the surface were prepared and analysed, and these particles were then used in multiple fingerprint examinations to examine the adherence on fingerprints of different ages. The surface modifications manifested great adherence to the fingerprint residue even after two weeks elapsed and showed great promise after a two year period.

# Contents

# Table of Figures

# Abbreviations

| | | |
|---|---|---|
| AFIS | - | Automated Fingerprint Identification System |
| APTMS | - | (3-Aminopropyl) trimethoxysilane |
| ATR | - | Attenuated total reflection |
| DI | - | Deionised |
| DNA | - | Deoxyribonucleic acid |
| EDX | - | Energy-dispersive X-ray |
| FTIR | - | Fourier Transform Infrared |
| IACP | - | International Association of Chiefs of Police |
| IPA | - | Isopropyl Alcohol |
| IR | - | Infrared |
| LCH | - | Long chain hydrocarbon |
| Ln | - | Lanthanide |
| LPA | - | Laser particle analyser |
| LUDOX | - | Colloidal silica |
| NBCI | - | National Bureau of Criminal Identification |
| NPIA | - | National Policing Improvement Agency |
| RE | - | Rare Earth |
| SEM | - | Scanning Electron Microscope |
| TEM | - | Transmission Electron Microscope |
| TEOS | - | Tetraethyl orthosilane |

| | | |
|---|---|---|
| UV | - | Ultraviolet |

# Chapter 1 – Introduction

## 1.1 Introduction to Phosphors

The word 'phosphor' was created in the 17th century after work was carried out on volcanic rock samples in Italy, which were fired in an oven with the aim of creating and developing new materials. Instead of a new metal the result yielded a material that gave out a red light after being exposed to sunlight. After being reported, more of these materials were found all over Europe and they were named phosphors, the word being derived from the Greek for light bearer. Later, the term 'phosphorescence' was used to describe these materials that emit light after the excitation source has been removed[1].

Records have been found in old Chinese texts that the Japanese used ground seashells and jade to make a phosphorescent paint in the 10th century, many years before the phenomenon was noticed in Europe. A Chinese manuscript, Xiang-Sham Ye-Lu[2], describes how the Japanese artists learned to make luminous paintings with these resources. The paintings were invisible during the hours of daylight at which time the sunlight was being absorbed but in the evenings after the sun had gone down the images began to glow, as the stored energy was slowly emitted until after a few hours the image was again dark. It is written that when the Emperor Zhao Tai Zhong asked why the animals in the paintings only appeared at night, the artists replied that the creatures spent the daylight hours grazing in secret, sacred groves. In 1768 an English physicist, John Canton, described the preparation of a phosphorescent material by calcinating oyster-shell with sulphur. This was known as Canton's phosphorus but was known commonly as calcium sulphide[3].

The word phosphor itself is not clearly defined and is dependent on the user. It is used to mean inorganic phosphors, usually those in powder form and synthesized for the purpose of practical applications. Other materials such as organic compounds and thin films which can exhibit luminescence are rarely called phosphors and instead are known as luminescent materials. As different materials

were found with variations on these properties, definitions were introduced to categorise them.

Fluorescence was introduced to describe the unnoticeable short afterglow of the mineral calcium fluoride (fluorite) following its excitation[4]. This distinguished it from phosphorescence which is denoted by a long emission after the excitation source has been removed. The word luminescence, which includes both fluorescence and phosphorescence, was first used by a German physicist, Eilhardt Wiedemann, in 1888[5]. This word originates from the Latin word lumen, meaning light. The word luminescence is now defined as a phenomenon in which the electronic state of a substance is excited by some kind of external energy other than heat and the excitation energy is given off as light.

The discussion between fluorescence and phosphorescence was very active in the first half of the 20$^{th}$ century; this was all due to the after-glow emission of the compounds once excitation ceased. However, this discussion has now become meaningless, as for inorganic compounds, fluorescence is the emission of light while it is being excited by a source and phosphorescence is the emission detected after excitation has ceased. Whereas for organic materials and compounds, fluorescence is the light emission from a singlet state and phosphorescence is the emission from a triplet excited state[6].

Research programs on phosphors started in the mid-19$^{th}$ century, when a version of a zinc sulphide phosphor was created unintentionally by French chemist Théodore Sidot[6]. From this accident the field of phosphor synthesis expanded. After this discovery, German physicist and later Nobel prize winner, Philip Lenard and his colleagues performed extensive research and prepared a broad range of sulphide and selenide, alkaline metal based phosphors, and other zinc sulphide specimens[7]. After investigating luminescence properties they introduced a variety of different metal impurities using heavy metal ions, and later rare earth elements which were later known as activators, into the host lattices during firing process which formed luminescent centres.

## 1.2 Fundamentals of Luminescence

In 1888 Eilhard Wiedemann[5] recognized luminescence as the opposite to incandescence. He classified the luminescence into six different areas according to the methods of excitation. These are described in the table below:

| | |
|---|---|
| Photoluminescence | The emission of light by absorption of photons |
| Thermoluminescence | The emission of light by certain crystalline materials by absorbing ionizing radiation |
| Electroluminescence | The emission of light in response to an electric field |
| Crystalloluminescence | The emission of light through crystallization |
| Triboluminescence | The emission of light by breaking of bonds |
| Chemiluminescence | The emission of light through a chemical reaction |

Since the first identification of luminescence, additional forms have been characterised. These new areas of luminescence all belong in the six categories described by Wiedemann and will be described in the following sections.

### 1.2.1 Thermoluminescence

Thermoluminescence is exhibited by certain crystalline materials such as some minerals. Electrons from ionizing radiation are stored in the imperfections in the crystal lattice. They cannot escape the lattice because they do not have enough energy to escape. When the material is heated these electrons return to their low energy positions, releasing light. The light released is proportional to the amount of energy that has been irradiating the sample[8-10].

This capability allows for thermoluminescence dating to be carried out on buried objects as the radiation received is proportional to the age of the object as shown in Figure 1.1. When the pottery objects are heated the thermoluminescent signature is reset and so after being dug up and tested the results can show the approximate age the pot etc. was last used. An example of this is the dating of

burnt flints as presented by Martini et al [11]. Dating was carried out on multiple flints found in three areas of Italy. A radiation dose for one sample was 90 Gy (The IS unit for absorbed dose 1 Gy=1 J/Kg) with a dose rate of 1.79 Gy/ka gave the age of the item to be approximately 50,000±8000 years.

$$\text{Age of Item} = \frac{\text{Accumulated Radiation Dosage}}{\text{Dosage per Year}}$$

Figure 1.1 - Thermoluminescent dating equation

### 1.2.2 Chemiluminescence

This is the emission of light from a chemical reaction. The most well-known reaction is the peroxidase-luminol reaction, in which hydrogen peroxide breaks down into $HO^{\cdot}$ in the presence of alkali and an iron catalyst. This then reacts with luminol to give an excited state of 3-aminophthalate which subsequently drops to a lower

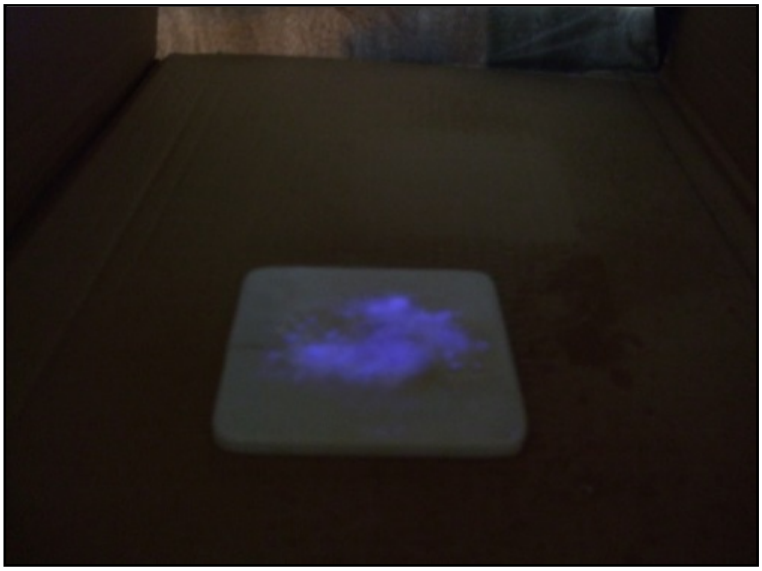

Figure 1.2 - Luminol reaction of blood splatter

energy level releasing energy in the form of light (see Figure 1.3). Both the $Fe^{2+}$ and $Fe^{3+}$ ions present in oxygenated and deoxygenated haemoglobin are able to catalyse this reaction allowing it to be used as a presumptive test for the detection of blood at crime scenes [12-17].

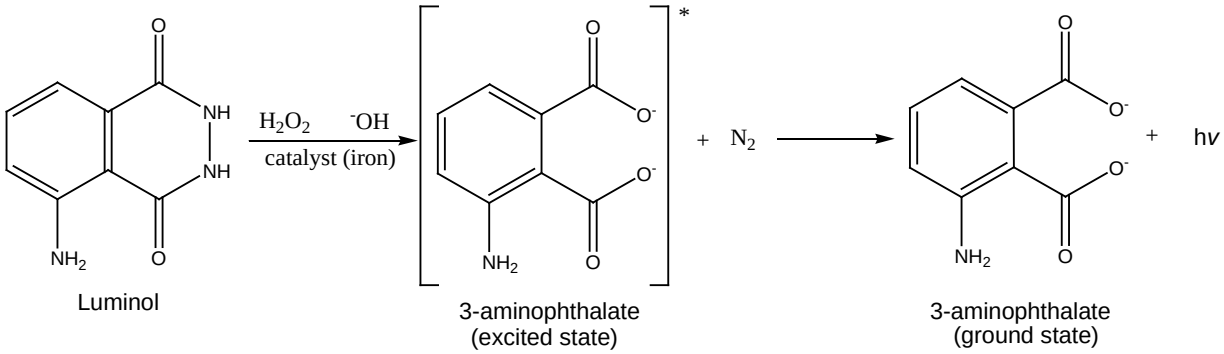


Figure 1.3 - Luminol reaction schematic [14]

## 1.2.3 Bioluminescence

This is the emission of light by an organism. It mainly occurs when luciferin reacts with oxygen. A luciferase enzyme catalyses the reaction and this produces energy in the form of light. There are many different ways life forms have evolved to use

Figure 1.4 - Female anglerfish showing bioluminescent trap

bioluminescence. For some, such as fire flies, it is used to attract a mate; they flash their abdomens to signal possible mates during mating season. The more frequent use for this form of luminescence is for feeding, to attract prey [18, 19]. The Anglerfish (Figure 1.4) is a prime example of this. The anglerfish live in the bathyal zone of the oceans, an area of the ocean between one and four kilometres below the surface and where there is not much light that reaches this depth. To help with attracting would-be prey the fish has a bacterial bioluminescent lure. The anglerfish move the bioluminescent lure around to resemble the motion of other small fish.

This entices predators to come in close which then allows the anglerfish to catch and kill these other fish for food.

### 1.2.4 Photoluminescence

Photoluminescence is described as a emission of light from a substance after absorption of a photon. There are two types of photoluminescence which each have a different emission length. Fluorescence and phosphorescence are both explained below.

### 1.2.5 Fluorescence

This is the emission of light from a molecule when an electron is excited by, for example, UV light from its ground state to a higher quantum state. The electrons then relax to its ground state emitting a photon of light[6]:

$$\text{Excitation: } S_0 + h\nu_{ex} \rightarrow S_1$$

$$\text{Emission: } S_1 \rightarrow S_0 + h\nu_{em} + \text{heat}$$

Figure 1.5 - Fluorescence mechanism

The equations (Figure 1.5) show that from a ground state ($S_0$) an energy source such as ultraviolet (UV) light ($h\nu_{ex}$) excites the molecule to an excited state ($S_1$).

The fluorophore is very unstable in high energy configurations and after a brief period ($10^{-15}$ to $10^{-9}$ seconds) it relaxes down to a more stable, lowest energy excited state. Finally the fluorophore returns to its ground state releasing the energy as light. Due to the drop in energy from the highest to the lowest energy excitation state, the light emission from the drop to ground state is always of a lower energy than the excitation wavelength[20].

Another pathway luminescence can take place is with the addition of a sensitiser molecule. In this way an excited molecule can transfer its energy to the sensitiser molecule which then releases the energy as light. This is a common reaction created with fluorophores such as 9,10-Diphenylanthracene (blue luminescence) and Rubrene (orange) which are present in glow sticks.

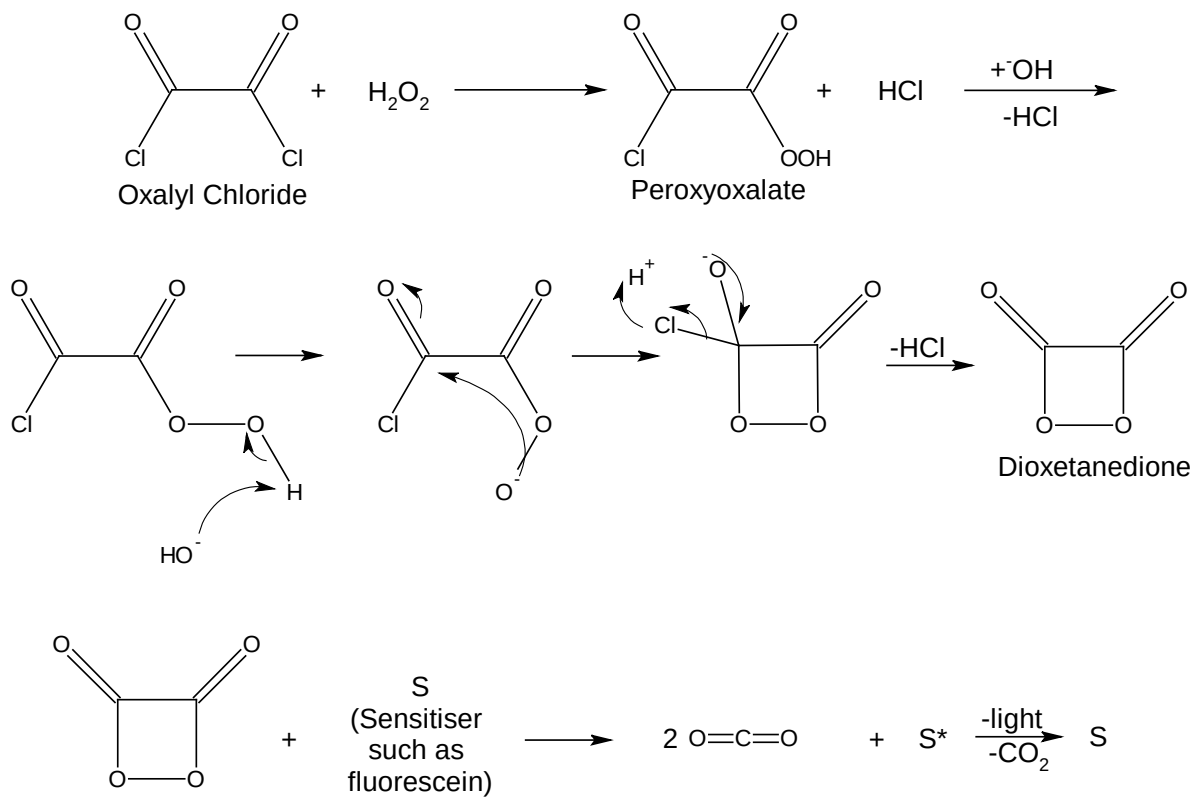


Figure 1.6 - Oxalyl chloride reaction schematic [12]

## 1.2.6 Phosphorescence

In phosphorescence, the energy absorbed by the substrate is emitted much slower than in the case of fluorescence. Under appropriate conditions this absorbed energy can undergo a spin flip which creates an intersystem crossing into a triplet state.

$$S_0 + h\upsilon \rightarrow S_1 \rightarrow T_1 \rightarrow S_0 + h\upsilon^1$$

Figure 1.7 - Phosphorescence mechanism

In this state, the energy is "trapped" and to be able to drop down to the ground state has to undertake another spin flip. This state can last between $10^{-3}$ to $10^{2}$ seconds. The energy emitted via this route is always of lower energy than the incident light due to the lower energy of the triplet state.

## 1.3 Introduction to Fingerprints

There are three types of fingerprints which are found at crime scenes. These are plastic, patent and latent[21, 22]. Plastic fingerprints are impressions made in mouldable materials such as wax or paint. Patent fingerprints are obvious to the human eye and are left on surfaces after being transferred through other material like ink or blood. Latent fingerprints are the most common found at crime scenes and have to be detected using a physical developer. The compositions of these fingerprints are made of material from two different sweat glands which are described in the following sections.

### 1.3.1 Eccrine

Eccrine based prints are made up of mainly aqueous materials and salts which are released through eccrine pores on the finger surface [11, 23-29]. Due to the decomposition and evaporation effects that occur after deposition on a surface these prints are harder to detect. The table below shows the abundance of the main chemicals that comprise an eccrine fingerprint.

| Components of Eccrine Sweat | Abundance (wt%) |
|---|---|
| NaCl | 43.83 |
| Lactic Acid | 29.22 |
| Urea | 11.69 |
| Amino Acids | 7.79 |
| Others | 4.97 |
| $NaH_2PO_4$ | 1.75 |
| Glucose | 0.44 |
| $K_2PO_4$ | 0.31 |

Figure 1.8 - Composition of eccrine fingerprints

### 1.3.2 Sebaceous

A second type of print that can be detected is known as a sebaceous print. These are more common over long periods of time and are made up of sebum. Sebum is predominately made up of triglycerides and other organic molecules [30-33]. Squalene, a lipid and precursor to cholesterol, is one of the largest single components of sebaceous fingerprints. This type of print arises when oily residue is transferred to the print by ways such as touching the neck or rubbing hands through hair. The components in this print can last much longer as these oils can survive for extended periods in a humid atmosphere.

| Components of Sebum | Abundance (wt%) |
|---|---|
| Wax Monoesters | 25 |
| Triglycerides | 41 |
| Free fatty acids | 16 |
| Squalene | 12 |

Figure 1.9 - Composition of sebaceous fingerprints

## 1.4 History

The use of fingerprinting as a tool for identification has been traced back all the way to ancient Egypt where Pharaohs used their fingerprint as a stamp in wax on important documents. It was also used in China in 650 BC; wax moulds of people's fingerprints were used to sign documents and deeds to properties. It was only in the late 19th century that scientists discovered the uniqueness of every person's print[34, 35].

Dr Henry Faulds published a letter in Nature in 1880 titled "On the Skin-furrows of the Hand"[36], detailing how fingerprints could be recorded using printer's ink and furthermore how they could be used in the forensic identification of criminals. Faulds showed two examples of how he previously used the technique in a hospital in Japan; first, to help convict an employee for stealing surgical alcohol from his

hospital, and second, to exonerate a man who was arrested for another burglary. A month after publication a letter was published by Sir William Herschel arguing his use of fingerprints in identifying people scamming benefit payments in India had been used 20 years prior. The feud between these two men lasted over fifteen years. When Faulds arrived back in the United Kingdom in 1886 he approached Scotland Yard to create a fingerprint bureau. This request was rejected due to the lack of evidence of the uniqueness of each individual's fingerprints. Faulds wrote to Charles Darwin for help in predicting the statistical probability of a unique fingerprint but his letter was passed onto Francis Galton, a cousin, who was too busy to work on the problem and little work was then carried out. Eight years later Galton was brought back to the problem via another route and published a paper, based on the analysis of 8000 fingerprints to show the chances of any two fingerprints being identical to be 64 billion to 1 [37]. This paper then lead to the introduction of fingerprint identification bureaus as an invaluable tool for the detection and identification of criminals. The bureau at Scotland Yard was set up in 1901 by Dr Edward Henry.

## 1.5 Henry Classification System

In 1823, Jan Evangelista Purkynje [38-40] noted the nine distinct fingerprint patterns that make up the human fingerprint shown in Figure 1.10, but it was not until 1880, when Dr Edward Henry properly characterised each template[41]. This system was used for over a hundred years and the templates formed the basis of the Automated Fingerprint Identification System (AFIS) which is used in many countries to identify a person's fingerprints. In recent years this method has been replaced by a ridge flow classification system[42]. These nine patterns are split up into 4 sub headings and are explained below[34].

Whorls

Spiral and Concentric

Whorls are patterns where the ridges form either a spiral, or concentric circles around the central core of the fingerprint. The whorl pattern consists of one or more free recurving ridges and two points of delta (an area which resembles the Greek letter). When the line of the fingerprint disc is placed on the two points of delta, it will bisect at least one of the ridges belonging to the core group.

Arches

Plain Arch

A plain arch has ridges which flow from one side of the print to the other. The centre has a much smaller uprising than other patterns. Like the plain arch, the tented arch flows from one side to the other but the middle uprising is much more pronounced and sometimes bisects other pronounced ridges. Approximately 5% of the population have an arched print and of this, 60% are plain with 40% tented.

Tented Arch

Composites

Twinned Loop

These composites were found which contained some of the characteristics of arches, loops and whorls. They were divided into four subcategories.

Central Pocket Loop

The Twinned Loop also referred to as the Double Loop consists of two separate loop formations which give rise to two deltas.

The main loop in the Central Pocket Loop recurve a second time forming a pocket within the loop. This pattern also contains two deltas.

Lateral Pocket Loop

The Lateral Pocket Loop is fairly similar to the Twinned Loop but the ridges bend sharply down on one side before recurving, forming a pocket which again gives rise to two deltas.

Accidental Loops

Accidental Loops are loops that are a combination of any two types of pattern with the exception of the plain arch that basically has no pattern. Due to this, there could be more than two deltas in this pattern.

Loops

Radial Loop

Ulnar Loop

Looped prints come in two different forms. The only difference between the two is the direction of the loop. To identify which loop a person has you first need to know what hand the print was taken from. The radial loop originates from the side nearest the thumb and goes towards the little finger whereas the ulnar loop heads from the little finger towards the thumb. The loop is the most prevalent pattern type with 60% of the population having it. The ulnar loop is the most common with 94% of people with loops having that type.

Figure 1.10 - The four main fingerprint patterns

## 1.6 Historic Cases

The introduction of fingerprint matching to identify suspects and provide evidence was noticeable by the speed with which this new technology was adopted and used around the world. This was helped by an increased investment into police forces, but also by some high profile cases that caught the imagination of both legislative and judicial professions, as well as the general public, who rapidly accepted the new technology as a vital and validated evidence procedure. The following show a small selection of some of the more high profile cases.

### 1.6.1 First case in the UK

1905 was the milestone for fingerprint evidence in the United Kingdom[43]. Thomas Farrow, the manager of a paint shop in Deptford, and his wife were found, murdered, in their home above their shop by an employee. He found the shop locked up and the shutters down which was unusual at that time of day. He checked through the windows, noticed the place was disturbed and called for help from a local shop owner. He forced open the door and found Mr Farrow dead on the ground floor and Mrs Farrow drifting in and out of consciousness in the couple's bedroom. The police were called and the scene was searched. The couple were found to be missing £10 and a print was found on the cash box.

Although the police already had a file built up of known criminals, the print was found to not match any that were already catalogued. After searching around the area witnesses led the investigators to two brothers. After having their prints taken, a match was made between the print found on the cashbox and their own prints. This led to them being arrested and charged for murder. The criminal case against them was very lengthy due to it being the first case for fingerprint evidence, but after two hours of deliberation the jury found them guilty and they were sentenced to be hanged and a new precedence was set in physical evidence.

### 1.6.2 First case in the US

The first real case of fingerprint evidence being allowed to be used in court in the USA was the case of People v. Jennings[44]. On the night of the 19th September 1910, an intruder broke into the home of the Hillers to rob it. It is shown that as he was creeping round the house he was met by Mr Hiller at the top of the stairs. A struggle ensued and both participants fell down the stairs; Mr Hiller was shot twice in the chest and died a few moments later. The intruder fled as the victim's wife came to investigate the noise. During the investigation it was found that the point of entry was the kitchen, and due to being newly painted, four fresh fingerprint imprints were imbedded into the window frame. The prints were taken and found not to be a match to anyone in the family. Hours later, the police found and questioned Jennings as to what he was doing out so late and after giving conflicting

statements, he was searched. This lead to the police finding him in possession of a loaded revolver and he was quickly arrested. He was found to have recently been released on parole and had a fingerprint card on file. This was compared to the prints found at the house and was found to be a conclusive match. During the trial, four leading expert witnesses were brought in by the prosecution and irrefutably proved the prints found on the window ledge were Jennings. He was found guilty of the murders. Jennings' lawyers appealed on the grounds of the admissibility of the evidence used but the court recognised the use of the fingerprints as evidence due to the long history of use in other countries. From this period the use of fingerprint evidence used in courts around the United States greatly increased.

### 1.6.3 Richard Speck

Richard Speck was a well-known American serial killer who was finally identified and caught by his fingerprints[45]. On the night of the 13th July 1966 he broke into a student nurses' dormitory with only a knife and over the course of the night methodically killed eight of the nurses who lived there. He kept them in their rooms and one by one brought them out and proceeded to strangle or brutally stab each one to death. His last victim was raped before being strangled. Only one nurse survived by staying under her bed until the morning when she climbed out of the bedroom window and called for help. During the examination of the scene, smudged fingerprints were found by the officer leading the search and these were part matched to fingerprints which the FBI had on file due to Speck's criminal background, and also an admission to the merchant navy where all applicants are required to give their fingerprints. Later that day, a better print was found on a door to the bedroom and with this the police were able to positively identify Speck as the suspect. A manhunt was started and he was later arrested after being recognised by a local doctor who had read in a local paper about a tattoo Speck had following a suicide attempt. After being found competent to stand trial by a panel of five psychiatrists and one general surgeon the trial took place and with the testimony of the surviving nurse and the fingerprint evidence he was found guilty and sentenced to be executed in the electric chair (a judgement that was later over turned - he was given life in prison where he died in 1991).

### 1.6.4 The Night Stalker

Another famous case is that of 22 year old drifter Richard Ramirez, known by the media as the Night Stalker, who kept residents of California in fear for the lives for 5 months[46]. On the 17th March 1985 in California he shot Angela Barrios, broke into her house, and immediately shot and killed another man, Dayle Ozakaki. Angela luckily survived the attack as the bullet had ricocheted off her keys. An hour later in a nearby park he pulled a woman out of her car, attacked her and then shot her several times. She was found still alive by a policeman but later died on her way to a hospital. The media latched onto the story and the residents around the area started to panic. The survivor was able to give the police a brief description of her assailant. He was said to have long curly hair, rotting teeth and bulging eyes. He was named the Walk-In Killer by the media.

Ten days later on the night of the 27th March he broke into the home of a sleeping Vincent and Maxine Zazzara. Vincent was shot in his bed and his wife's body was mutilated, having several stabs wounds and her eyes gouged out. Police matched the bullets used in the previous murders and also found footprints outside the windows, which was the first real evidence the police had on the now labelled serial killer. This brought a major police investigation into operation but having no real evidence, they didn't manage to get any closer to catching Ramirez. Two months later he struck again, breaking into the house of Harold and Jean Wu. Like his last break in, Harold was found shot in the head but this time Jean was found alive. She had been physically assaulted, raped and bound but was able to give the police the same description as before. The police were able to collect more evidence but due to the lack of DNA fingerprinting available at the time nothing could be done with the evidence.

Over the next three months he stepped up his attacks and left at least seven people dead with many others assaulted physically and sexually. He began moving around California leaving Los Angeles and moving to San Francisco, where he carried on attacking and murdering people in their homes. As the residents of California became more fearful of this serial killer and started securing their homes better, his tactics changed from just climbing through open windows to breaking and entering.

This made the media change the name they used to describe him to The Night Stalker.

Ramirez then again moved south of San Francisco where he broke into the house of Bill Carns and his fiancée Inez Erickson. Like he had done many times before, Bill was shot in the head and Inez bound and raped. After he left she was able to crawl to a window, get a good look and then describe him to the police when they arrived. With this new evidence the police put out an all-points bulletin and gave the media the description. The next day the car was reported by a teenager who gave the licence plate number. The car was finally picked up and examined by police a few days later. After thoroughly dusting and inspecting every part of the car a single useable fingerprint was found on the rear view mirror. The prints were run through AFIS and a single name was output with a criminal record image which matched all previous descriptions of the renowned serial killer. It belonged to Richard Munoz Ramirez, who was found to have a long criminal record predating his initial attacks for drug possession and traffic violations.

The media was given his photo and only two days later he was spotted and was set upon by an angry mob that surrounded and brutally beat him. The police managed to arrest him and had to disperse the mob which would have likely killed him. He was charged and convicted of sixty seven felonies and fourteen counts of murder and was still on Death Row awaiting execution until his death from blood cancer in June 2013.

### 1.6.5 The Theft of the Mona Lisa

In 1911, the Mona Lisa was stolen from its place in the Louvre, Paris. It was found to have been taken during the gallery's closed period[47]. The thief managed to get through security, undo the glass around the Mona Lisa and then take the painting down and move it out through the back stairway. It was not noticed for a while due to the museum curator being away on holiday and the regular guard being away to tend to his sick son. It was first noticed by a painter, Louis Beroud who had come down to see it. After walking into the room and noticing it was missing he went and

informed the head of security only to be told the painting was probably away for cleaning.

Hours later he came back and spoke again to the security personnel and then it was found the painting had been stolen and the police were called. Sixty investigators scoured the museum but apart from the frame of the painting which was found on a stairwell, the painting itself had gone. The frame was meticulously searched and one thumb print was found. The police called in Alphonse Bertillon, a well renowned fingerprint expert who tried to match the thumb print to a print he had gathered from previous cases. After many days it was found the print had not been collected previously and one of the only leads broke down.

It took three years before the culprit was finally apprehended in a sting operation in Italy. Once the suspect was in custody Alphonse was finally able to match the suspect's prints to the print found on the frame. He was convicted of the theft and sent to prison but was released shortly afterwards during the war.

## 1.7 Identification Technology

### 1.7.1 Automatic Fingerprint Identification System

In 1903, fingerprints were accepted by New York Civil Service Commission as a suitable replacement from the previously used Bertillonage system of anthropometric measurements which were used in court for twenty years. The system relied on a technique created by Richard Edward Henry and had already been used in India for three years and Britain for two years. Quickly, it was decided that a national database should be started to hold fingerprint records from anyone convicted of a crime to be used in future in case the convict reoffended. In 1904 The International Association of Chiefs of Police created what was known as the National Bureau of Criminal Identification (NBCI), the first national fingerprint repository of its time. In the database's first few years of use, fingerprint record cards were taken of all prisoners in the United States and this was then built upon slowly with criminals who had been newly convicted after its setup period. From 1905 other departments started using their own fingerprint databases including the

Army and Navy. This would help quickly identify soldiers' bodies during war time situations.

Over the years the system was changed and updated as the courts agreed on how many reference points could give a positive identification. In 1914 renowned forensic pioneer Edmond Locard wrote an article on how twelve points of reference would be sufficient to give a positive match between two suspected similar prints. By 1946 the NBCI contained 100 million fingerprinting record cards and this increased to 200 million in 1971. Even though these cards were separated into groups by the Henry Classification system it still gave a large amount of records to be searched through especially as each record could have up to ten prints on it. Most of the time the database was only properly used for serial crimes and any prints found were added to the crime file until a suspect was found. This would then be verified and the prints checked on the database for any other outstanding crimes.

As computerisation started to take over the US Department of Justice decided that a computerised system needed to be put in place to firstly alleviate the problems with keeping such large amounts of paper, and also to make it quicker to identify people without having to go through such a large number of records. The Automatic Fingerprint Identification System (AFIS) was created to help this and after the record cards were slowly put into the first database it was found there were many duplicates; after all 200 million were entered, there were found to only be approximately 30 million individuals in the system.

Although the use of AFIS reduces the length of time it takes to identify a fingerprint manually, each positive result still has to be checked by hand to double check the result. When a fingerprint is scanned into the database, the system looks for twelve specific reference points and the record is then given a numeric identifier related to the points. This number is then searched in the database and any file with the same number is flagged. If no record is found then it looks for the largest amount of reference point positives on file and then these are each checked by an expert. In this way, partial fingerprints can also be checked on the database.

The largest database in the world at the moment (2014) is held by the US Department of Homeland Security's Office of Biometric Identity Management (OBIM) which contains 120 million records of all persons when they arrive in the United States. There is also a large AFIS system used by INTERPOL which contains over 150,000 records for international criminals which can be accessed by all countries. The UK IDENT1 database contains over 18.6 million sets of fingerprints which belong to known individuals and 1.9 million unidentified records.

## 1.8 Detection Techniques

### 1.8.1 Dusting

The primary way of searching for latent prints is by surface dusting. This is where a brush usually made of camel or squirrel hair [48] (Figure 1.11) is first placed into a

Figure 1.11 - Dusting using a squirrel hair brush

pot of powder and this is then applied to a material's surface with a twisting motion to slowly deposit powder onto the particular surface. From the beginning, graphite powder was the most used powder and has only been replaced fairly recently with newer more specific powders such as titanium dioxide and aluminium. Dusting of an area often leads to many different prints. Each has to be lifted from the surface

with tape and then catalogued ready for examination and analysis. The graphite powder had its disadvantages, for example it was very hard to spot graphite coated prints on dark surfaces which often lead to prints being overlooked. As time went on, newer methods were researched and developed to help give forensic scientists a larger arsenal when looking for prints [24, 49-51].

### 1.8.2 Magnetic Powders

The magnetic powders don't use a brush but instead make use of the magnetic properties to be pulled over the print by a magnetic wand (Figure 1.12). This is

Figure 1.12 - Magnetic wand

becoming more common because it is more precise and also is much cleaner as all excess powder can be picked up again so only the print gets covered. The powders are usually $Fe_3O_4$ shelled particles which are paramagnetic and are then covered in silica to stop any degradation the chemical would give to the print[52].

### 1.8.3 Bichromatic Powders

These powders can be used with either a magnetic wand or with a usual brush. These powders are usually made of aluminium mixed with an anticaking agent and unlike graphite reflect light to an extent that the powder shows up on both dark and light surfaces.

### 1.8.4 Other Techniques

Although dusting is the quickest and most used form of locating latent fingerprints, some surfaces do not allow dusting to take place. This is usually due to the surface being too porous and the oils from the print being absorbed into the surface making dusting useless, or that the surface is too electrostatic and the powder is attracted more to the surface than the print. In cases like this other techniques can be utilised either at a scene or back in a lab.

#### 1.8.4.1 Ninhydrin

For porous materials such as paper, a solution of ninhydrin can be sprayed onto the surface and then heated in an oven to convert latent prints into a visible print by

Figure 1.13 - Ninhydrin reaction

converting the amino acids in sweat to a purple colour (Figure 1.13) which is named after the discoverer Siegfried Ruhemann [53-59]. Results can vary due to the composition of the paper and the quantity of amino acids in the fingerprint material (a large amount could mean an over developed print which would have lost all definition). The ninhydrin is dissolved in a solvent, usually ethanol, so any information needed form the document has be photographed first or another detection method has to be used.

1.8.4.2 Silver Nitrate

Like the Ninhydrin, a silver nitrate solution can be applied to a paper surface and this reacts with the sodium chloride in latent eccrine prints to produce silver

Figure 1.14 - Silver nitrate reaction

chloride. When exposed to UV light the print will darken and can then be photographed as shown in Figure 1.14. Silver nitrate is a destructive test and therefore has rather a large disadvantage. It is only used when all other tests such a ninhydrin and iodine fuming have failed to generate an image. The reduction process from silver nitrate to silver metal can lead to overdeveloped images if there is too much expose to UV light.

1.8.4.3 Iodine Fuming

Iodine fuming is a very old technique used before the development of ninhydrin and silver nitrate. It is still used as it is one of the best non-destructive ways to locate latent fingerprints.

Other fuming techniques and even dusting processes, if used incorrectly, can lead to the print being unusable in further examination. In this method iodine is sublimed and the vapour fumed over the surface. Any fats or oils temporarily absorb the iodine vapour turning a dark brown. This can then be photographed ready for analysis. After a short while the iodine will evaporate from the print making it colourless again. This process can be stopped with the use of a starch solution if necessary [11, 60-63].

Due to its non-destructive nature iodine fuming is usually the first technique applied to a porous surface. If no reaction is observed this is then followed by ninhydrin and finally silver nitrate[64].

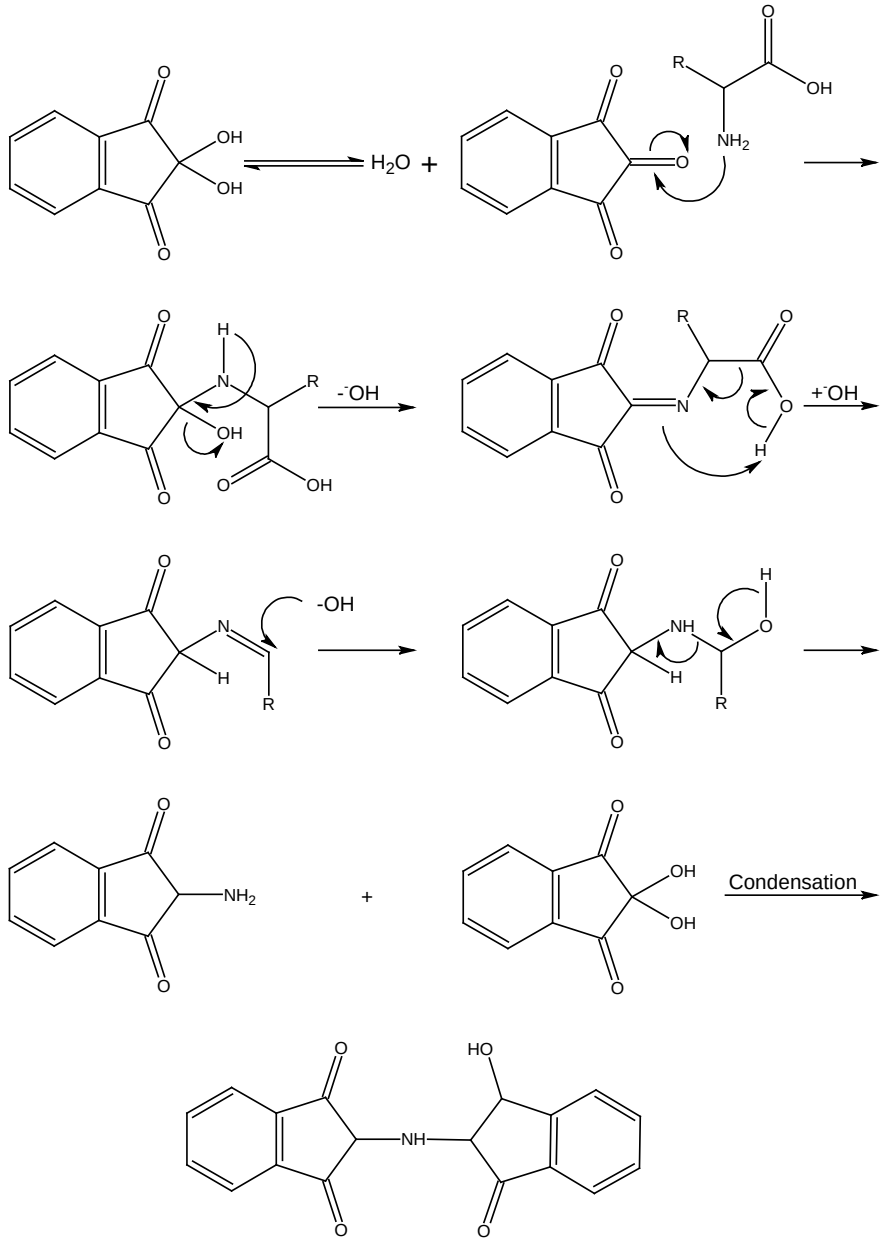


Figure 1.15 - Ninhydrin schematic

1.8.4.4 Cyanoacrylate fuming

Fingerprints on surfaces that hold an electrostatic such as black sacks and other large plastic items are able to take advantage of a cyanoacrylate fuming method, which allows large items to be processed quickly. In this technique, a small amount

of cyanoacrylate was warmed in a humid environment which contained an object on which a possible print may be found [65]. The cyanoacrylate vapourises and then polymerises on the surface of the print (Figure 1.16). This would lead to a white print being made visible and from there analysis can occur. The method needs to be watched carefully as too much vapour can lead to the print being overdeveloped and so useless for any further analysis [11, 60-63].

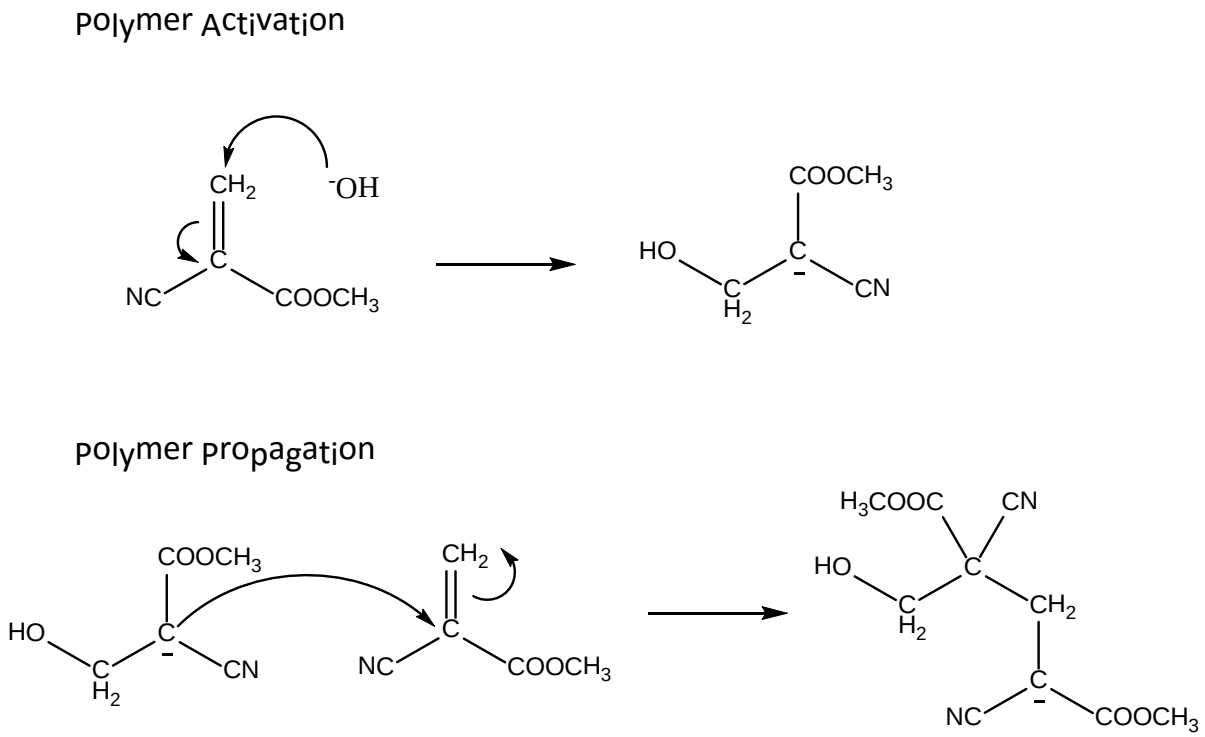


Figure 1.16 - Cyanoacrylate schematic

## 1.9 Problems with Existing Techniques

As discussed, the existing techniques that have been developed have all improved upon the original graphite methods [66-76]. Its inability to work effectively on porous or black surfaces resulted in the use of new materials and new techniques.

Although these techniques have improved the detection rate of latent prints there are still many disadvantages and problems which are not solved. An example is the

detection of fingerprints on textured surfaces which are problematic for powders of large particle size. To this end phosphors of particle sizes of between 100-250nm were chosen for the study

However none of them have brought together all the requirements into one easy to use high contrast system. This research is aimed at investigating the use of nano phosphors as a dusting medium, with careful design of particle size, morphology, coating, fluorescent performance and ease of use to enable it to replace and enhance existing solutions. To this end a variety of phosphors were synthesised and then coated to allow for modification to increase the ability for the particles to adhere to aged latent prints.

# Chapter 2 – Experimental Techniques

## 2.1 Introduction

In this chapter, the synthetic methods used to prepare nanometre-sized rare earth doped phosphor powders followed by the methodologies for silica coating and for making surface modifications are described.

Various yttria based host lattices were tested, each doped with a rare earth element phosphor, which would fluoresce under UV light [6, 20]. This new phosphor powder was to be used to help in the detection of latent fingerprints by allowing for the easier viewing of powder dusted fingerprints under UV light on any type and colour of material. This would help save time trying to uncover a possible fingerprint. In addition it was intended that the particles could be modified to adhere to different molecules in fingerprints [77-83]. For example, by dusting a location with a powder containing a phosphor modified with a drug antibody; the use of one UV wavelength may show the site of the fingerprint and by using a different UV wavelength if the fingerprint had contained some drug metabolites these particles would fluoresce under a different wavelength. This could lead to the identification of a motive for the crime or help disprove a motive if it conflicted with a statement.

## 2.2 Solid State Synthesis

### 2.2.1 Synthesis of $YVO_4:RE^{3+}$ phosphor by solid state synthesis

$YVO_4:Eu^{3+}$ was prepared by solid state synthesis[6]. $Y_2O_3$ (10.7g) (Ampere Industries (French), 99.99%), $Eu_2O_3$ (0.88g) (Aldrich, 99.99%), $NH_4VO_3$ (12.9g) (Sigma Aldrich, 99%) were milled together in a pestle and mortar for 1 hour to fully blend the compounds and break down any large clusters of material. The resulting mixture was fired in an alumina crucible for 1 hour at 1000$^oC$ and then for an additional hour at 1200$^oC$. The resulting solid was cooled, washed with a strong solution of NaOH, left to dry, then fired again at 1200$^oC$ for 1 hour to give a slightly yellow powder due to the formation of metavandates[10]. The whole procedure is illustrated in the flow diagram below (Figure 2.1)

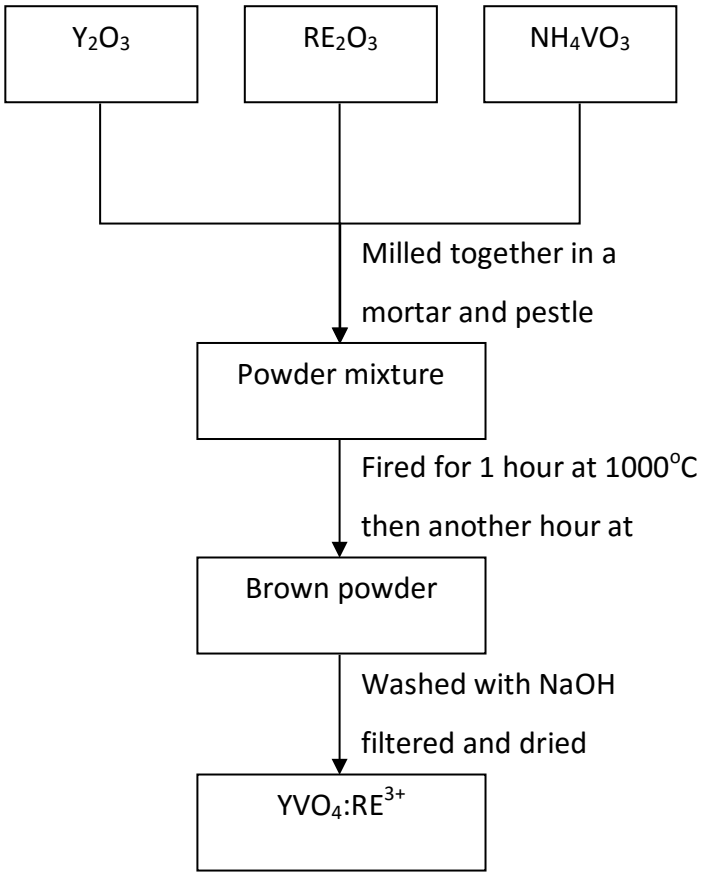


Figure 2.1 - Solid state $YVO_4:RE^{3+}$ synthesis flow chart

## 2.2.2 Synthesis of $Y_2O_3:RE^{3+}$ phosphor by solid state synthesis

$Y_2O_3:Eu^{3+}$ was prepared by solid state synthesis[6]. $Y_2O_3$ (Ampere Industries (French), 99.99%) and $Eu_2O_3$ (Aldrich, 99.99%) were milled together in a pestle and mortar for 1 hour to fully mix. This mixture was then fired in an alumina crucible for 6 hours at 1000$^{o}$C to give the $Y_2O_3:Eu^{3+}$ phosphor.

$Y_2O_3:Tb^{3+}$ was prepared as above using $Y_2O_3$ and $Tb_2O_3$. The procedure is illustrated in the flow diagram below (Figure 2.2)

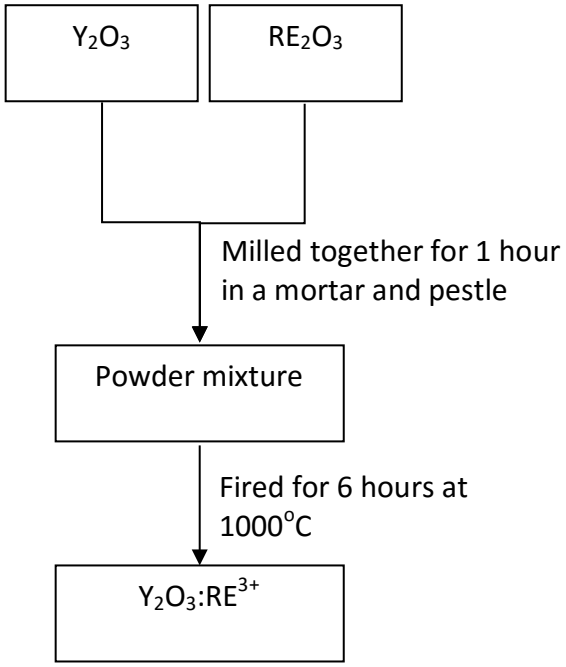


Figure 2.2 - Solid state $Y_2O_3:RE^{3+}$ synthesis flow chart

## 2.3 Homogeneous Precipitation Synthesis

### 2.3.1 Preparation of stock solutions

$Y_2O_3$ (Ampere Industries (French), 99.99%), $Tb_2O_3$ (Aldrich, 99.99%) and $Eu_2O_3$ (Aldrich, 99.99%) were used as starting materials, all chemicals were used as received with no further purification.

The stock solution of $Y(NO_3)_3$ (0.5M) was synthesised by heating 56.52g $Y_2O_3$ in distilled water (400mL). To this was slowly added diluted $HNO_3$ (100mL 70%) until the solution became clear showing the formation of the nitrate. The solution was raised to boiling and then cooled and left to stir overnight. The solution was then topped up to 1 litre.

The stock solution of $Eu(NO_3)_3$ (0.01M) was synthesised by first heating 1.761g $Eu_2O_3$ in distilled water (300mL). A solution of diluted $HNO_3$ (10mL 70%) was then carefully added to the solution containing the $Eu^{3+}$ cations until the solution grew clear showing europium nitrate had been formed. The solution was then cooled and stirred overnight before being made up to 1L with distilled water.

The stock solution of Tb$(NO_3)$3 (0.01M) was synthesised by heating 1.851g $Tb_2O_3$ in distilled water (300mL). A diluted solution of $HNO_3$ (10mL 70%) was carefully added until the solution became clear showing the formation of the terbium nitrate. The solution as then cooled and stirred overnight before being made up to 1L with distilled water.

The general procedure for the creation of the stock solution is below (M = Y, Eu, Tb)

$$M_2O_3 + 6HNO_3 \rightarrow 2M(NO_3)_3 + 3H_2O$$

## 2.3.2 Reaction Schematic

The decomposition of urea above 85 $^{o}$C gives an ammonium cation and cyanate anion which under acidic conditions (pH <3) reacts as shown below.

$$H_2NCONH_2 \rightarrow NH_4^+ + OCN^-$$

$$OCN^- + 2H^+ + 2H_2O \rightarrow H_2CO_3 + NH_4^+$$

The hydronium ions from the weakly hydrolysed yttrium ions promotes the decomposition of the urea and the release of the carbonate ions triggers precipitation once the concentration of reactants reaches saturation.

$$[YOH(H_2O)n]^{2+} + H_2CO_3 \rightarrow Y(OH)CO_3.H_2O + (n-1)H_2O$$

## 2.3.3 Synthesis of $Y_2O_3:RE^{3+}$ phosphor by homogeneous precipitation

$Y_2O_3:Eu^{3+}$ was synthesized using a two stage homogeneous precipitation method [84, 85]. Firstly, Aqueous solutions of $Y(NO_3)_3$ and $Eu(NO_3)_3$ were mixed to appropriate molar ratios in a glass beaker and then heated to 85$^{o}$C whilst being continually stirred on a hot plate. Once at temperature, excess urea was added and after turbidity was observed the solution was left for 2 hours to complete the precipitation of the hydroxycarbonate. After this time the precursor was filtered, washed with distilled water and the soft white powder dried at 50$^{o}$C overnight. This precursor was then fired at 1000$^{o}$C for 6 hours to obtain a soft white powder of 2% doped $Y_2O_3:Eu^{3+}$ phosphor.

The $Y_2O_3$:Tb phosphors were synthesised using the same method as shown above with the exception of using 25mL of $Y(NO_3)_3$ stock solution and 25mL of $Tb(NO_3)_3$ stock solution. The method is shown in the flow diagram below where RE = Eu, Tb.

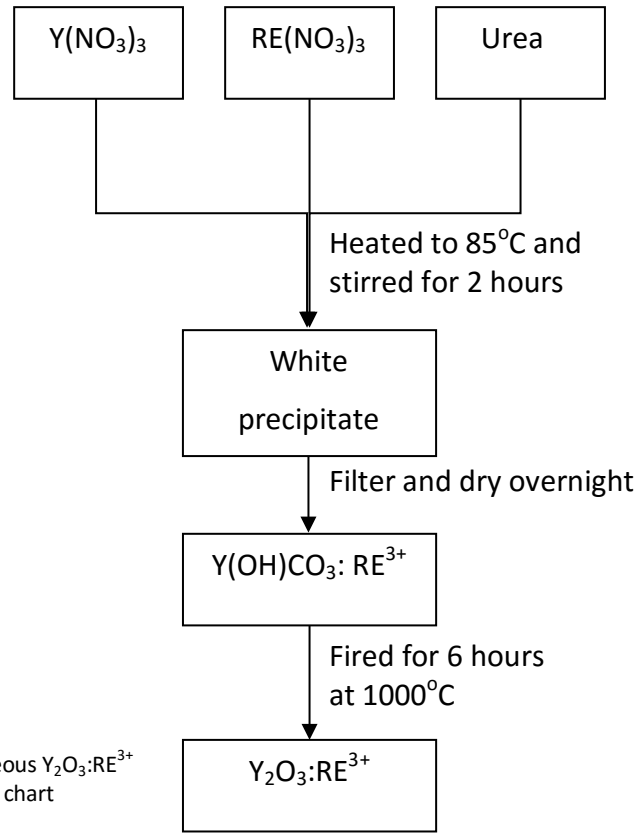


Figure 2.3 - Homogeneous $Y_2O_3:RE^{3+}$ synthesis flow chart

### 2.3.4 Synthesis of $Y_2O_2S:RE^{3+}$ phosphor particles by homogeneous precipitation

$Y(OH)CO_3:Eu^{3+}$ hydroxycarbonate precursor particles were synthesised using the homogeneous precipitation method shown above. To obtain the $Y_2O_2S:Eu^{3+}$ phosphor particles the precursor particles then were converted to oxysulfides by a reaction with sulfur[86]. The precursor was thoroughly mixed with $NaCO_3$ (Aldrich, ≥99.99 %) and S (Aldrich, ≥99.99 %) before being transferred and carefully packed into an alumina crucible. A top layer made up of a ratio of 1:1.5:2 $Y_2O_3$ (in the same ratio as the precursor), $NaCO_3$ and S were then mixed up and again carefully packed above the precursor. This layer was used to give an inert atmosphere in order to exclude as much oxygen as possible for the reaction to take place. The crucible was fired in oxygen for 6 hours at 1000$^oC$ and then left to cool. The top layer was removed and discarded while the bottom layer of white powder was removed from the crucible and added to boiling water where it was stirred for 1 hour to remove the flux and any impurities. The precipitate was then filtered and dried in an oven to obtain a fluffy white powder of $Y_2O_2S:Eu^{3+}$. The same method was used to create the $Y_2O_2S:Tb^{3+}$ phosphors by using the $Y(OH)CO_3:Tb^{3+}$ as a starting material. The full method for synthesis is illustrated below in Figure 2.4 where RE = Eu, Tb.

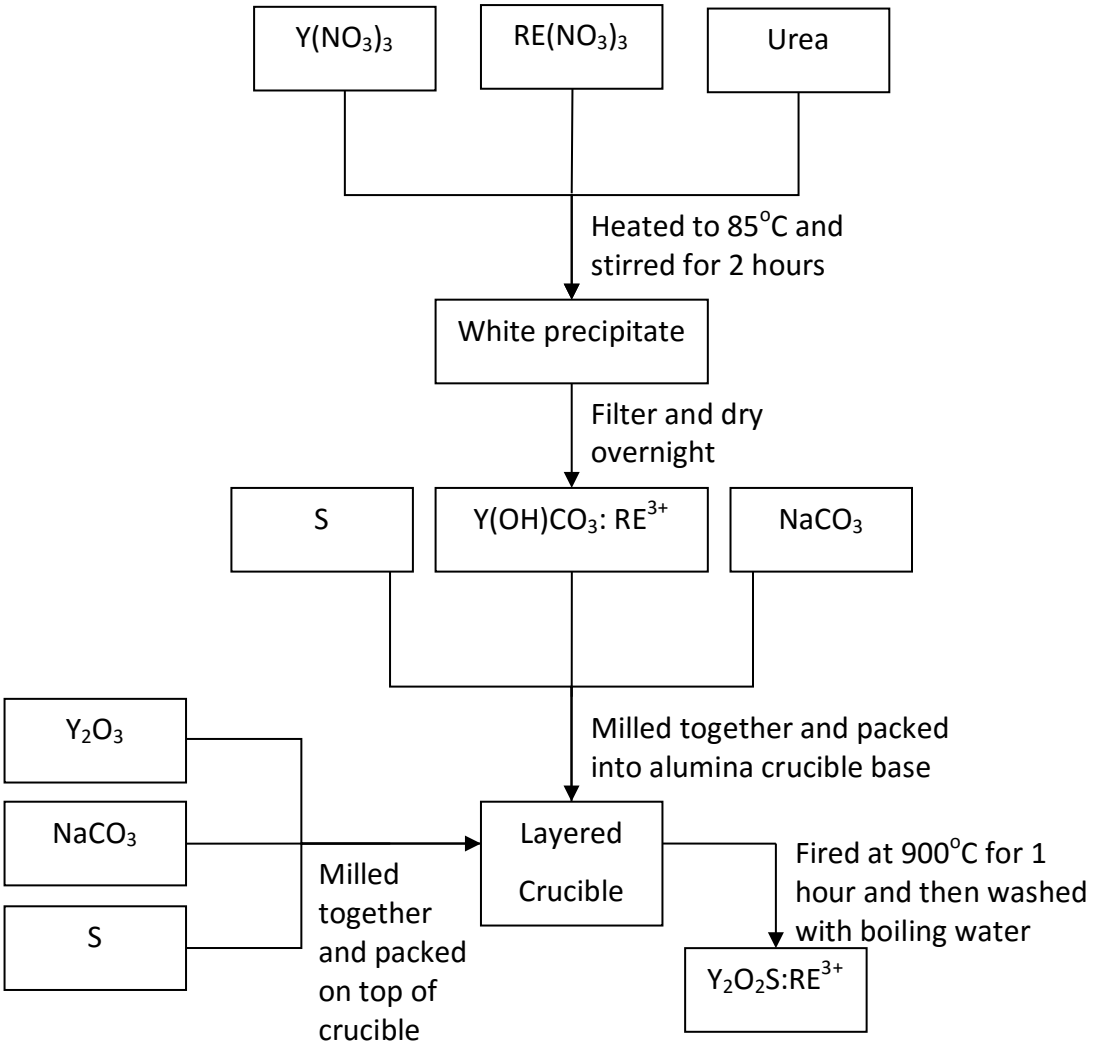


Figure 2.4 - Homogeneous $Y_2O_2S$:$RE^{3+}$ synthesis flow chart

## 2.3.7 Synthesis of $YVO_4:RE^{3+}$ phosphor particles by homogeneous precipitation

$YVO_4:Eu^{3+}$ was prepared by homogeneous precipitation[27]. Two initial solutions were produced. Solution A consisted of 2.34g $NH_4VO_3$ (Aldrich, 99.99%) dissolved in water and then the pH made up to 12.5 with a solution of NaOH. Solution B was made by combining 7.27g of $Y(NO_3)_3$ in water (200mL) with 0.37g $EuCl_3$ in water (200mL). Solution B was added dropwise whilst stirring to Solution A and then heated to 60°C for 3 hours. The resulting yellow precipitate was filtered and dried. The precipitate was added to a crucible then fired at 1000°C for 1 hour. After cooling the sample was then washed with concentrated NaOH and finally filtered and dried to produce the $YVO_4:Eu^{3+}$ phosphor. A schematic of the overall reaction is shown in Figure 2.5 (RE= Eu).

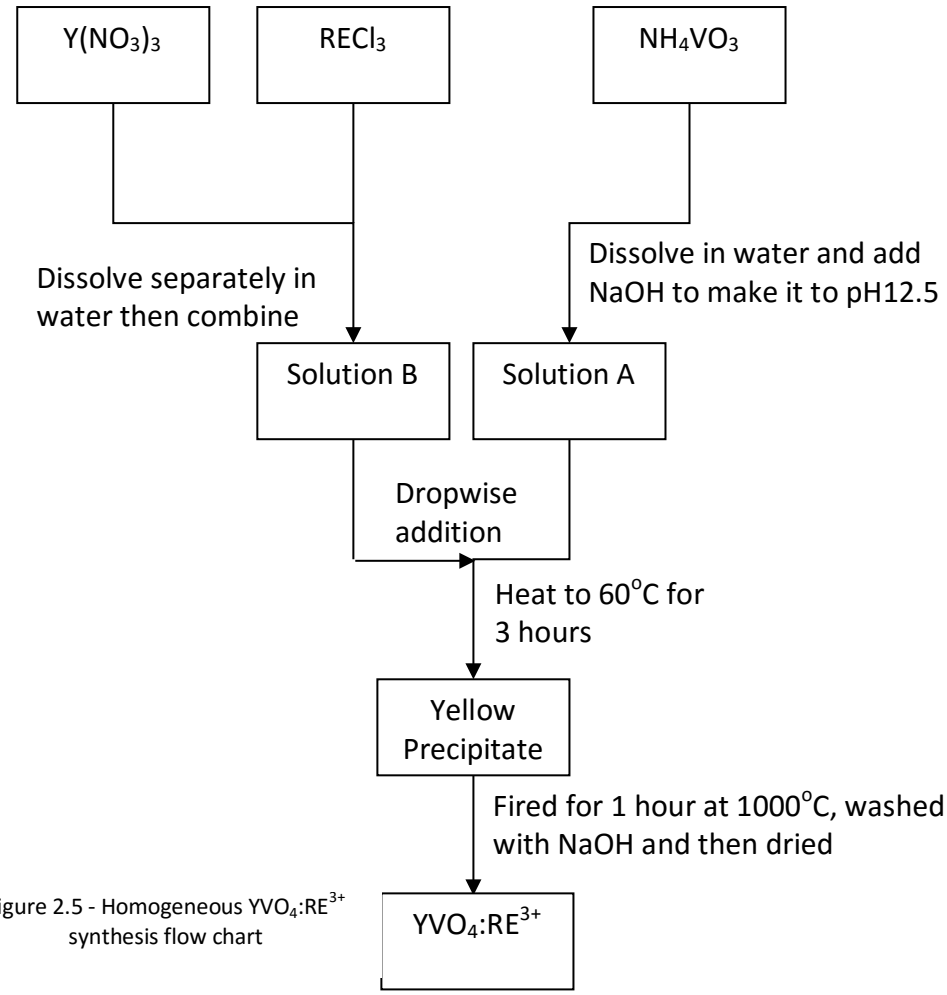


Figure 2.5 - Homogeneous $YVO_4:RE^{3+}$ synthesis flow chart

## 2.4 Preparation of Coatings and Modifications

### 2.4.1 Introduction

The phosphors were coated in silica to create a standardised surface for the modifications. This allows a straightforward surface for the modifications to be deposited onto rather than having to create a new deposition method for each new phosphor. An additional use for the coating is to improve the agglomeration of phosphor particles during the sintering process. The hydroxycarbonate precursors are coated in silica before being heated. Once the firing process has been completed the silica was etched to break apart the particles and create a porous surface. Two methods were used for the silica coating. The first is a well-known method for creating silica particles[87] while the second utilises a colloidal silica dispersion.

Modifications to the surface were attached to the silica coating to improve the adhesion of the phosphor powders to the latent fingerprints. Two modifications were employed to increase the adhesion to either eccrine or sebaceous fingerprints. For eccrine fingerprints an aminosilane was applied and for the sebaceous prints the surface was modified with an octylsilane.

The preparations for each of the coatings and modifications are presented in the following sections

### 2.4.2 Preparation of coated phosphor particles by tetraethyl orthosilane

Phosphor powders and precursors were coated with silica to using a modified version of the Stöber method [87-90] (See Figure 2.6). A sample of phosphor (1g) (or phosphor precursor powder) was dispersed in 400mL ethanol. The solution was fully dispersed by using an ultrasonic probe for 1 hour. 25mL $Si(OC_2H_5)_4$ (Aldrich, 99.999%) and 20mL distilled water was added to the flask and the solution slowly stirred for 10 minutes. 8mL ammonium hydroxide was added to the solution and

the stirring was increased momentarily. After this time the stirring was brought back down to 100rpm. The solution was left slowly stirring for 1 hour at room temperature. The precipitate was washed 3 times with ethanol and filtered by centrifuge. The collected powder was then dried overnight in an oven. The phosphor particles were examined after this coating was applied, whereas the coated precursor hydroxycarbonate particles were then fired for 6 hours in a furnace at 1000$^{o}$C. In both cases a coating as shown in Figure 2.7 was produced. An illustration of the process is shown below in Figure 2.6.

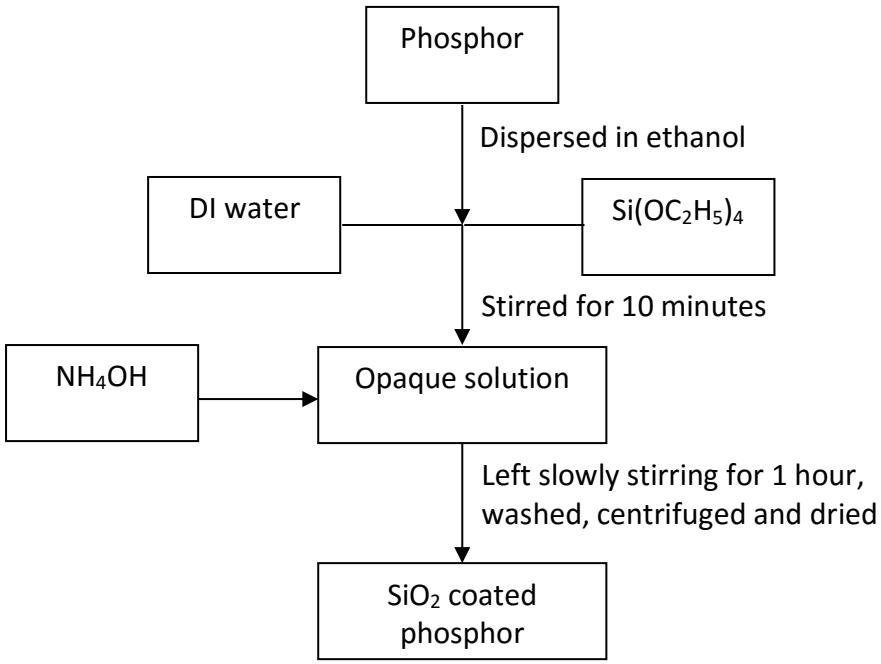


Figure 2.6 - TEOS coated synthesis flow chart

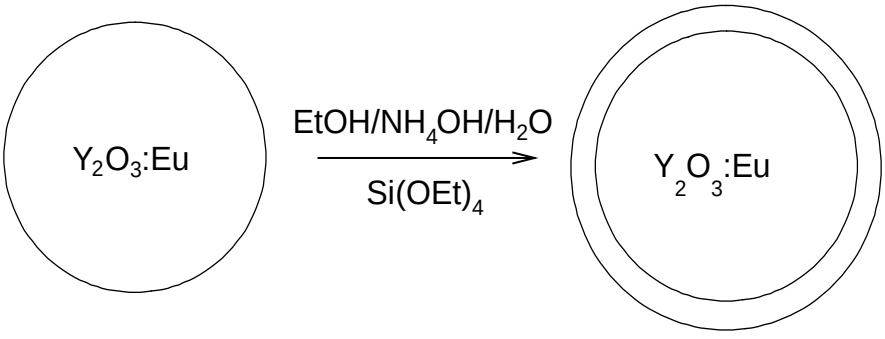


Figure 2.7 - Coating of phosphor particle with silica

## 2.4.3 Preparation of silica coated phosphor particles by addition of a colloidal silica dispersion

LUDOX (Aldrich 30 wt. %) is a colloidal silica dispersion in water containing discrete spherical particles of silica between 80-100nm, was used as a starting material[91-94]. 1g of phosphor powder was dispersed in 100mL of water and to this LUDOX AM-30 (10mL) was added and gently left to stir for 1 hour (Figure 2.8). The particles were separated by centrifuge, washed three times with ethanol and dried to give the silica coated phosphor (as seen in Figure 2.9). To adhere the silica to the phosphor the dried particles were then fired at 400$^{o}$C for 2 hours.

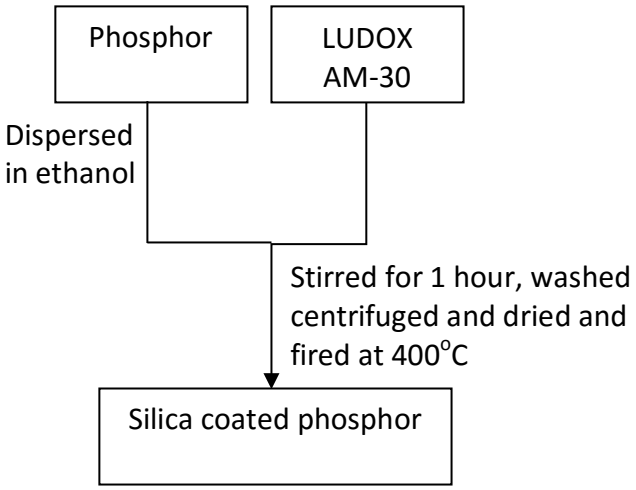


Figure 2.8 - Ludox AM-30 coating flow chart

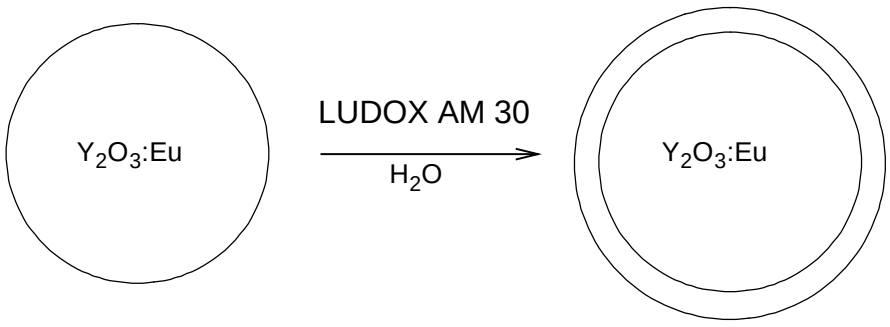


Figure 2.9 - Coating of phosphor particle with silica

## 2.5 Modification of Silica Coated Phosphors

### 2.5.1 (3-aminopropyl) trimethoxysilane modified silica

The surface of the silica coated phosphor was modified (using (3-aminopropyl)trimethoxysilane (Aldrich 97%)) to be covered with long chains ending with an amine group when dispersed in water[95-97]. In a typical experiment 1g phosphor powder coated with silica was dispersed in 100mL ethanol. The solution was then ultra-sonicated for 1 hour to fully disperse the powder in the ethanol. The flask was transferred to a magnetic stirring plate and stirred. 20mL (3-aminopropyl)trimethoxysilane was slowly added to the stirring solution and this was left stirring for 48 hours before being separated by centrifuge, washed three times with ethanol and left to dry. Figure 2.10 displays the modification schematic for the reaction.

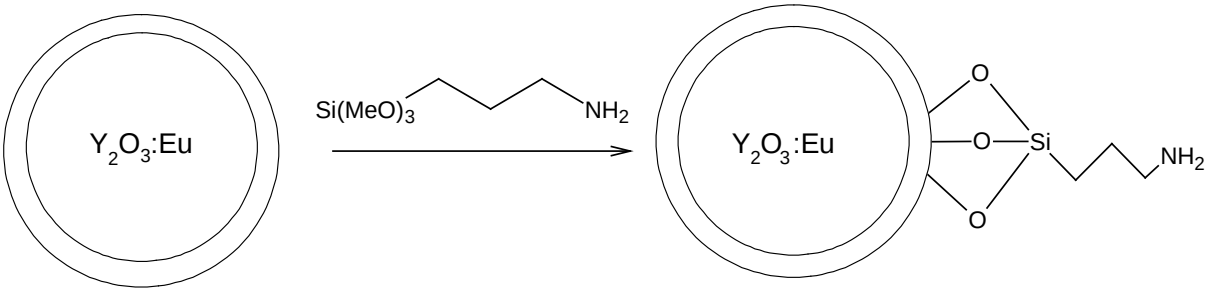


Figure 2.10 - Modification of silica coating with amine groups

### 2.5.2 Triethoxy(octyl)silane modified silica

To modify the surface of the phosphors for better adherence with sebaceous prints 1g of one of the silica coated phosphors was dispersed in 100mL ethanol. The solution was stirred and 10mL water and 20mL triethoxy(octyl)silane was added. This was left stirring with samples being taken every 24 hours with each being separated by centrifuge, washed three times with ethanol and dried.

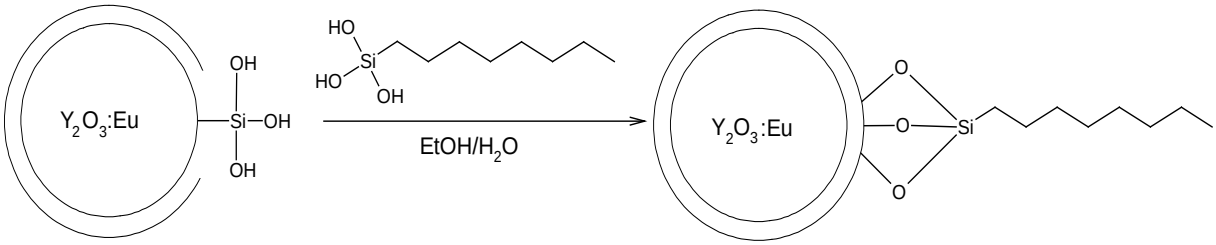


Figure 2.11 - Modification of silica coating with triethoxy(octyl)silane

## 2.6 Etching Studies

### 2.6.1 Introduction

Etching studies were carried out on silica coated hydroxycarbonate precursors [98] to break up any agglomerated particles after the sintering process had taken place and to reduce the size of the silica coating surrounding the phosphor particles. The SEM images of the coated phosphors indicated that the LUDOX coated phosphors were very inconsistent in size and the TEOS coated powders showed a coating of approximately 100nm in diameter. This procedure was carried out to facilitate control of the coating diameter and also to test the possible quenching of a silica coating on the photoluminescent properties of the phosphor as research has shown previously that the use of a silica coating can absorbs short wavelength UV light which would impair the phosphors ability.

## 2.6.2 Methodology

The coated precursors were added to a solution of NaOH and stirred to etch away the silica coating[8].This method has been well documented in previous papers[99] The hydroxide ions target the Si-O bonds to create a sodium silicate which is soluble in water as shown below.

$$nSiO_2 + 2NaOH \rightarrow Na_2O.nSiO_2 + H_2O$$

In a typical experiment 10mL 10M solution of NaOH was made up using NaOH pellets ( Sigma Aldrich, ≥98%) and left stirring on a magnetic plate. 0.1g of silica coated hydroxycarbonate precursor powder was added to 10mL distilled water and ultra-sonicated to fully disperse the powder. After ten minutes the dispersed solution was added to the alkaline solution and left to wash whilst stirring for 24 hours. The reaction was then quenched with water, separated by centrifuge and then washed three times with ethanol. The powder was then left to dry overnight in an oven at 70$^{o}$C before being fired at 1000$^{o}$C for 6 hours to obtain a finer silica coated phosphor powder. Figure 2.12 shows a schematic for the etching of silica coated particles.

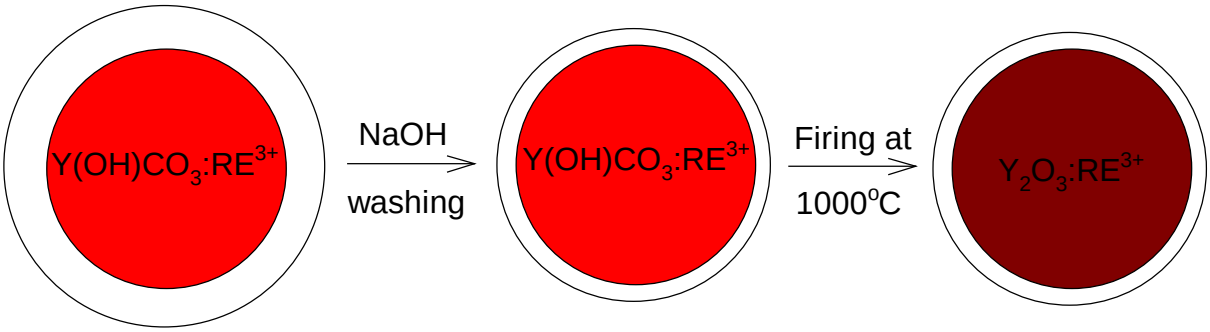


Figure 2.12 - Method of etching silica coating

# Chapter 3 – Instrumentation

## 3.1 Introduction and Sample Preparation Methodologies

Phosphor powders were characterised with scanning electron microscopy, transmission electron microscopy, Raman spectroscopy, photoluminescence spectrometer, FTIR spectroscopy and their sizes established by a laser particle analyser. In this chapter the instrumentation and equipment used to generate the images and spectra of the materials synthesised for the project (coated and uncoated phosphor powders) will be presented/discussed together with sample preparation methods.

## 3.2 Photoluminescence Spectrometer

A photoluminescence spectrometer consists of three main parts: a light source, filters and a detector. The Bentham spectrometer used in this work contained two monochromators rather than filters to allow selection of the excitation and emission light as illustrated in Figure 3.1. Luminescent properties of phosphors were introduced in Chapter 1.2. The photoluminescence emission and excitation spectra were recorded on a Bentham spectrometer. The emission spectra were taken from 350nm to 800nm using a 254nm light source for $Eu^{3+}$ doped phosphors and 274nm for $Tb^{3+}$ doped phosphors while the excitation spectra were recorded by monitoring at the most intense emission peak.

### 3.2.1 Sample Preparation

To quantify the emission and to examine the emission potential of the coated and modified phosphors 1g of each phosphor was added and compressed into a 10mm aluminium boat. This allows a quantifiable emission from each of the coated and modified phosphors. The boat was then placed under the light source of the spectrometer and the spectrum of the phosphor was recorded.

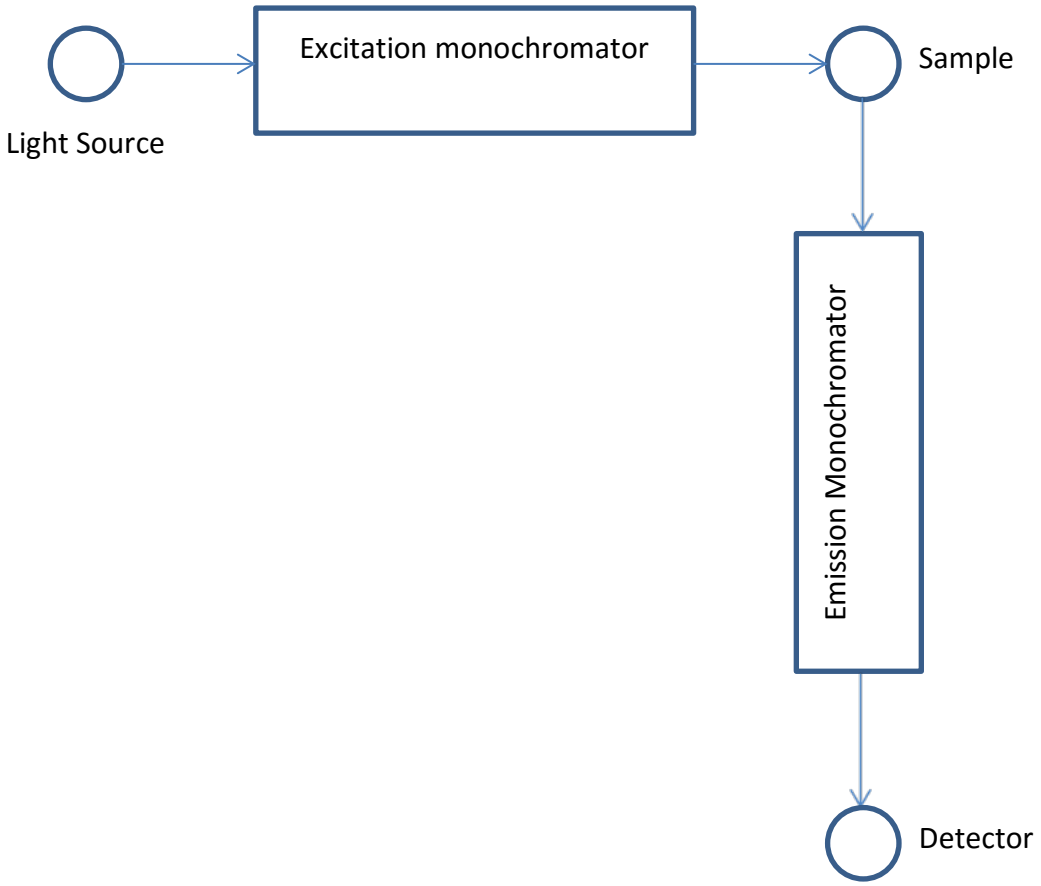


Figure 3.1 - Components of a photoluminescent spectrometer

### 3.2.2 Example Spectra

Figure 3.2 is an example of a photoluminescent spectrum with both an emission and excitation line. The emission spectrum is produced by exciting the sample material (i.e. a phosphor) with photons of higher energy than the bandgap. This energy absorption can occur either in the host lattice or at the luminescent centre. If the absorbance is in the host lattice then it is followed by a transfer to the luminescent centre before the emission can occur (Figure 3.3). When these luminescent centres show too weak an absorbance a sensitiser molecule can be added which firstly absorbs the energy before transferring it to the luminescence centre. The host lattice is always excited by high energy excitation such as electron beams, X-rays and γ-rays whereas the luminescent centres are only directly excited by low energy excitation such as UV, visible and IR light.

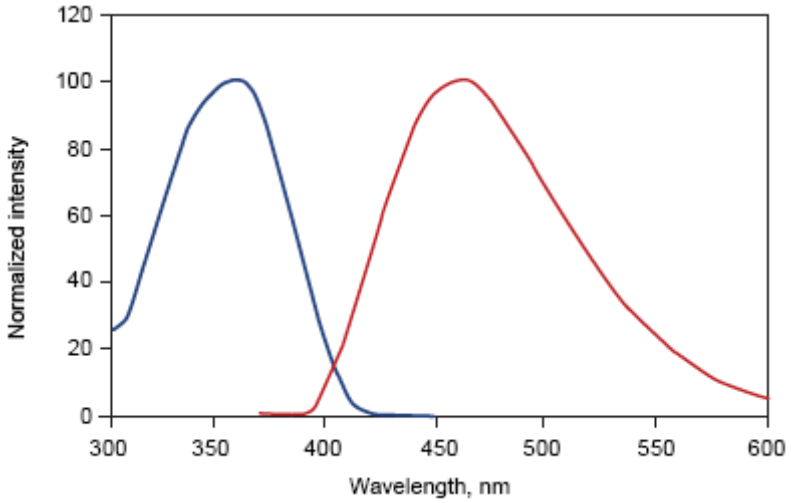


Figure 3.2 - Example emission and excitation spectrum

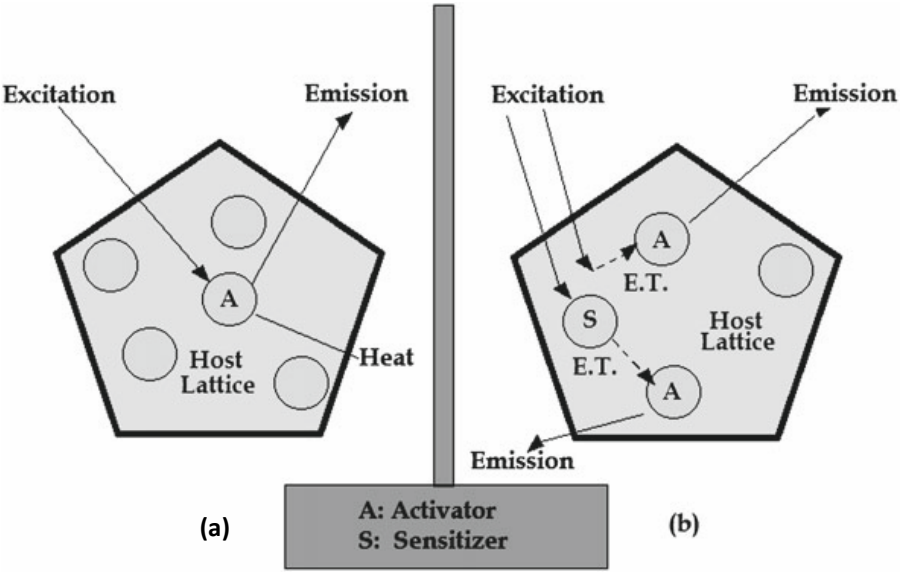


Figure 3.3 - Schematic diagram showing (a) direct and (b) indirect excitation[100]

Figure 3.4 - Bentham Spectrometer

## 3.3 FTIR Spectroscopy

The samples were scanned on a Perkin Elmer Spectrum One Fourier Transform Infrared (FTIR) spectrometer, using a Specac Golden Gate Single Reflection ATR accessory, consisting of a Diamond crystal at a fixed angle of 45°. The spectrometer passes infrared radiation, through the sample and the absorptions made by each type of bonding vibration in the sample is recorded. The energy induces vibrational excitation of the atoms to either stretch or bend. Molecules in different environments absorb varying intensities and frequencies of energy. This allows a spectrum to be produced which can be directly correlated to the bonding within the sample.

### 3.3.1 Sample Preparation

The phosphor powders were dried overnight in an oven. The sample area was opened and the powder was placed on the chamber. The diamond was closed onto the sample and then the spectra were collected over the 4000 $cm^{-1}$ to 650 $cm^{-1}$ wavenumber range, at a resolution of 4 $cm^{-1}$. 10 accumulations were collected for the samples.

Figure 3.5 - Perkin Elmer Spectrum One FTIR

### 3.3.2 Example spectra

When the Infra-red beam interacts with a covalent bond which has an electrical dipole the absorbed energy starts an oscillation in the bond. An asymmetric molecule such as O-H can absorb IR radiation but a symmetric molecule such as H-H cannot. Figure 3.6 is an infrared spectrum of ethanol[101] and the most prominent peaks are very noticeable. These include the large absorbance at 3300$cm^{-1}$ which is indicative of an O-H stretch, a sharp absorbance at around 3000$cm^{-1}$ of a C-H stretch and the two large peaks at around 1050 and 1100$cm^{-1}$ showing the C-O stretch.

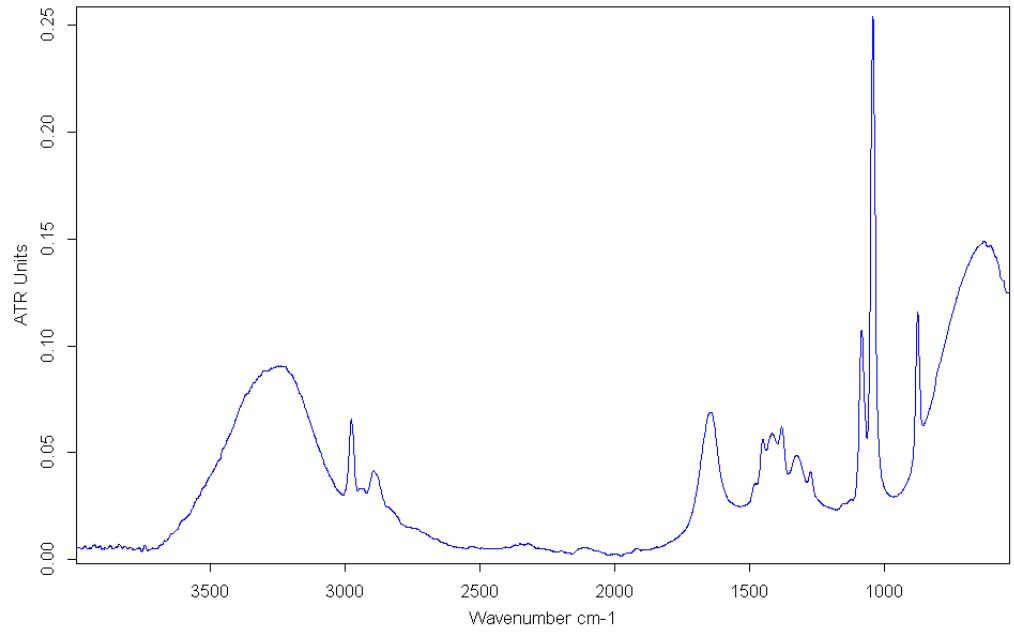


Figure 3.6 - IR spectra of ethanol

## 3.4 Raman Spectroscopy

The Raman spectra were recorded on a Horiba Jobin Yvon LabRAM HR800 spectrometer[102, 103]. It is used to observe the vibration and rotation of molecules which scatters monochromatic laser light. The lasers used for the analysis were either an $Ar^{+}$ green laser of 514.5nm wavelength, a He-Ne 20 mW red laser 632.8nm or an infrared 1064nm laser. The laser is focussed onto the sample, this excites the lattice or molecules from its or their ground state to a virtual state. The excited molecules then relax returning to a different vibrational state. This scattered light is collected and sent through a filter to remove wavelengths close to the laser line due to Rayleigh scattering. The light is then focused onto a detector and a signal is collected.

The Raman spectrometer was calibrated using a silicon sample. The microscope was focussed on the surface of the sample and then the auto calibration function was started using the LabSpec program. This program then calibrated the spectrometer to the 520.7$cm^{-1}$ shift of the silicon sample.


Figure 3.7 - Horiba Jobin Yvon LabRAM HR800

### 3.4.1 Sample Preparation

For the phosphor powders, a sample was added to a glass slide and then slightly compressed. The slide was placed on the stage and the focal point was verified to make sure it was at its strongest. The spectrum was then run using a multi window accumulation mode on the LabSpec 5 program.

### 3.4.2 Example Spectra

Figure 3.8 is an example of a Raman spectrum of the pigment vermillion collected using a 632.8nm laser from a Hans Holbein sketch at the Royal Collection in Windsor. The spectrum shows a strong band at 253 and 343cm$^{-1}$ which is indicative of vermillion which has been well documented [104-112]. A Raman spectrum allows for the identification of vibrational states of molecules by the shift in the wavelength of the inelastically scattered radiation. Figure 3.9 gives the three types of scattering which occur. In Rayleigh scattering a photon interacts with a molecule raising it to a short lived virtual energy state. The relaxation to the ground state

releases a photon which results in scattering. As the molecule returns to its ground state the energy of the released photon is the same as the energy before the interaction which results in the photon having the same wavelength. In Raman scattering the photon can gain or lose energy during the scattering process and therefore the resulting scattered photons wavelength increases or decreases respectively. If the molecule relaxes from an excited state to a vibrational state the scattered photon has less energy than the incident photon and therefore a longer wavelength then this is known as Stokes scattering. If the molecule was already in a vibrational state then after relaxation the scattered photon will have less energy and therefore a shorter wavelength. This is known as Anti-Stokes scattering. More photons undergo Stokes scattering than Anti-Stokes scattering but these are both less than the Rayleigh scattering which is far more prominent. Due to this only the Stokes scattering is used in a spectrum due to the larger intensity.

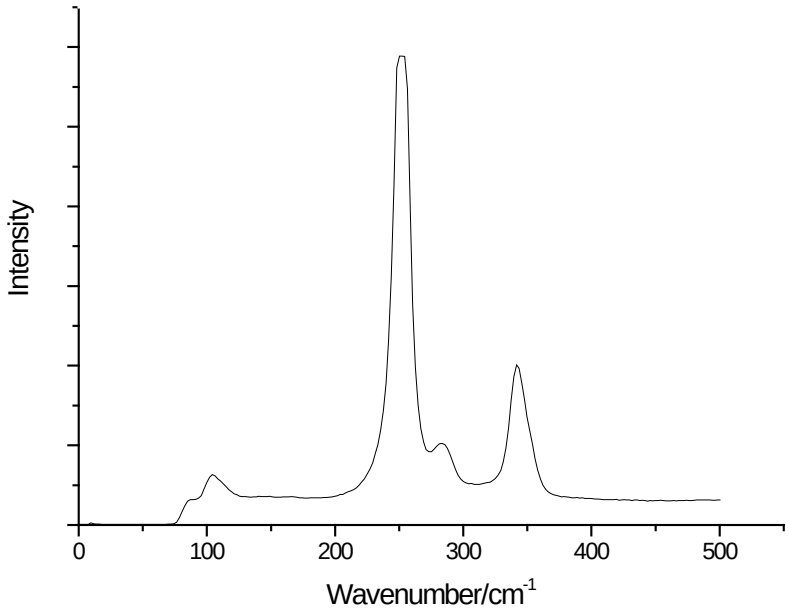


Figure 3.8 - Raman Spectra of Vermillion[112]

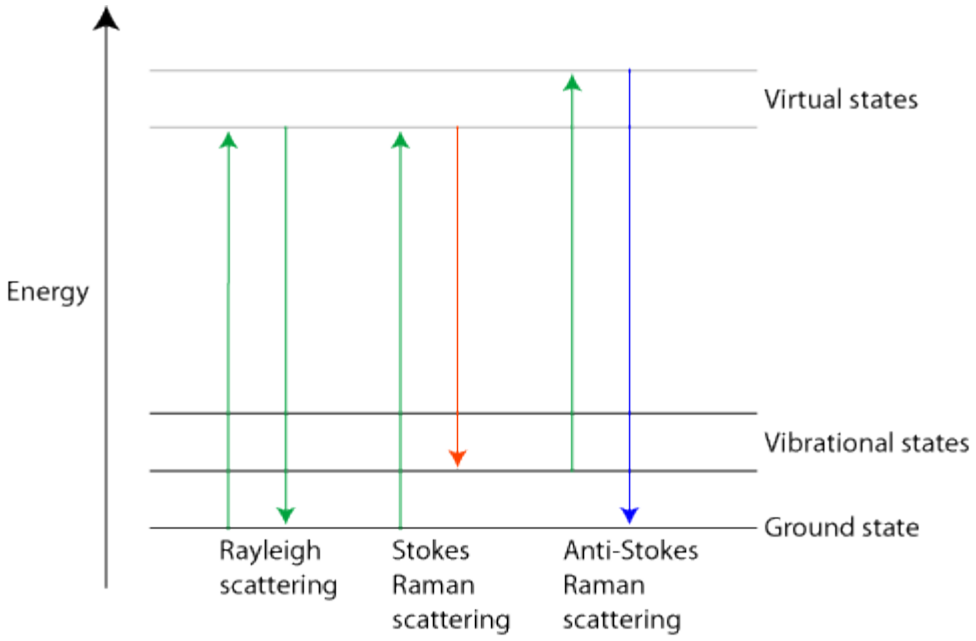


Figure 3.9 - Three different forms of scattering

## 3.5 Laser Particle Analyser

The laser particle analyser (Figure 3.11) utilises Frahnhofer diffraction to allow sizes of particles to be determined. The sample is first dispersed in a pure non particulate liquid and then ultrasonicated for five minutes for maximum dispersion[113]. The particles then pass through a laser beam which has been broadened with spatial filters in order to increase the interaction with a maximum amount of particles. The particles scatter the incident beam onto a Fourier lens which focusses the light onto a detector (Figure 3.10). This detector uses the Frahnhofer diffraction equation [16] (see below) to give a particle size distribution.

$$\frac{W^2}{L\lambda} \ll 1$$

Where W is the aperture size, L is the distance from the aperture and λ is the wavelength. The method of dispersion is of great importance when determining the size of nanoparticles as the particles tends to cluster together in a mass which changes the distribution curve.

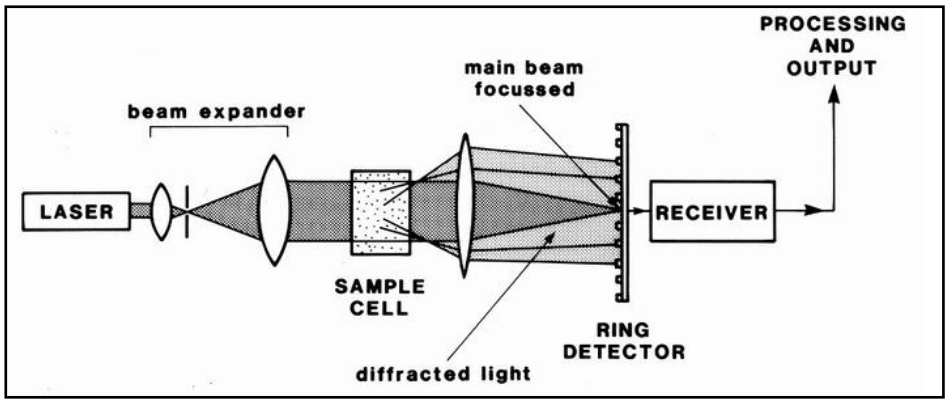


Figure 3.10 - Schematic diagram of the laser particle analyser


Figure 3.11 - Horiba LA-920 Laser Particle Size Distribution Analyser

### 3.5.1 Sample Preparation

A 0.1g sample of phosphor was ultrasonically dispersed in ethanol to create a weak solution. The solution was then transferred to the analyser and ultra-sonicated again. The program was then set and the solution passed through the laser and a spectrum of the particle size was output.

## 3.6 Transmission Electron Microscopy

For the Transmission Electron Microscopy (TEM) images, the microscope used was a JEOL JEM 2000 FX. The layout of a TEM is much like an optical microscope. At the top of the vacuum chamber sits a high voltage electron gun which generates a beam of electrons down the column through the sample. As it travels the electrons pass through a series of lenses which focus the beam through the sample and onto a phosphor screen below. The lenses can be used to change the image.

### 3.6.1 The Electron Gun

The electron gun is made up of lanthanum hexa-boride filament which can be operated at up to 200kV. The filament is superheated by an electric current to higher than the materials work function (around 2.5eV). The crystal then emits electrons which have a Boltzmann energy distribution. These then need to be focussed into a tight beam and then sent down the column towards the sample.

### 3.6.2 The Lenses and Apertures

The first of the electromagnetic lens (Figure 3.12) the beam passes though is the condenser lens. This lens determines the spot size of the beam on the sample. The beam then travels through the condenser aperture which condenses and maintains the beam at a certain size. The beam then travels through the sample and then hits the objective lens which magnifies and focuses the image. The beam then goes through the objective aperture which controls the contrast of the image and finally through the projector lenses which then increase the magnification further. The beam then hits a phosphor screen or electronic detector which then lets a user view their sample.

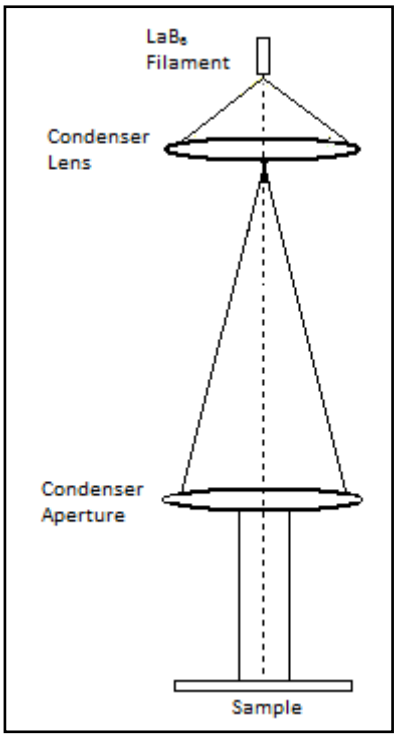


Figure 3.12 - TEM lens diagram

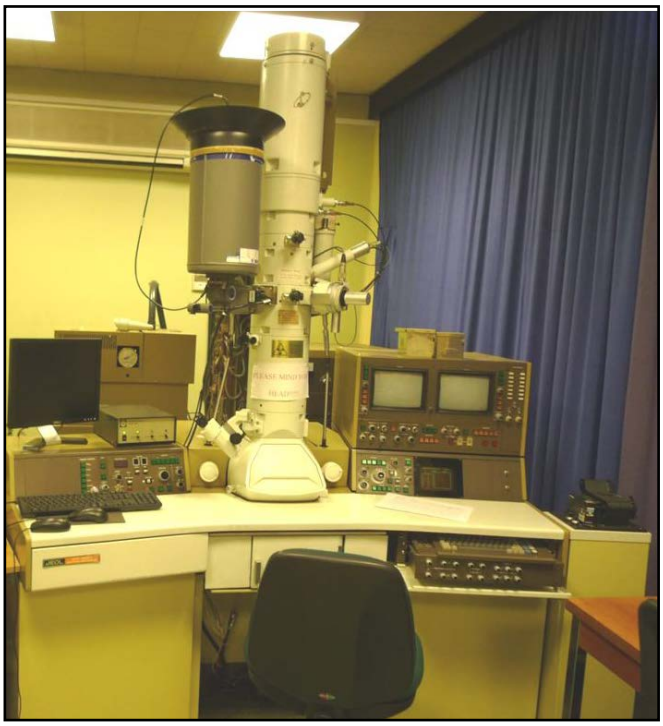

Figure 3.13 - JEOL JEM-2000FX Transmission Electron Microscope

### 3.6.3 Sample preparation

A very small sample of the phosphor was added to an amount of isopropyl alcohol (IPA). This was then ultra-sonicated for 10 minutes to fully disperse the phosphor in the alcohol. A drop of solution was then added to a carbon coated copper grid and left to dry in an oven. Once the sample was dry it was transferred to a sample probe and inserted into the microscope.

## 3.7 Scanning Electron Microscopy

All Scanning Electron Microscopy (SEM) images were taken using a Zeiss Supra 35VP. The working of an SEM is very much like the top half of a TEM. A beam from a field emission electron gun passes through a set of lens and apertures and then hits the sample. The beam knocks an electron from the surface of a sample which is then detected by a secondary electron detector inside the sample chamber. There is also an X-ray detector for the detection of X-rays for Energy Dispersive X-Ray (EDX) analysis.


Figure 3.14 - ZEISS SUPRA 35 VP Scanning Electron Microscope

### 3.7.1 Sample preparation

For uncoated phosphor powders a small sample was added to isopropyl alcohol (IPA) and ultra-sonicated for ten minutes to fully disperse the powder. An aluminium stub was also sanded to a smooth and shiny surface and fully cleaned to remove any contamination with ethanol. A drop of the IPA solution was added to the stub which was then left to dry for 10 minutes in an oven to give a thin phosphor layer. The sample was then ready for analysis.

For coated and modified samples the powders were again dispersed in IPA and after ultra-sonication a drop was added to a smoothed cleaned aluminium stub. Due to the insulating effect of the silica coating the stub was then placed into a sputter coater and coated with gold. This was then transferred to the stage ready for analysis.

To view the phosphor dusted fingerprints, a silicon wafer was cut up and attached to an aluminium stub with carbon adhesive tape. A fingerprint was then placed on the wafer after the finger was washed with ethanol. The wafer was then dusted with the phosphor powder and then excess removed before being placed on the stage ready for observation.

The results of the studies on the materials explained in this chapter will be reported and discussed in the next chapters.

# Chapter 4 – Luminescent Studies of RE Doped Phosphors

## 4.1 Introduction

For years these rare earth doped phosphors have been used in display technologies and their properties are well recorded [6, 86, 114-128]. These nanophosphors have not been used as a dusting powder before and because of this a few different versions were produced using different synthesis methods and rare earth element dopants. These have been previously reported in Chapter 2 and will be analysed and the coatings and modifications presented. To be used as a fingerprint powder the phosphors need to be produced at a uniform shape and size. If the particles differ in either of these values then the detail in the developed print might not be easily distinguished. The synthesis routes also need to be easy to upscale to produce large amounts of the phosphor. Likewise the coating and modification process needs to give a thin even coating which will not quench the fluorescence.

## 4.2 Analysis of $Y_2O_3$:Eu and $Y_2O_3$:Tb phosphors

$Y_2O_3$:Eu phosphors were first synthesised by the homogeneous precipitation method. The hydroxycarbonate precursor particles precipitated out of solution and were then sintered at 1000$^{o}$C for 6 hours to produce the phosphor. The particles were analysed by SEM and shown to have a uniform spherical structure of approximately 250-300nm as shown in Figure 4.1. It was observed that after the sintering process had finished the particles had formed large clusters. To try and break these apart into smaller clusters or single particles the powder was dispersed in ethanol and vibrated in an ultrasonic bath. The particles were then analysed on the laser particle analyser to examine whether the vibrational effect of the ultrasonic bath had any effect.

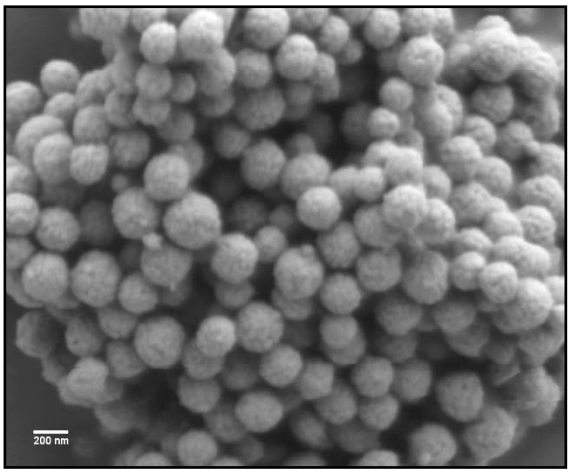


Figure 4.1 - SEM of $Y_2O_3$:Eu particles

Figure 4.2 displays the results from after the ultrasonic test took place. The LPA showed a median particle size of around 4-5µm. At close to 100 µm an anomalous reading was noted but this was not noted in further studies with the particles. To try and improve on the size the sample was replaced in the ultrasonic bath and subjected to further vibration. After further analysis no further breaking of the agglomeration was noted.

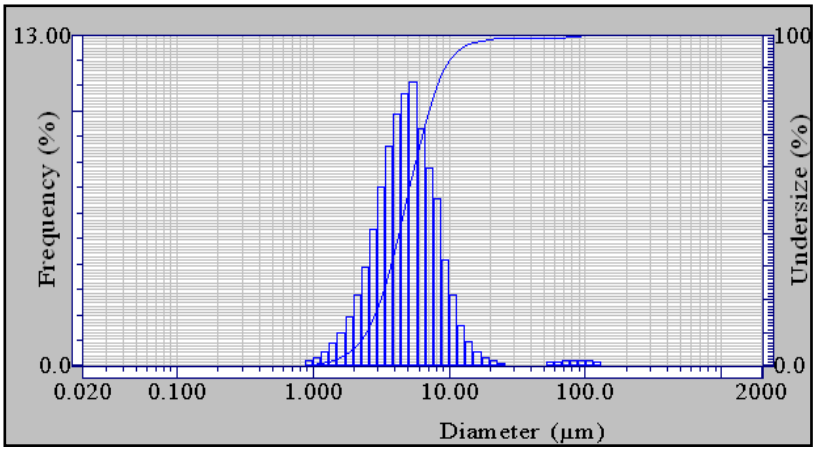


Figure 4.2 - LPA of $Y_2O_3$:Eu particles synthesised by homogeneous precipitation

Particles of $Y_2O_3$:Tb were also synthesised using the routes shown in 2.3.3. Using SEM and the laser particle analyser the particles were found to be approximately 250-300nm as shown in Figure 4.3 and had a particle distribution relatively similar

to that of the $Y_2O_3$:Eu particles of around 4µm after ultra-sonication. Techniques to reduce the clustering effects of the particles were examined to improve the definition detail for when the powder is dusted on a latent fingerprint. These are described later in Chapter 4.5.

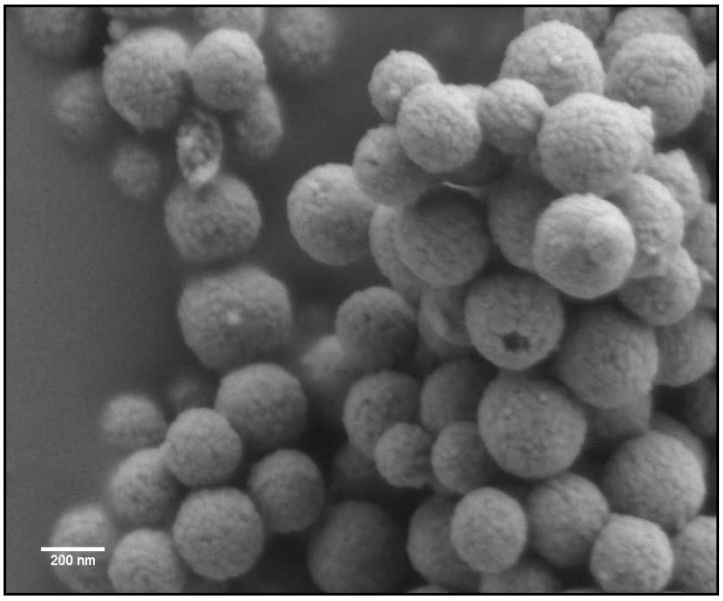


Figure 4.3 - SEM of $Y_2O_3$:Tb particles synthesised by homogenous precipitation

Phosphors of $Y_2O_3$:Tb were also synthesised using the solid state method presented in 2.2.2. These particles were found to have much larger and less uniform structure as presented in Figure 4.4. Due to the non-uniformity the particles were shown to be over 2µm in diameter but these particles agglomerated into much larger clusters of over 10µm in size. Dispersing the powder in ethanol and vibrating in an ultrasonic bath did help break apart the agglomerations, but wasn't able to modify the size distribution due to the high number of 10µm+ particles. These solid state particles were broken down in a pestle and mortar to try to reduce to the particle size further but the size distribution was approximately the same after this period. These particles weren't taken forward to be used as a dusting powder because the sheer size differences between the particle clusters would severely reduce any detail or definition in the fingerprints dusted with this new powder. This would make it harder to distinguish any relevant features when making a comparison.

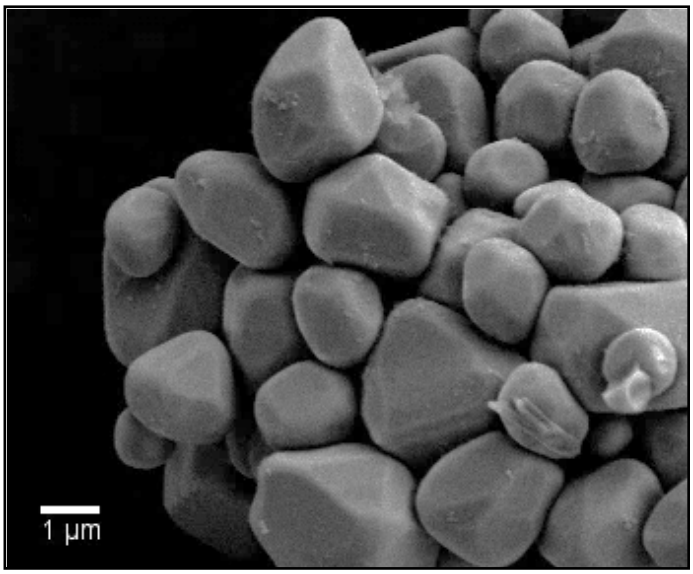


Figure 4.4 - SEM of $Y_2O_3$:Tb synthesised by solid state synthesis

Particles of $Y_2O_3$:Eu and $Y_2O_3$:Tb were analysed on the Bentham photoluminescent spectrometer. The results shown in Figure 4.5 show a maximum emission point of 611nm with an excitation wavelength of 254nm. The paper by Silver et al [118] concurred with this result giving a "very very strong" emission at 611.1nm. This emission is due to the electric dipole transition of $^5D_0 \rightarrow {}^7F_2$.

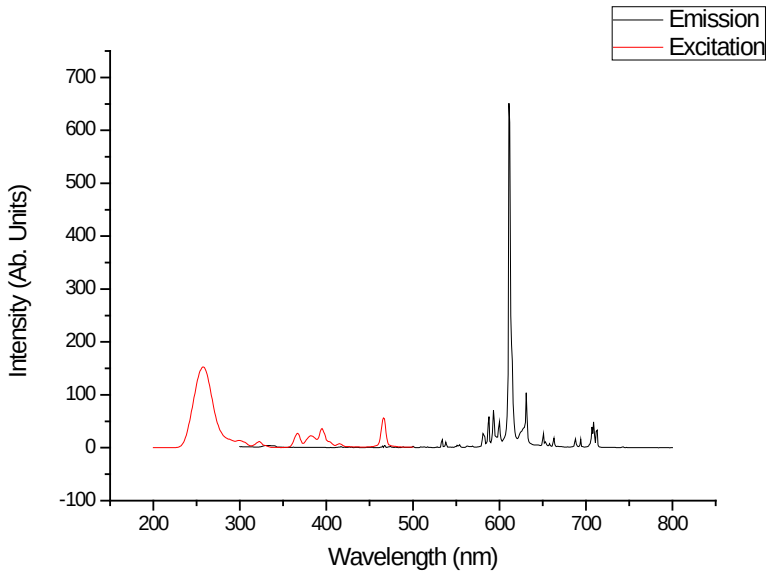


Figure 4.5 - Luminescent spectra of $Y_2O_3$:Eu phosphors

$Y_2O_3$:Tb phosphors showed a maximum emission point of 545nm with an excitation of 273nm (Figure 4.6) The main emission transitions are the $^5D_4 \rightarrow {}^7F_J$ (J= 6, 5, 4, 3) due to the electric dipole transition of the $Tb^{3+}$ ions at $^5D_4 \rightarrow {}^7F_6$ (490nm), $^5D_4 \rightarrow {}^7F_5$ (545nm), $^5D_4 \rightarrow {}^7F_4$ (587nm), $^5D_4 \rightarrow {}^7F_3$ (619nm) with the $^5D_4 \rightarrow {}^7F_5$ being the most intense all which were confirmed by Cho et al[129] and Muenchausen et al[130].

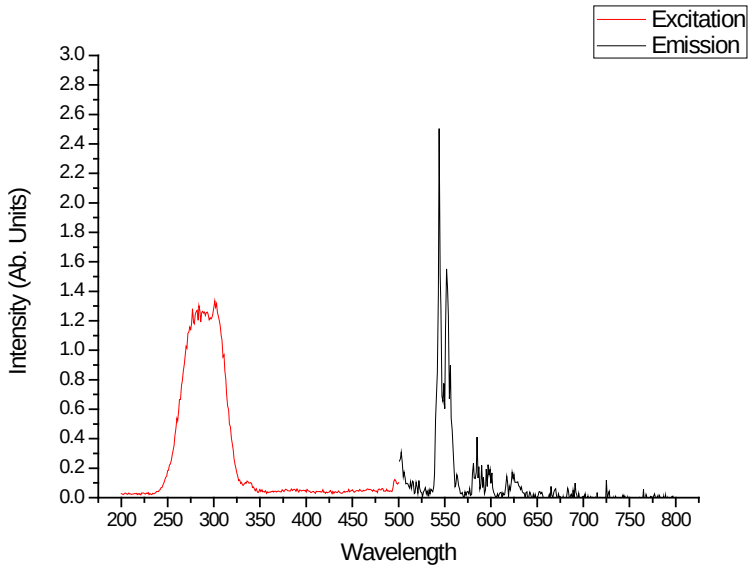


Figure 4.6 - Luminescent spectra of $Y_2O_3$:Tb phosphors

## 4.3 Analysis of $YVO_4$:Eu phosphors

$YVO_4$:Eu was synthesised using homogeneous and solid state methods. Both methods were picked to examine the differences between phosphors created using each technique. The first set of particles were synthesised by the solid state method. These particles were shown to be non-uniform and extremely varied in size. The SEM image in Figure 4.7 shows the differences in the sizes of the phosphors range from 2µm to over 20µm.

These sizes were confirmed by the laser particle analyser shown in Figure 4.8 as well as showing the particles cluster to create agglomerations of over 100 µm. These large particles weren't taken forward for testing on latent fingerprints as all definition would be lost in the print using a large powder.

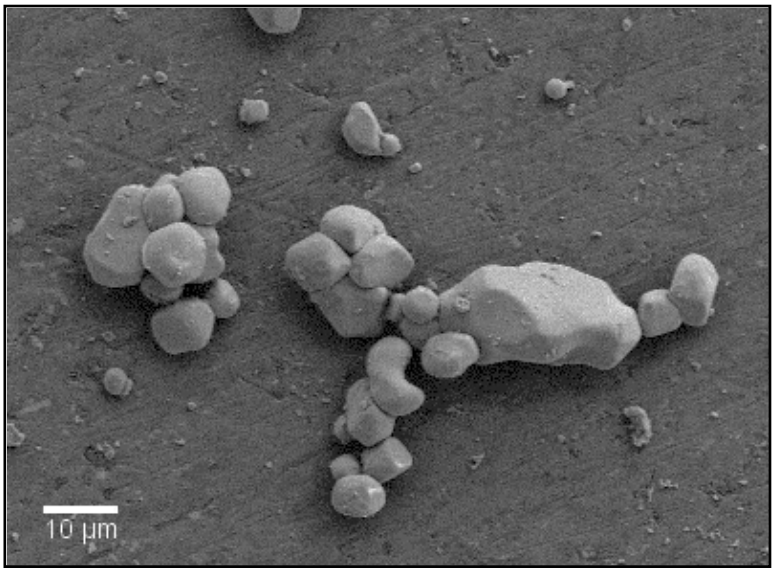


Figure 4.7 - SEM of $YVO_4$:Eu synthesised by solid state process

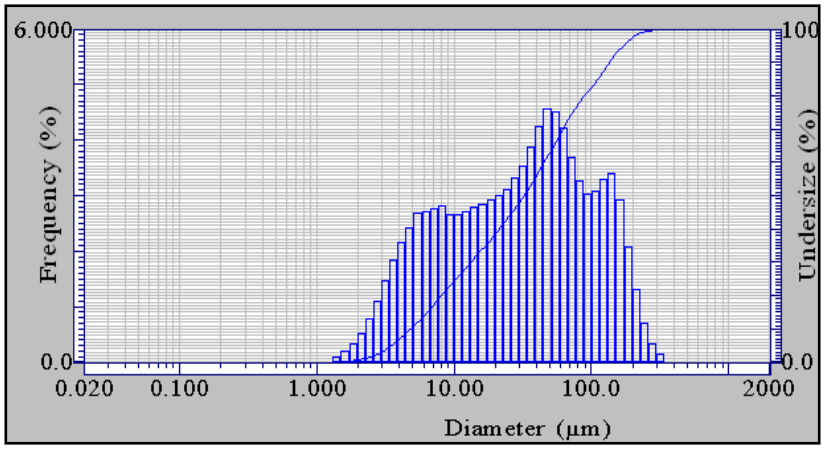


Figure 4.8 - Laser particle analysis of $YVO_4$:Eu particles

The particles created using the homogeneous precipitation method (Figure 4.9) showed a much smaller particle size than using the solid state synthesis method. Figure 4.9 demonstrates the particle size ranges between 1-2 µm but does also display the size of the agglomerations synthesised using this technique. Figure 4.10 displays an EDX spectra of the $YVO_4$:Eu particles which is also confirmed by Xiu et al [131].

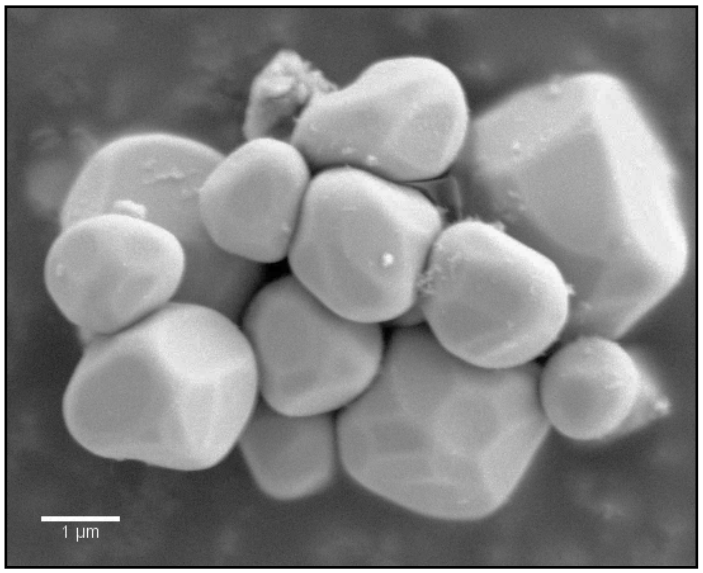


Figure 4.9 - SEM image of $YVO_4$:Eu synthesised by homogeneous precipitation

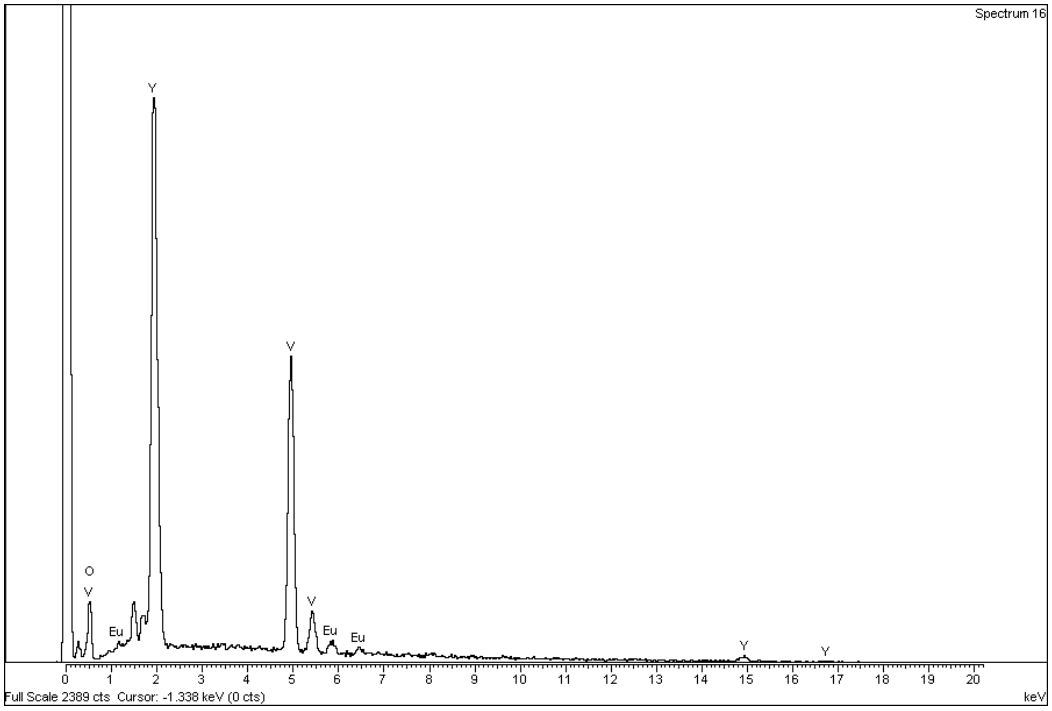


Figure 4.10 - EDX spectrum of $YVO_4$:Eu

## 4.4 Analysis of $Y_2O_2S$:Eu and $Y_2O_2S$:Tb

Particles of $Y_2O_2S$:Eu and $Y_2O_2S$:Tb were synthesised using the homogeneous precipitation method shown in 2.3.4 and prepared previously by this department [132]. The hydroxycarbonate precursors produced in 2.3.3 were firstly mixed with sodium carbonate and sulphur before being transferred into a crucible. A top layer of material was then added using molar ratios of yttria, sodium carbonate and sulphur to create a seal and not allow oxygen into the mixture. This was then sintered at 1000$^{o}$C for 6 hours. After firing the top layer was removed and the bottom layer was boiled in DI water for 20 minutes. The soft white phosphor powder was subsequently dried and analysed.

The particles of $Y_2O_2S$:Tb (Figure 4.11) displayed a small but non-uniform shape and size between 50-300nm. The particles were also shown to be rather agglomerated even after multiple sessions in an ultra-sonic bath. An EDX analysis (Figure 4.12) of $Y_2O_2S$:Tb phosphors demonstrates correct elemental composition as identified by Giakoumakis et al[133] but also includes an aluminium peak due to the composition of the stub used for the analysis.

$Y_2O_2S$:Tb and $Y_2O_2S$:Eu were analysed using the Bentham photoluminescent spectrometer and the emission and excitation spectra are shown in

Figure 4.13 and Figure 4.14 respectively. The spectra were compared and confirmed against the work of multiple sources[86, 129, 133-141]. The main emission peak in the $Y_2O_2S$:Eu was observed to be at 625nm due to the $^5D_0 \rightarrow {}^7F_2$ transition[129]. The main emission peak for the synthesised $Y_2O_2S$:Tb phosphors was observed at 550nm due to the $^5D_4 \rightarrow {}^7F_5$ transition[140].

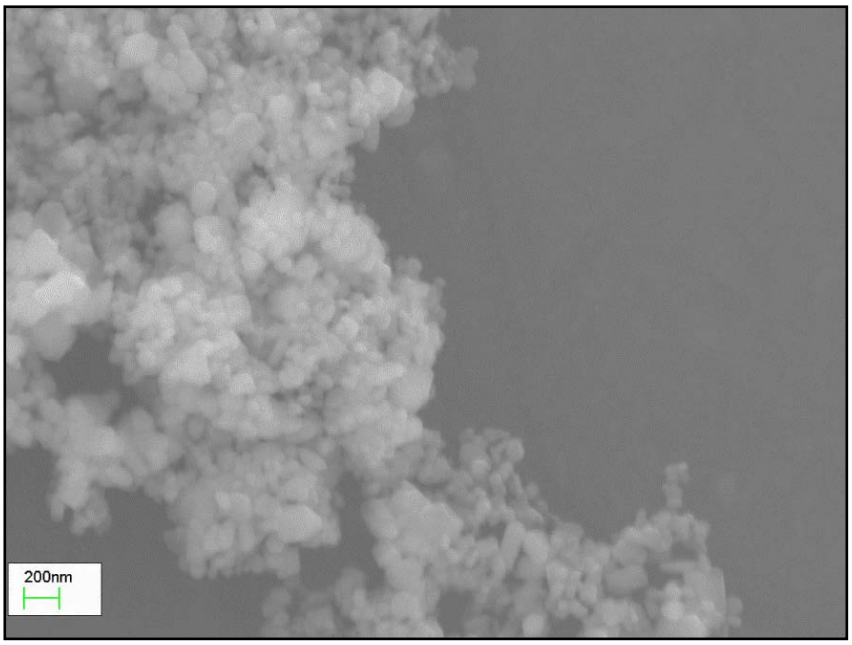


Figure 4.11 - SEM image of $Y_2O_2S$:Tb

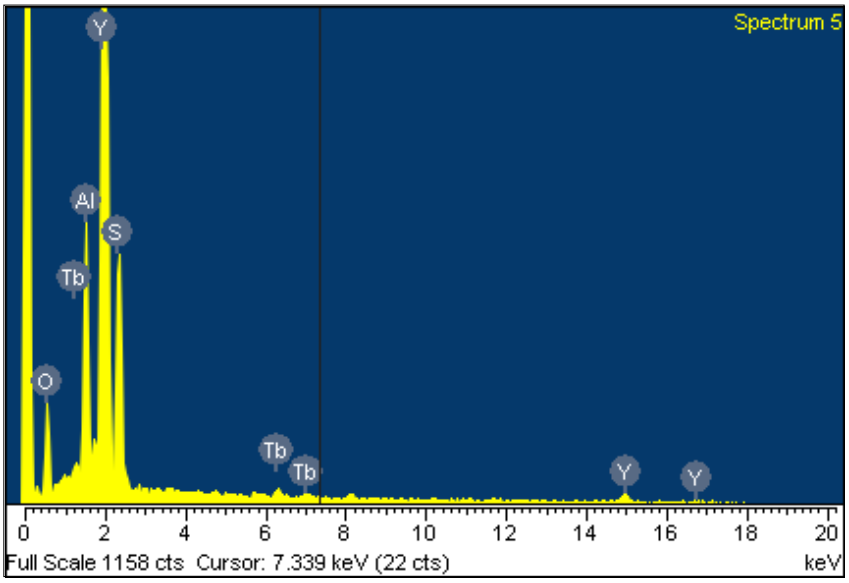


Figure 4.12 - EDX Analysis of $Y_2O_2S$:Tb

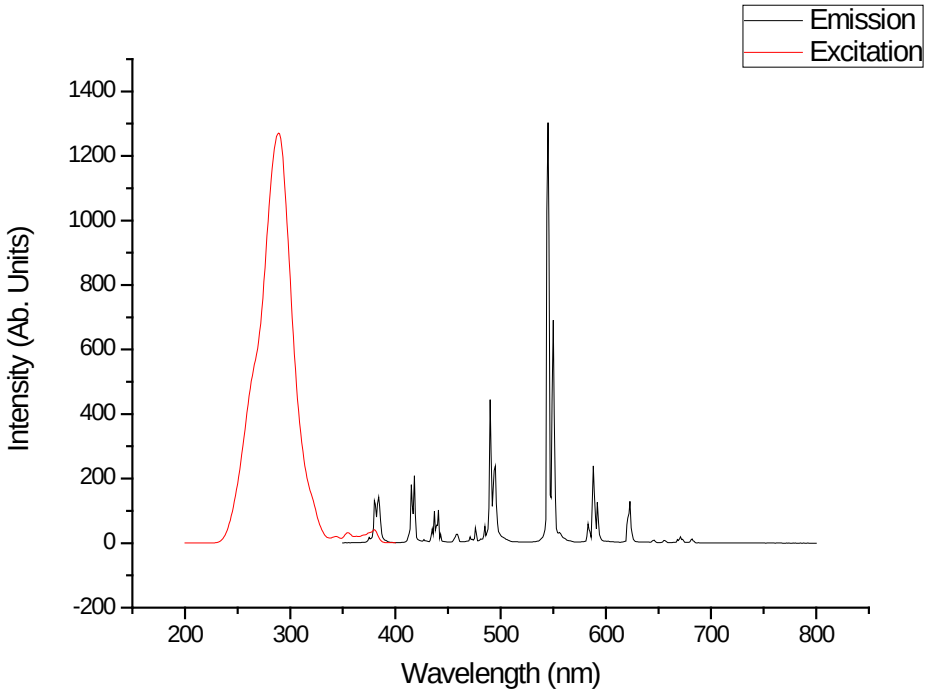


Figure 4.13 - Luminescent spectrum of $Y_2O_2S$:Tb

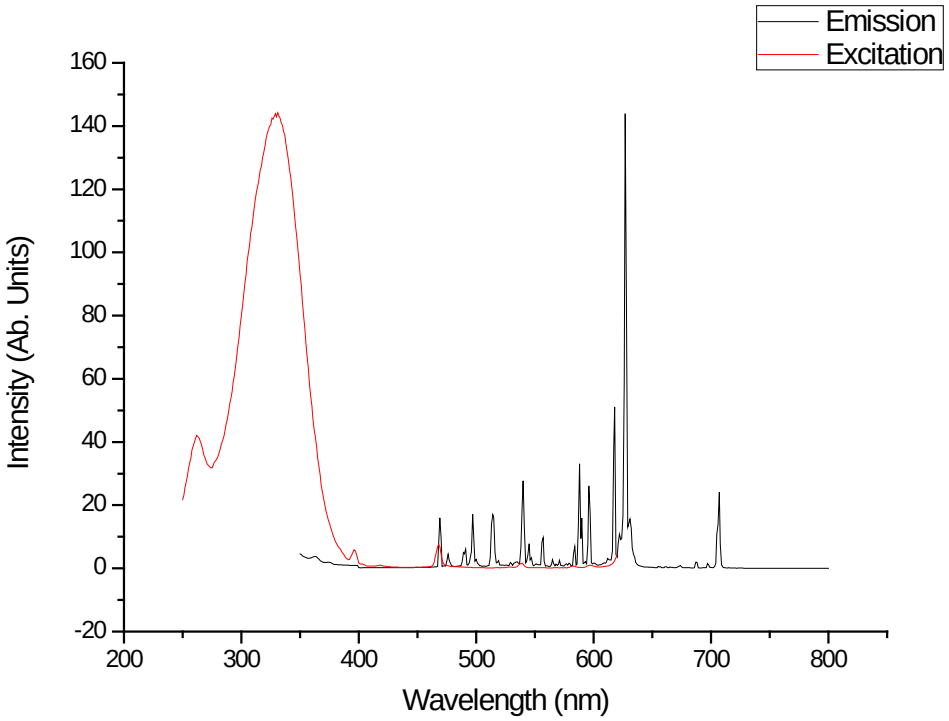


Figure 4.14 - Luminescent spectrum of $Y_2O_2S$:Eu

## 4.5 Coating Analysis

The coating of phosphors in $SiO_2$ served two purposes. The first was to minimise the agglomeration during the firing process. The phosphor precursors were coated with silica before being fired and then subsequently etched. The etching process was carried out using concentrated NaOH to break apart particles which may have fused together. It also allowed for the phosphor to be easily modified with other compounds by bonding them to the silica on the surface. To this end, two different methods were chosen to be studied. The first was a modified version of the Stöber method[142-147] in which an intermediate group of the ethoxy groups of Tetraethyl orthosilicate (TEOS) dispersed in water with ethanol was created, catalysed by the ammonia (Figure 4.15). Immediately following this a condensation reaction takes place either between an ethoxy group of another TEOS molecule or by the hydroxyl group of another intermediate to form the $SiO_2$ which encapsulates the phosphor. The quantities of ammonia and $H_2O$ were adjusted to ensure a good coating was achieved.

$$Si(OC_2H_5)_4 + xH_2O \rightarrow Si(OC_2H_5)_{4-x}(OH)_x + xC_2H_5OH$$

$$Si(OC_2H_5)_{4-x}(OH)_x + OH - Si \rightarrow Si - O - Si + C_2H_5OH$$

Or

$$Si - OH + HO - Si \rightarrow Si - O - Si + H_2O$$

Figure 4.15 - $SiO_2$ condensation reaction

The use of LUDOX, a Sigma Aldrich colloidal silica dispersion, to coat the particles was carried out to analyse a possible faster and more straightforward coating process. The addition of the colloidal LUDOX to the dispersed particles creates a heterocoagulation reaction allowing the silica to be adsorbed electrically onto the phosphor surface.

The differences between particles coated with LUDOX and TEOS was very noticeable. LUDOX coated particles were found to not be uniformly coated with silica but were covered in nanosized silica spherical balls as shown in Figure 4.17 which, even after many washes, still remained due to the bonding to the surface layers. Although this structure was not as uniform as anticipated, the particles were fired and then etched to assess the agglomeration reduction potential. The Stöber processed particles were found to show a much more uniform coating on the surface which could be modified in diameter depending on the quantities of the reactants used. A coating width of approximately 100nm (Figure 4.18) was created and chosen for subsequent experiments. After imaging of the coated phosphors was completed an EDX elemental spectra was acquired of a $Y_2O_3$:Eu phosphor coated using the Stöber process (Figure 4.16). This analysis was compared to the work of Abe et al[148] and presented the Y, O and Eu peaks of the phosphor along with the Si of the coating and an Al peak from the stub used to hold the phosphor.

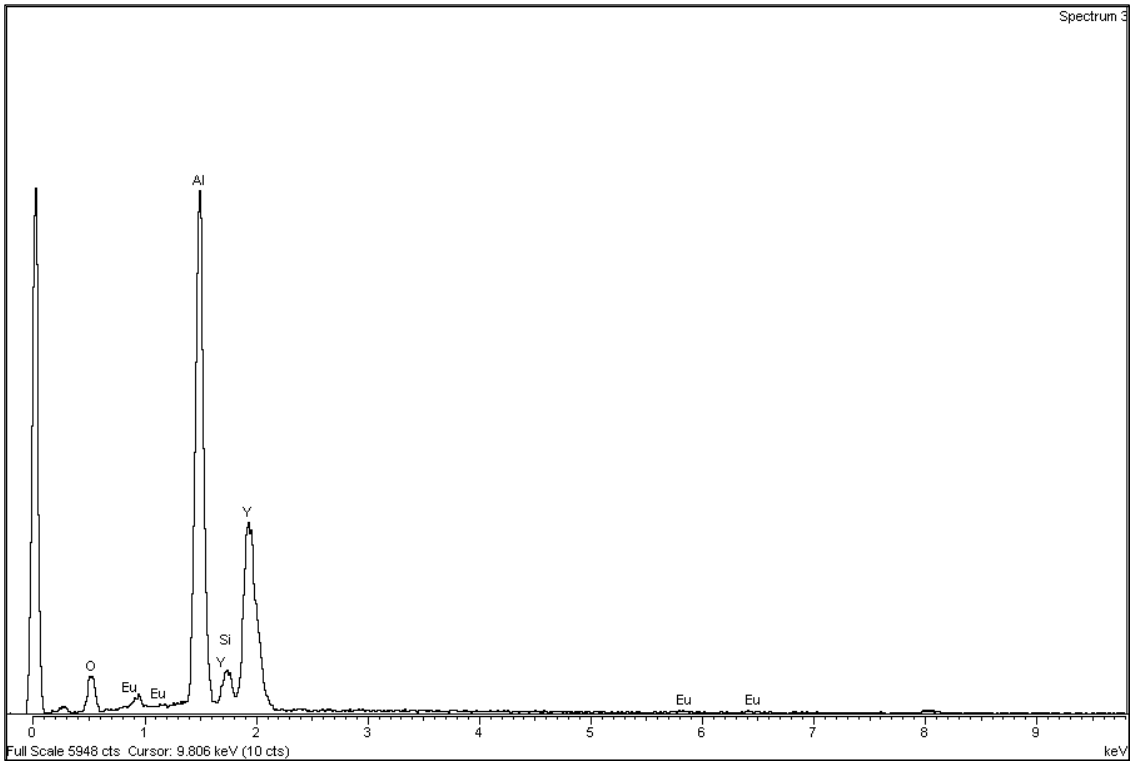


Figure 4.16 - EDX of silica coated $Y_2O_3$:Eu particles

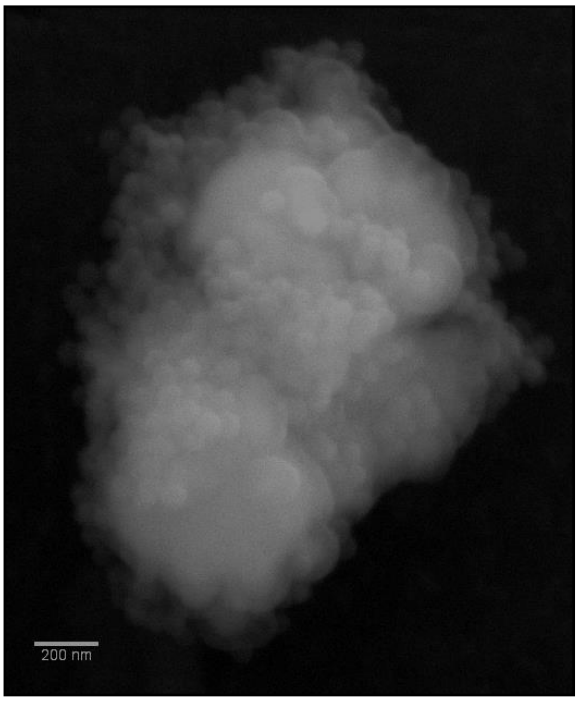


Figure 4.17 - LUDOX coated $Y_2O_3$:Eu particles

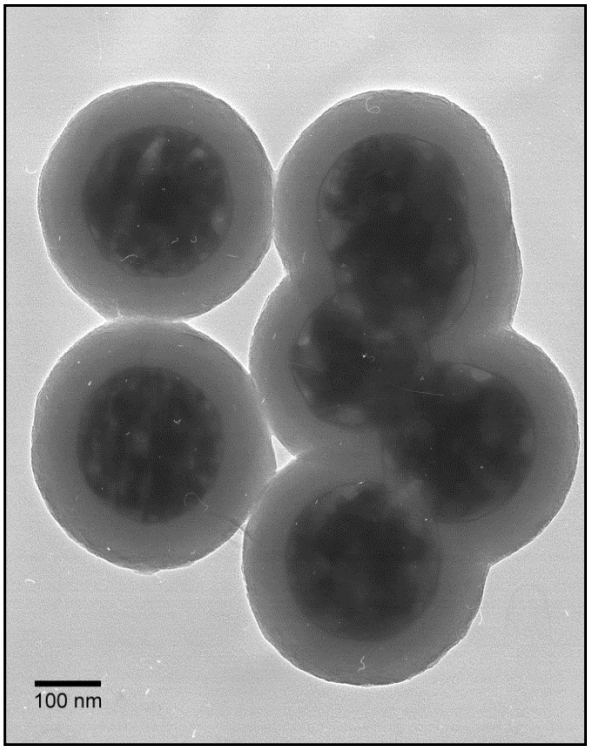


Figure 4.18 - SEM image of TEOS coated $Y_2O_3$:Eu particles

## 4.6 Etching of $SiO_2$ Coating

Etching studies using NaOH were performed to try and decrease the $SiO_2$ around the particles to reduce the quenching effect. Although many methods are available for etching of the silica[149-154] The NaOH method was chosen due it being the easiest to upscale. The methods are well documented by others[99]. They were performed to try and break down agglomerates that may have formed during the firing process as well as to allow for maximum luminescence from the phosphor[155].

The etching process was carried out using the method described in 2.6 by dispersing the particles in a concentrated solution of NaOH (4M). The samples were left stirring in NaOH for 24 hours and after centrifuging were imaged by SEM. The process was then continued until the silica shells were thinner and the excess silica particles were etched away.

The etching of the LUDOX coated particles occurred much faster than the TEOS coated and to a much greater extent. 24 hours after etching showed a small change in the spherical silica spheres around the particles (Figure 4.19). After 48 hours there had been a dramatic change in the coating as well as with the excess particles. The particles showed a removal of the coating and with subsequent analysis the LUDOX process was found to give a non-uniform coating once the excess particles had been removed. Due to this the LUDOX coating process was not used when testing the phosphors on fingerprints.

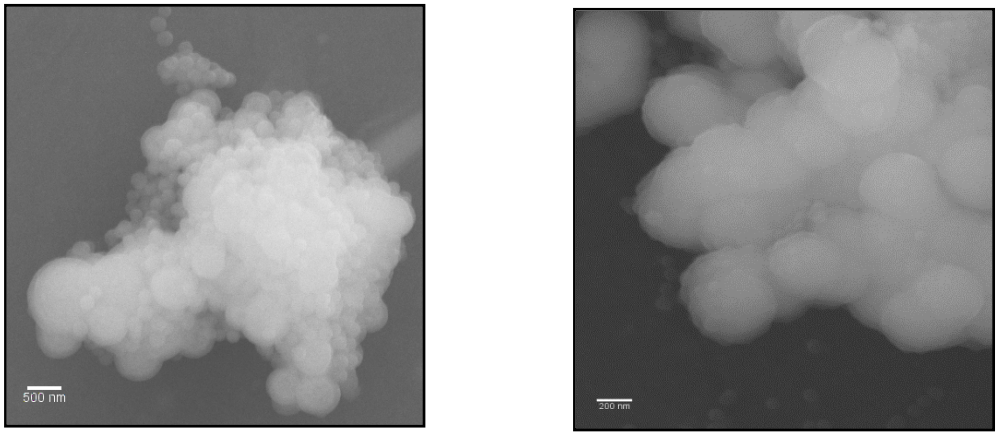


Figure 4.19 - LUDOX coated $Y_2O_3$:Eu after 24 hours (l) and 48 hours (r)

The TEOS samples showed a much more stable etching. After 24 hours the coating had reduced in size by a small amount and there was an increase in quantity of single particles on the stub. Figure 4.20 shows that although some of the coatings were still in the range of 100nm more single particles were noticeable under the microscope. After leaving the etching process for another day the coatings were down to approximately 60nm in width and there were many more free particles in the solution (Figure 4.21).

A sample of pre etched and post etched TEOS coated particles were analysed to examine the difference the etching process has on the agglomeration of particles using the laser particle analyser. Figure 4.22 illustrates that the coating of the particles firstly increases the agglomeration compared with a completely uncoated surface shown earlier (Figure 4.2). Once etching has taken place further analysis (Figure 4.23) demonstrates a decrease in size of these clusters to levels around an uncoated phosphor sample.

These studies show a success in the etching process to reduce the coating of the phosphors as well as keeping the level of agglomeration to a level consistent with an uncoated phosphor powder.

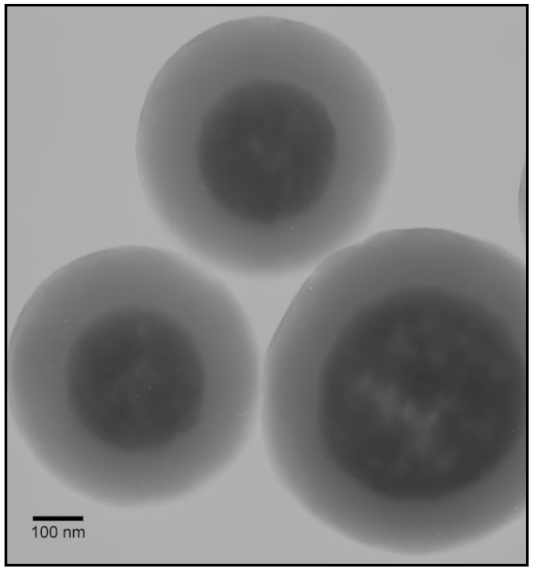


Figure 4.20 - TEM micrograph of TEOS coated particles after 24 hours

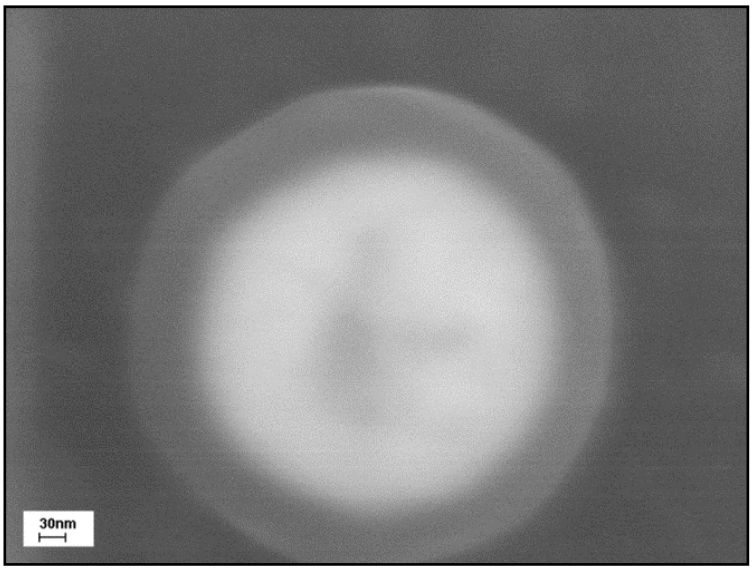


Figure 4.21 - SEM micrograph of TEOS coated particle after 48 hours

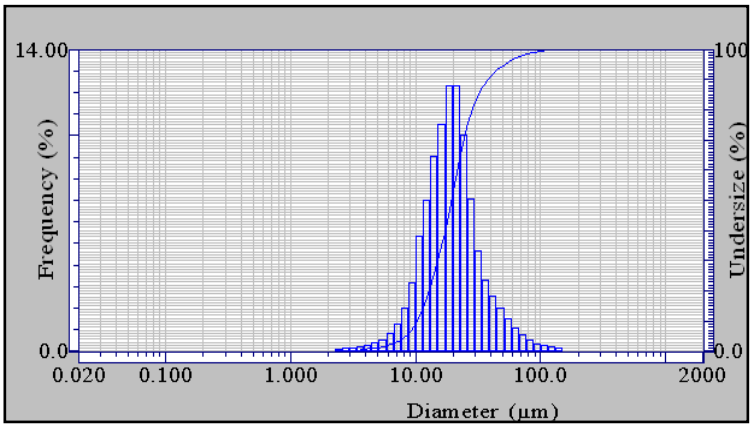


Figure 4.22 - Laser particle analysis of $Y_2O_3$:Eu before etching

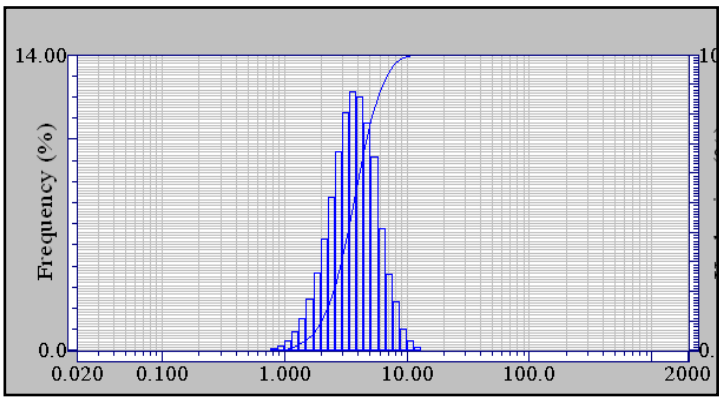


Figure 4.23 - Laser particle analysis of $Y_2O_3$:Eu after etching

## 4.7 Luminescence Intensity of Coated Phosphors

The luminescence potential of the particles was analysed using the Bentham spectrometer to examine whether the coating of the particles had any effect on the luminescent intensity. The samples were tested at an excitation wavelength of 254nm. To allow slight quantification when comparing the three samples; 0.1g of each phosphor sample was measured out and flattened into a small aluminium disks. These samples consisted of an uncoated, coated and etched quantity of $Y_2O_3$:Eu particles. Figure 4.24 showed that the coated phosphor still gave an intense emission at 612nmn and that the etching of the particles increased the intensity to levels on par with the uncoated phosphor.

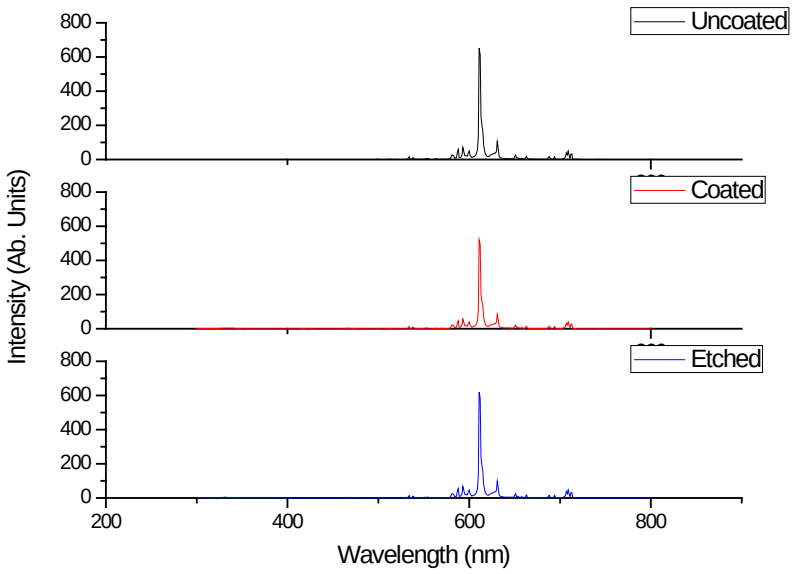


Figure 4.24 - Comparison of luminescent intensity of $Y_2O_3$:Eu

## 4.8 Modifications of Coated Phosphors with Functional Groups

The modification of the coated and etched phosphor particles were carried out using the methods shown in section 2.5. The modifications were included to allow testing of whether functional groups have an effect on adherence to latent fingerprints.

## 4.8.1 (3-aminopropyl) trimethoxysilane modified phosphors

The coated phosphors were dispersed in ethanol and a quantity of APTMS added to the solution and this was then left stirring for 48 hours. The APTMS hydrolysed in the solution and condensation reaction with the $SiO_2$ took place adding an aminopropyl silane to the surface of the coated phosphor as shown in section 2.5.1[156, 157].

The solution was washed and centrifuged multiple times with the resulting particles analysed for the presence of the modification. The powders were analysed using Raman spectroscopy.

Figure 4.25 shows the Raman spectra of the uncoated phosphor and APTMS modified silica coated phosphor taken with an excitation wavelength of 632nm. A strong Raman band at 377 $cm^{-1}$ appears due to the cubic phase of $Y_2O_3$:Eu, along with emission bands due to $Eu^{3+}$ in the 600-2500 $cm^{-1}$ region. The APTMS modified silica coated phosphor exhibits a broad Raman band due to C-H stretching vibrations in the 2800-3000 $cm^{-1}$ region that is not evident in the uncoated phosphor. These bands have been increased in intensity to show the difference between the two powders.

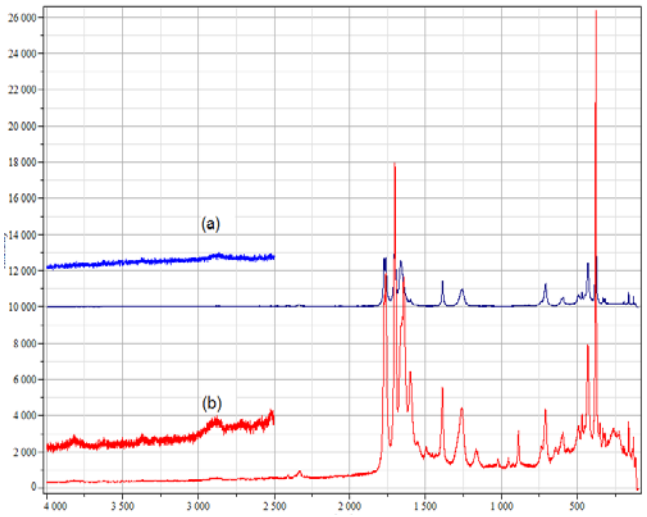


Figure 4.25 - Raman spectrum of $Y_2O_3$:Eu (a) and $Y_2O_3$:Eu with APTMS (b)

### 4.8.2 Triethoxy(octyl)silane modified phosphors

The modification of the silica surface with triethoxy(octyl)silane allowed for the addition of long chained hydrocarbons (LCH) as shown in section 2.5.2. It was hypothesised that modifications to the phosphor with these compounds would allow for the particles to enhance the appearance of older prints as well as more sebaceous fingerprints due to the increase of oils.

The silica coated particles were dispersed in ethanol and a quantity of triethoxy(octyl)silane was added to the solution. The resulting reaction like 4.8.1 was a condensation polymerisation at the surface. The solution was set stirring and samples were removed from the solution every 24 hours. These samples were washed and centrifuged multiple times to clean the phosphor sample.

The samples were then analysed by IR spectroscopy to show how the surface modification changed over time. Over time there was a gradual increase in the bands between 2800cm$^{-1}$ and 3000cm$^{-1}$ which is due to an alkyl absorption[156, 157]. As Figure 4.26 and Figure 4.27 show, there is an increase in the alkyl band up to a coating time of 96 hours when the surface is either saturated with alkyl groups or there was no more APTMS left in solution.

The majority of this work was published for the International Conference on Raman Spectroscopy in 2010. The full abstract and poster is presented in Appendix A Part 3.

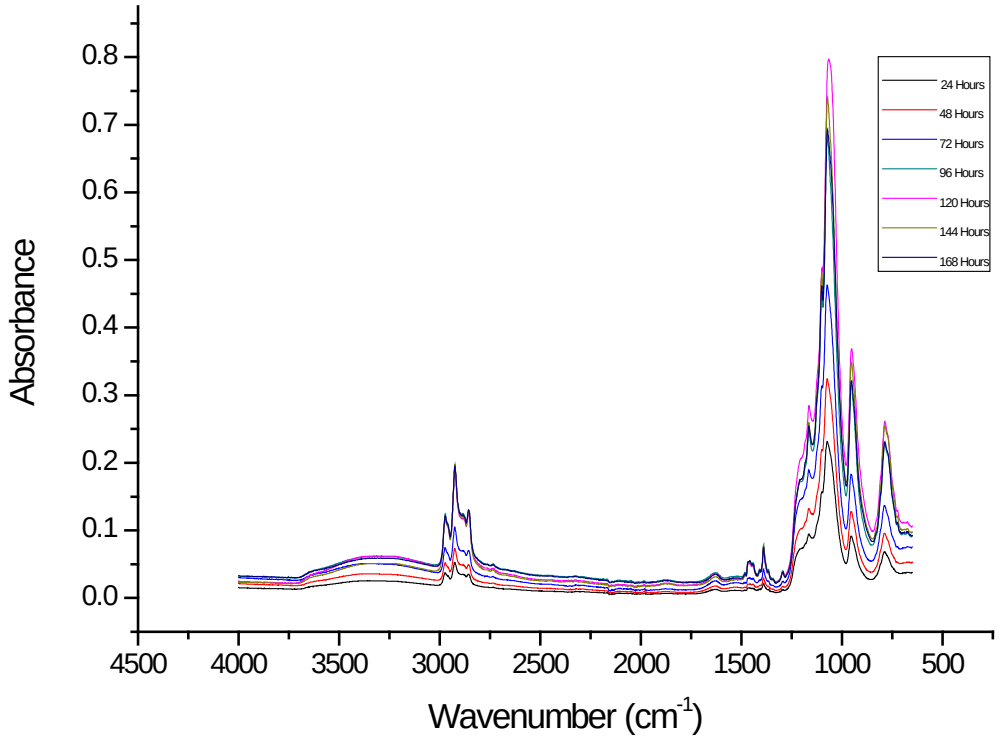


Figure 4.26 - IR spectra of modified $Y_2O_3$:Eu particles over time

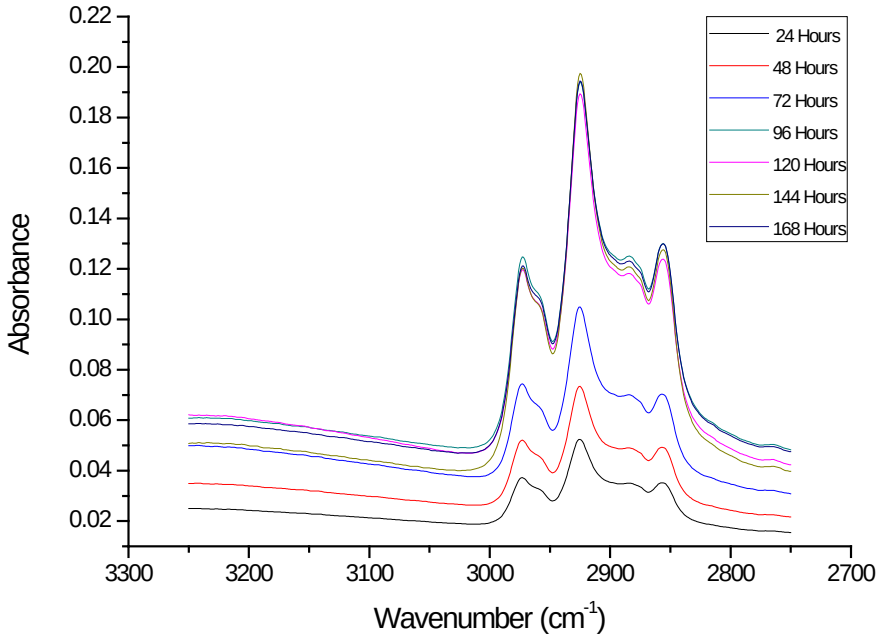


Figure 4.27 - Increase in the alkyl absorption band over time

# Chapter 5 – Latent Fingerprint Analysis

## 5.1 Introduction

To determine the ability of a phosphor powder to adhere to a latent fingerprint, tests were carried out using three commercial dusting powders. From the images and spectra obtained in Chapter 4 the $Y_2O_3$ phosphors were chosen to continue with the fingerprinting examinations. This was due to the fast synthesis, comparable size of particles to the commercial fingerprinting powders and the intensity of the luminescence. The two commercial powders that were used for comparison are aluminium and a magnetic bichromate powder shown in Figure 5.1.

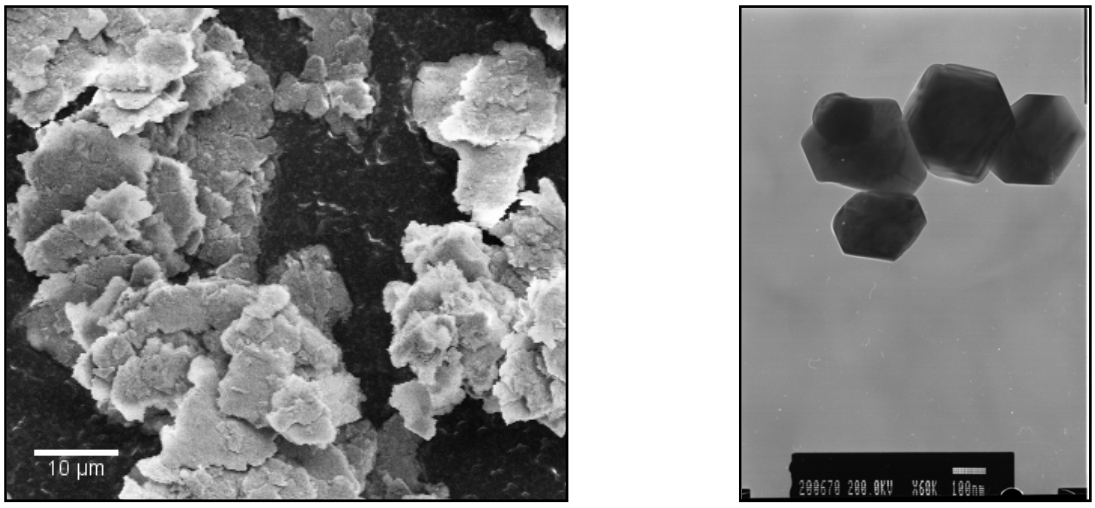


Figure 5.1 - SEM of Al powder (L) TEM of bichromate powder (R)

These powders were tested on a depletion series and compared with the phosphor powder. The phosphor and aluminium powders were dusted on the surface using a standard squirrel hair brush while the magnetic bichromate powder was brushed using a magnetic wand. A depletion series is made of 20 latent prints that are created one after another on a surface. This creates a set of prints with each having less residue deposited on the surface than the one before. As objects are touched the sweat does not get replaced quickly and therefore each placed fingerprint will have less material in it. Using this set of prints gives a good indication of how a

specific powder will function in a real world environment where the fingerprint left by a suspect may not always be fresh[158].

## 5.2 Depletion Series

Two sets of depletion series were created on a glass sheet to test the main different compositions. For the eccrine series, a finger was first washed in water and then ethanol to clean it of all oily impurities. A set of 20 prints were then made on the glass. For the sebaceous series, the print was cleaned as above then rubbed on the back of the neck and then rolled between fingers to make sure the oil for the sebaceous series is fairly distributed around the finger and another series was made. Although this is a subjective test a real sebaceous fingerprint would contain far more material as the finger wouldn't have been cleaned beforehand and the oils would not have been spread in such a way[159]. This demonstrates that these tests would give a much lower result than in a real situation.

The powders are then dusted onto the surface and analysed to see whether a workable print could be lifted. For the eccrine prints the APTMS modified phosphors were used due to the hydrophilic nature of their functional groups. The LCH modified phosphors were tested on the sebaceous prints.

### 5.2.1 Eccrine

The bichromate powder was tested first and showed up on 12 out of the 20 prints. Although by the end, of the noticeable prints the powder was almost unnoticeable and a lot of the time only a partial print was recognised. The aluminium powder gave a better result with a 15 print series and although, like the bichromate powder, the powder gave partial prints at the high levels, the parts of the print that were covered had a much larger coating. The phosphor dusted prints were able to be seen very well up to 13 prints with the naked eye, but with the use of a UV light these could be easily seen up to 17 partials.

### 5.2.2 Sebaceous

The use of LCH modified phosphor powders on the sebaceous depletion series gave very encouraging results and all 20 fingerprints were seen when UV light was used. The use of the phosphor powder was expected to give a better result due to the composition of oils in a fingerprint. The bichromate powder also displayed high definition when dusted on to the all 20 of the prints. The aluminium powder started off overdeveloping the prints which made them much less useful for analytical purposes by removing definition in the pores but after the $10^{th}$ print the definition had improved. Due to the excellent adherence of the sebaceous powders they were examined on aged prints.

## 5.3 Aged Print Analysis

A set of fingerprints were placed on glass slides and left at room temperature for one month. These prints were then dusted with phosphor powders to determine whether the powders would be able to visualise older, more decomposed latent fingerprints.

A fingerprint powder needs to have the capability to work on old prints just as well as on new prints. Some crime scenes are only found after a long period of time and to make sure that officers have a chance in catching whoever was responsible, the powders need to be able to attach to these old prints. When prints are first left on a surface they are made up of oils and sweat. As time goes on the moisture slowly evaporates leaving behind salts. Due to the nature of the oils they will last for much longer, and in the right conditions, they can last for years. To analyse the effect of time on the fingerprints, three separate sets were created and placed on glass and silicon wafers and then left for three different time periods. The creation of these prints were generated in the same way as in 5.2 except to encompass a full print rather than a particular composition after washing the finger was left to replenish before the prints were made. The prints were also created on silicon wafers for easy analysis by SEM after the powder has been deposited. These prints were then left in a wooden slide case. Once the time had come to test the print, it was

removed from the case and each powder was dusted over the print using a squirrel hair brush or magnetic wand. The prints were then photographed in natural light and also under 254nm. The samples were also imaged on the SEM.

### 5.3.1 Minutes old

Figure 5.2 and Figure 5.3 show that the phosphor powder dusted onto the fresh prints displayed great adherence. This was expected due to the photos taken of the depletion series. After the powder had been dusted on the surface the excess powder was removed by use of a small pressurised air can. After the phosphor was removed, the photos showed complete coverage of the ridges and the print was easily imaged under UV light as shown in Figure 5.5.

Figure 5.2 - Image of phosphor deposited on new print

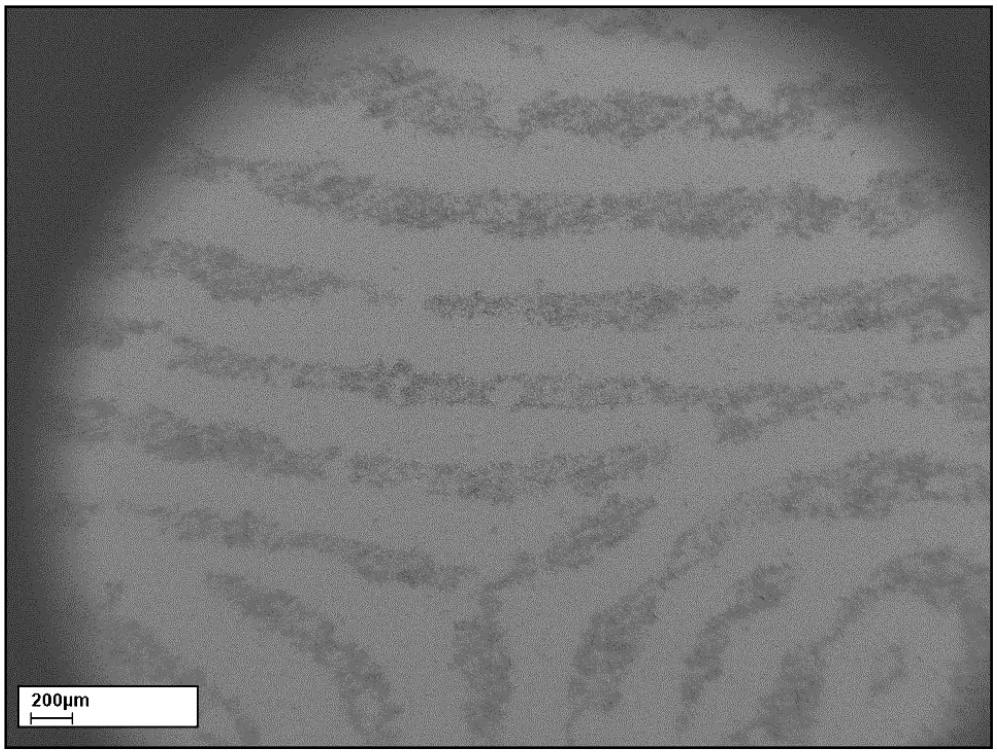


Figure 5.3 - SEM image of phosphor deposited on new print

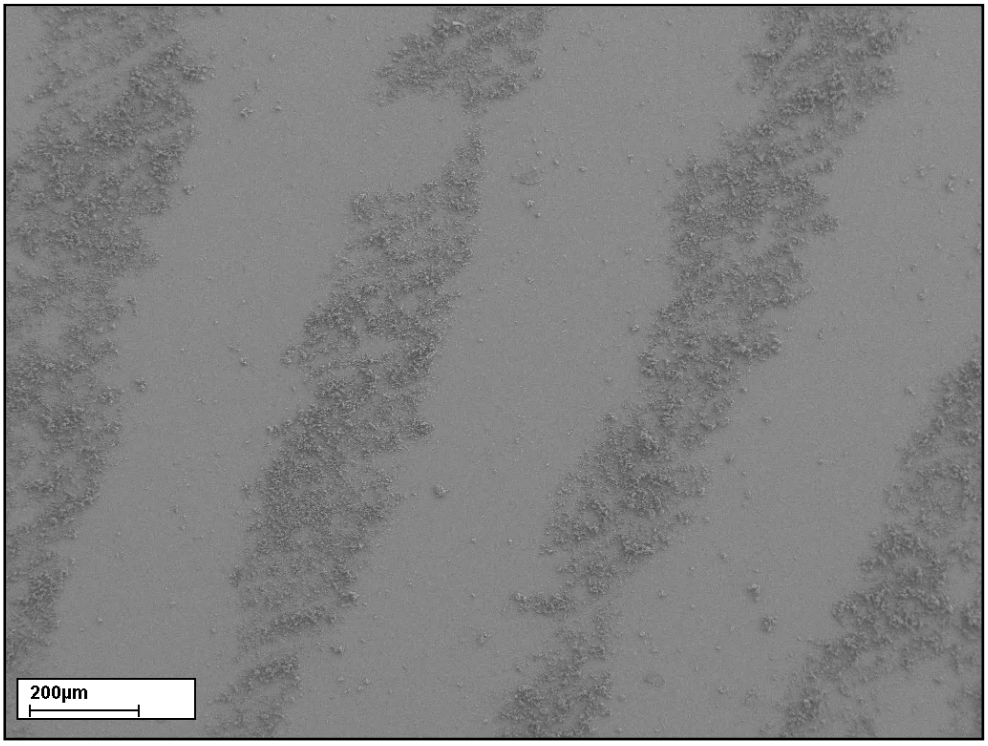


Figure 5.4 - Higher mag of phosphor deposition on new print

SEM images showed the ridges were covered with phosphor powder and the troughs were empty of powder. The aluminium and bichromate powders also gave a good adherence to these new prints. The aluminium powder very quickly over-developed the print which made it become useless for analysis.

Figure 5.5 - Coated fingerprint shown under 254nm UV light

### 5.3.2 Two weeks old

The two week old prints were dusted as above (5.3.1). No visible differences were noted after the excess powder had been removed. Both natural and UV photos showed clear differences between the troughs and ridges. When compared under SEM analysis Figure 5.3 showed a much larger concentration of phosphor on the surface than Figure 5.6. This was likely due to the evaporation of moisture from the fingerprint over the two week period. This can be demonstrated by the visible large crystals that had appeared in the print. After EDX analysis (Figure 5.10) these were found to be composed of sodium, calcium and chlorine. Comparison of Liu et al [160] identified the same Na and Cl peaks in NaCl at 1.0 and 2.6keV respectively

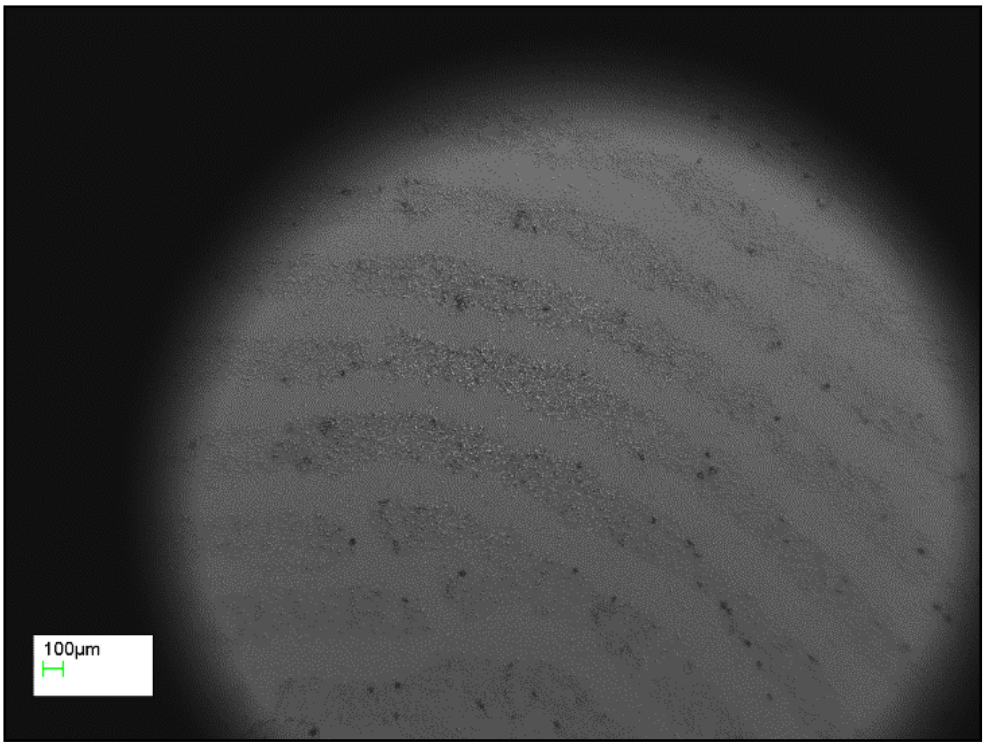


Figure 5.6 - SEM image of phosphor deposited on two week old print

When two week old prints were tested with the aluminium and bichromate powders they again showed a relatively good adherence to the print when imaged with the naked eye. The bichromate powder was the stronger of the two at this stage as the aluminium powder was again shown to overdevelop the fingerprint (Figure 5.11) leading to a reduction in the definition. Figure 5.8 shows the bichromate and phosphor powders side by side to give an indication of the coating ability on a two week old print. Figure 5.9 shows the ability of graphite and the phosphor powder to adhere to a fingerprint after two weeks. The graphite powder is much more difficult to observe over this timeframe.

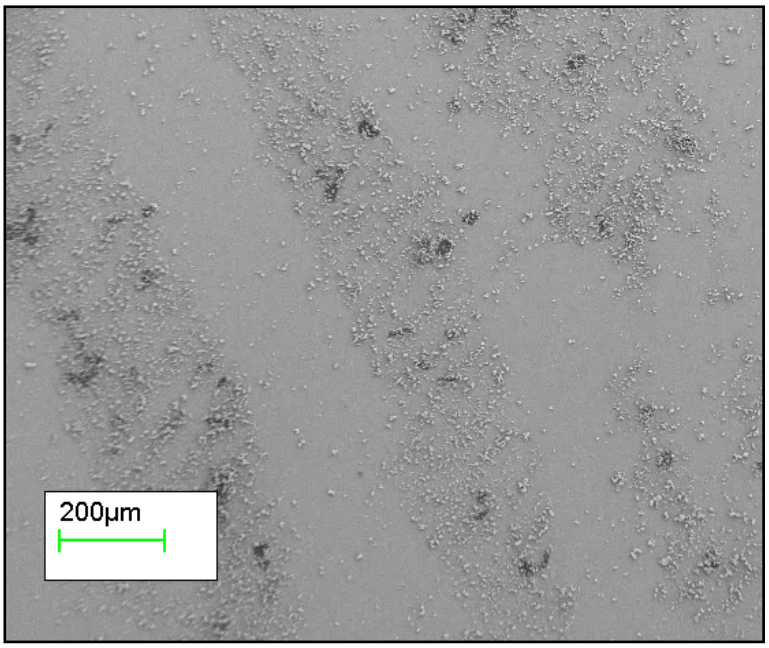


Figure 5.7 - Higher mag SEM image of phosphor deposited two week old print

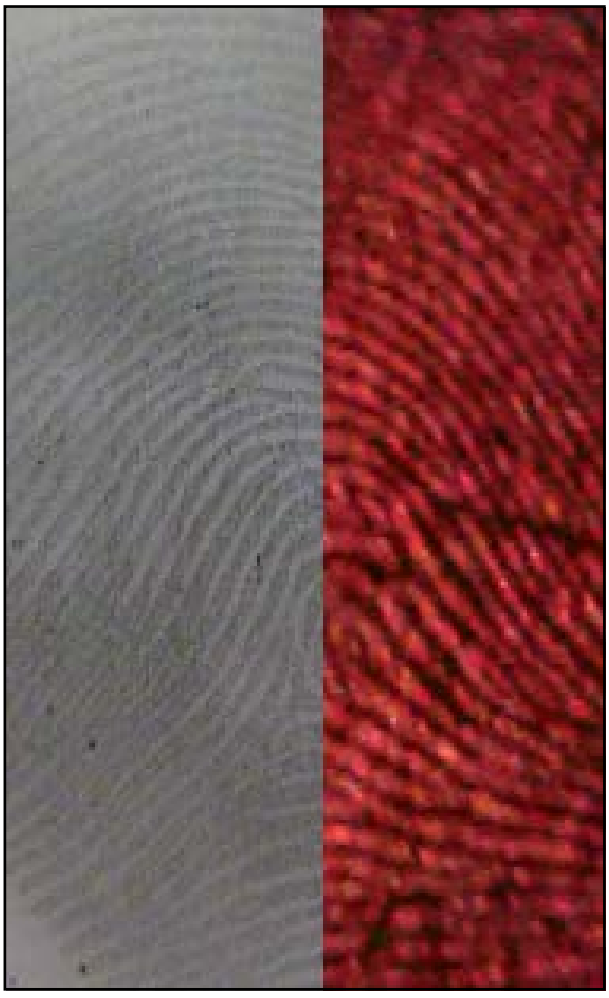

Figure 5.8 - Built image of bichromate powder (L) and phosphor powder (R)

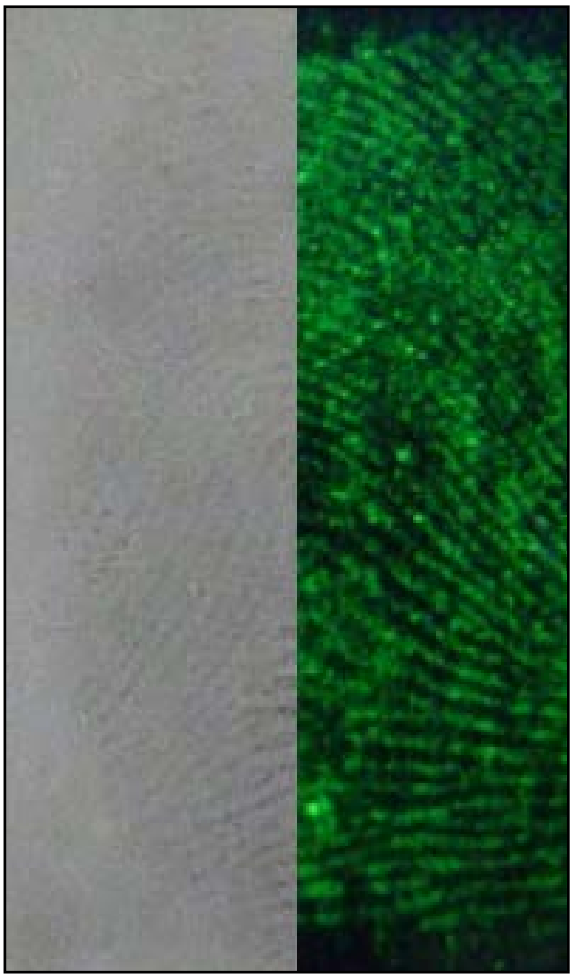

Figure 5.9 - Built image of graphite powder (L) and phosphor powder (R)

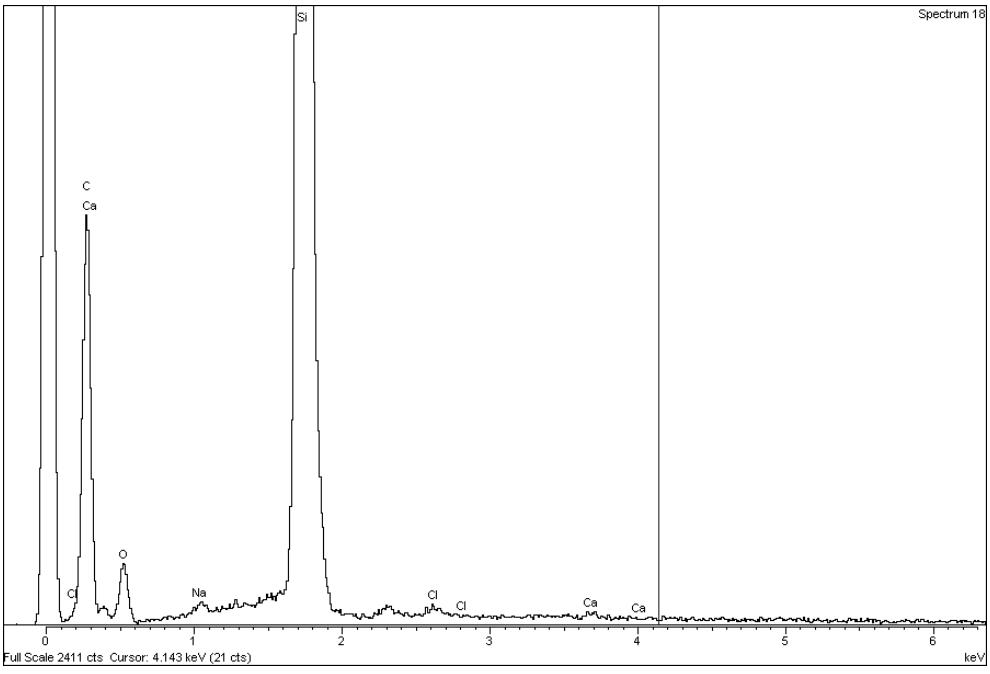


Figure 5.10 - EDX Analysis of NaCl crystals from fingerprint

Figure 5.11 - Aluminium powder dusted onto 2 week old print

### 5.3.3 Two years old

Before the dusting analysis took place, the two year old print looked different to the naked eye. After dusting the powders the phosphor showed a much lower adhesion rate than in the previous two tests as with the naked eye. Although the ridges were still noticed under natural and UV light when analysed in the SEM, the image showed many fewer phosphor particles than in previous tests. There were also noticeable brush strokes in the print due to the lower levels of oils for the phosphor to adhere too as can be shown in Figure 5.12.

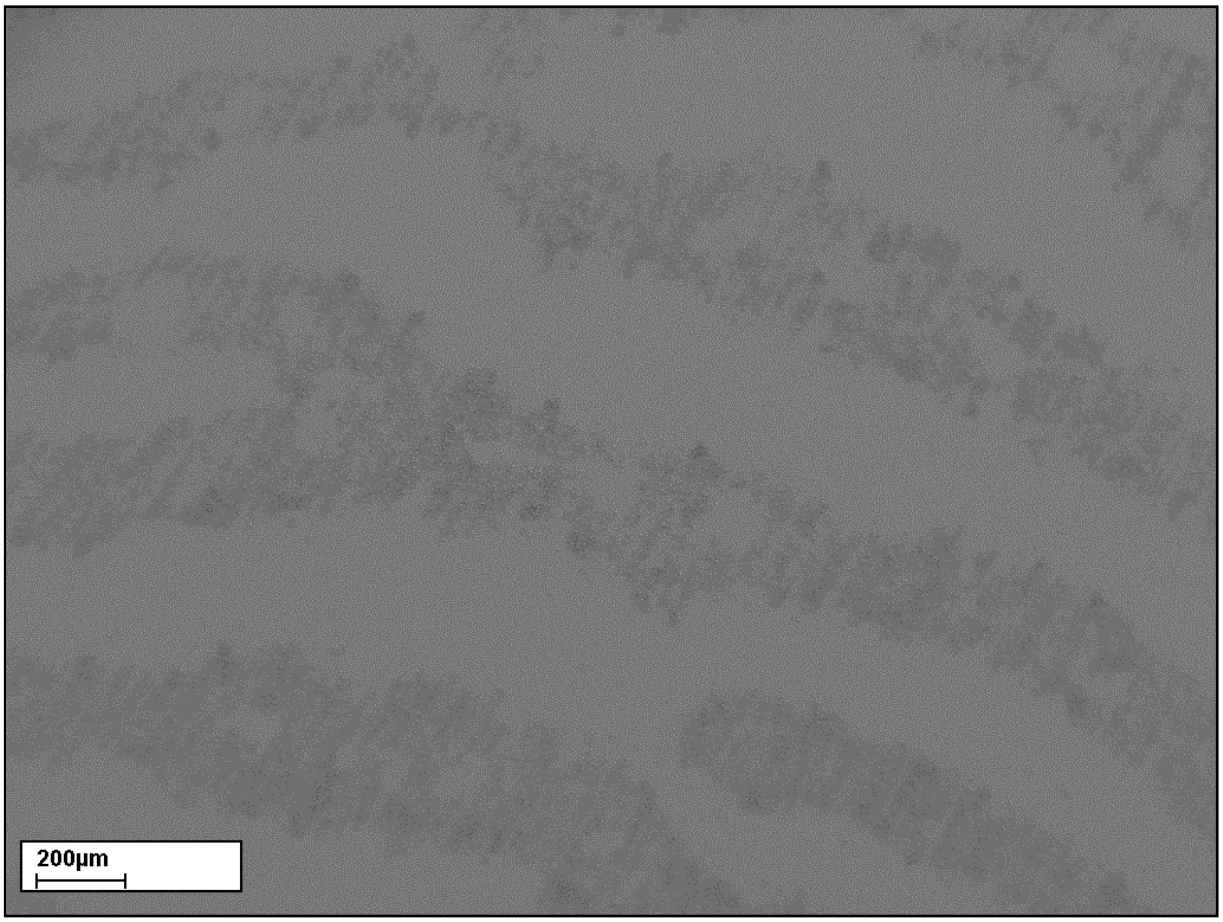


Figure 5.12 - Phosphor dusted two year old print showing brush strokes

At this stage the aluminium powder showed no adherence and even when imaged under SEM showed particles randomly clustered on the surface. The bichromate powder did show some adherence but then was very light and it was very hard to identify any features in the print. Under SEM the bichromate powder could be seen attached to the ridges of the print.

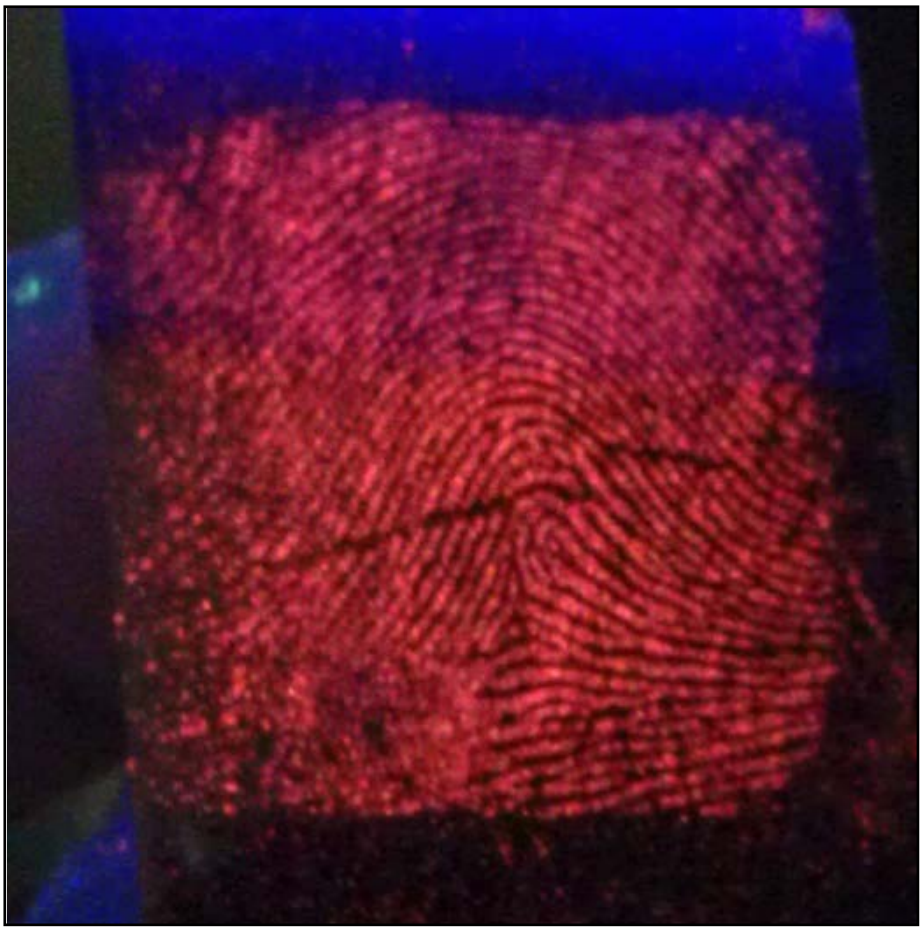

Figure 5.13 - Noticeable brush strokes on two year old print

## 5.4 Processing of Phosphor Dusted Fingerprints

The use of phosphor powders have shown to be very effective against aged and minimised prints but the use of red emission phosphors may be harder for fingerprint software to analyse. This was assessed by editing the fingerprint using image editing software ImageJ[14]. The image was firstly split into the RGB colour channels (Figure 5.15). The green image had its colours inverted (Figure 5.16) and finally was made into a binary image to change it to a more recognised image which could then be searched through on a fingerprint database (Figure 5.17). A side by side view can be seen in Figure 5.18 showing how the definition in the print has been retained. Figure 5.19 shows a magnified view of the pore structure identified from the newly masked image.

Figure 5.14 - Phosphor dusted fingerprint

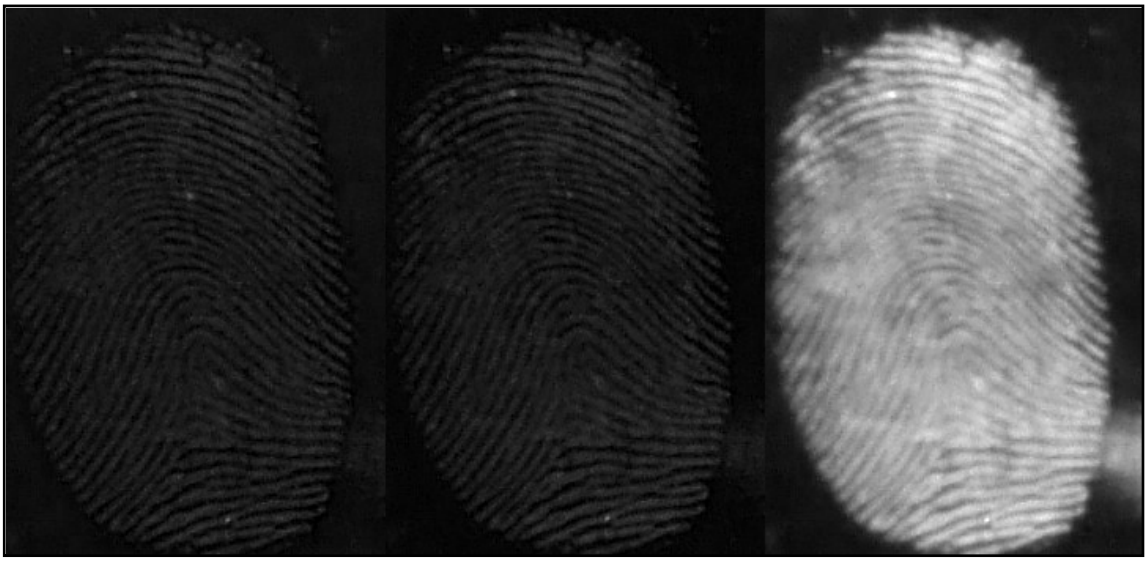

Figure 5.15 - RGB colour channels of dusted image

Figure 5.16 - Green colour channel with colour reversed

Figure 5.17 - Binary image of dusted fingerprint showing ridge detail

Figure 5.18 - Effects of fingerprint post production

Figure 5.19 - Ridge detail in produced print

Although this should allow for a better identification using the IDENT1 searchable fingerprint database the final confirmation should always be carried out by a fingerprint examiner to remove all doubt about the possibility of a technological

mistake [15, 18, 19]. This already takes place as part of the detection and classification procedure by Thames Valley Police as well as most other forces[161, 162].

# Chapter 6 – Project Discussion

## 6.1 Introduction

Although nanophosphors have been shown to suitably operate as a fingerprinting powder, there are positives and negatives for using them as a technique in a 'scene of crime' setting. Each of these will be discussed in this chapter.

## 6.2 Positive Uses of Nanophosphors for Fingerprinting

The size of the nanopowders synthesised allowed for a good coverage of latent fingerprints. The phosphors were comparable in size to the commercial bichromate powders but showed a better adherence to the prints than both other tested powders.

The synthesis method of homogeneous precipitation as well as the modified Stöber process used to coat the phosphors allows for a fast batch production process which can easily be scaled up to make large quantities of these phosphors. Only small amounts of the phosphor were needed to develop a workable fingerprint which makes the process more economical. Due to both processes being “wet chemistry” processes this reduces the health risk up the final firing process of the particles.

The ability to coat the phosphors allows for multiple useful applications. Firstly the coatings can allow for the particles to be more easily dispersed in different liquids which can change the use of the particles from a dusting technique to a dip coating technique. Secondly, and carrying on from the primary example, is that the coated particles can be modified (as shown in 2.5) to attach various compounds to the surface which can add additional benefits to the powders. The addition of drug antibodies to the powder along with dispersion in a carrier liquid can allow for a previously captured print to be tested for the presence of a certain drug. This

process would work well using a different doped phosphor to allow for a colour change on the print.

The ability of the phosphor powder once modified to adhere to older prints allows for a greater advantage in increasing the definition and the likelihood of a match. Although most scenes are found at a relatively early stage i.e. days to weeks there have been times when a scene is found after longer periods of time i.e months to years. At these times evidence can be rare and so any process that allows for a better chance of finding fingerprints is in demand. The coated phosphors were shown to have the ability to allow for higher definitions even after two years. The prints were kept in a wooden environment and so were not subject to environmental issues which could come about but the ability to get anything from a print after that length of time in other commercial processes is low.

The main product on the market which uses a fluorescent component to allow the prints to be visualised under UV light is a CdSe quantum dot process[78, 163-167]. The cost and health implications of using this process make nanophosphor powders a much less hazardous option in the areas in which they will be used. The very small size of the QD's has already raised issues, plus their constituents can cause concern.

For the scene of crime officers who would be using the powders in the field, there would be no need for any extra training as the use of these particles would be similar to the other latent fingerprint powders. The forensic specialist whose job it is to try and identify the fingerprint would only need a small amount of training on some relevant software to allow for the images to be converted into a black and white image, to be used in identification software.

## 6.3 Possible Issues in Using Phosphor Powders

The first major concern with using nanophosphors for dusting purposes is the material cost. Whereas the host lattice components are relatively cheap, the cost of the rare earth metals dopant is significantly more expensive, and is expected to remain so for the foreseeable future, principally due to the high usage of the compounds for creation of high definition displays. Although there has been

significant development of natural resources across the world, the principal supplier is still China, and as such they control a significant proportion of the world supply.

The impact and significance of the European Union's assessment of the risks associated with Nanomaterials needs also to be addressed. This in turn drives the REACH legislation (Registration, Evaluation, Authorisation and restriction of Chemicals) which not only limits the potential use of certain Nanomaterials, but can also limit their availability.

As mentioned in 6.2 the health implications for the production of the phosphors are low due to the wet chemistry process in which the nanoparticles are formed. Most of the dusting of latent fingerprints is carried out in open areas and as other powders of comparable sizes are already in use the examiners should not be at any more risk, and indeed are already trained in the use of equivalent materials. That said, the implications of using the powders for dusting in enclosed areas have not been researched and would need to be examined before the powders could be used on a large scale.

Storage of the particles is another issue that arises with using coated phosphors as a dusting powder. The use of a silica coating to allow for greater adherence to aqueous prints means that any moisture that penetrated through the storage medium (jar, sealed packet etc) could increase the particle agglomeration and therefore either make the powder less effective at adhering to the print or creating such large groups of particles that all definition is lost in the dusting process. The implication is that either the materials would be supplied as single shot disposable sachets, where unused materials were discarded, or further work would need to be done to develop additional coatings or modified coatings so as to reduce the effect of moisture[168, 169].

## 6.4 Future Improvements

Having finished the project and after processing through the data along with spending the last two years working in an industrial setting, it can be concluded that there are a number of extra ideas and analytical details which could be developed to add to the results gained so far to make the project tighter, more relevant to operational requirements and with a higher level of validation for future exploitation.

Having taken luminescent spectra of some of the main phosphors used in the study it would have been preferred to have taken more to allow for a baseline when working on the coating experiments. This would have allowed for a more detailed analysis of the luminescent properties before and after the coating process. This would have led to a faster focus on which phosphors would have been the best test subjects for the continued trials.

Seeing that the phosphor powder worked well on a two year old latent print if more samples had been created a better look at the process could have been completed. At the start of the project the chance of the powders being able to adhere to two year old prints was negligible so only a single sample of prints were left. This gives a chance for a larger study to be carried out on more prints of different ages as well as to see whether different subjects fingerprint compositions make for better or worse adherence over long timeframes.

For example, PhD theses could have been examined and any external fingerprint assessed, these are not regularly studied, details of when they are released from the library can be ascertained and the fingerprints potentially matched to the borrower if they were still present within the university system.

The phosphors created for the study were all in the range of 150-200nm diameter. Changing the size of these particles to understand whether smaller or larger particles give better definition would allow for the process to be refined. Changing the concentration of the dopant in the phosphor would allow for the possible reduction in the overall cost of the process when upscaling to large production.

Spending longer on sample preparation for examining the particles under SEM and TEM would have given better ideas of the agglomeration and also would have given better focused images for analysis. These techniques along with capturing more images at different magnifications would have given better examples.

The use of commercial grade fingerprinting powders was helpful in the comparison between the phosphor powders. The one test which would have been useful to have carried out would have been the analysis of the captured fingerprints in the UK's IDENT1 system. This system is the central database for the UK crime agencies to search and identify fingerprints. Unfortunately the use of this system for research purposes was not possible in the timeframe. This would have given a good impression as to whether the technique would be viable. This would also have allowed for an analysis in whether the captured images would need to be processed or whether the system would be able to handle the fluorescent im45age.

More in depth analysis of the phosphors using techniques such as XRD would have given a fuller story as to the reactions of the modifications on the surface as well as whether any changes between the $SiO_2$ and host lattice during the firing process.

Finally due to the ease of use of the magnetic bichromate powders a powder could be produced with a magnetic core covered by a phosphor shell. This would allow the powder to be dusted on the surface using a magnetic wand and any particles not adhering to the print could be easily removed with the wand after deposition which would make for less powder waste.

# References


1. Ayto, J., *Word Origins*. 2nd edition ed. 2005: A&C Black. 576.
2. Kilsby, P. *Lux*. LUX 2015 [cited 2014; Available from: http://www.paulkilsby.com/page4.htm.
3. Herbert, K.B.H., *John Canton FRS (1718-72).* Physics Education, 1998. **33**(2): p. 126-130.
4. Stokes, G.G., *On the Change of Refrangibility of Light.* Philosophical Transactions of the Royal Society of London, 1852. **142**: p. 463-562.
5. Wiedemann, E., *Ueber Fluorescenz und Phosphorescenz I. Abhandlung.* Annalen der Physik, 1888. **270**(7).
6. Yen, W.M., S. Shionoya, and H. Yamamoto, *Phosphor Handbook*. 2nd Edition ed, ed. H. Yamamoto. 2006: CRC Press. 1080.
7. Lenard, P., *Ueber Kathodenstrahlen in Gasen von atmosphärischem Druck und im äussersten Vacuum.* Annalen der Physik, 1894. **287**(2): p. 225-267.
8. Bos, A.J.J., *High sensitivity thermoluminescence dosimetry.* Nuclear Instruments and Methods in Physics Research Section B: Beam Interactions with Materials and Atoms, 2001. **184**(1–2): p. 3-28.
9. Lian, O.B., *LUMINESCENCE DATING | Thermoluminescence*, in *Encyclopedia of Quaternary Science (Second Edition)*, S.A.E.J. Mock, Editor. 2013, Elsevier: Amsterdam. p. 643-652.
10. Yusoff, A.L., R.P. Hugtenburg, and D.A. Bradley, *Review of development of a silica-based thermoluminescence dosimeter.* Radiation Physics and Chemistry, 2005. **74**(6): p. 459-481.
11. Kent, T., *Visualization or Development of Crime Scene Fingerprints*, in *Encyclopedia of Forensic Sciences*, J.A.S.J.S.M. Houck, Editor. 2013, Academic Press: Waltham. p. 117-129.
12. Reip, A., *Comparison of presumptive blood detection and major interferences*. 2008, University of Reading.
13. Middlestead, C. and J. Thornton, *Sensitivity of the Luminol Test with Blue Denim.* Journal of Forensic Sciences. **55**(5): p. 1340-1342.

14. Barni, F., et al., *Forensic application of the luminol reaction as a presumptive test for latent blood detection.* Talanta, 2007. **72**(3): p. 896-913.
15. Larkin, T. and C. Gannicliffe, *Illuminating the health and safety of luminol.* Science & Justice, 2008. **48**(2): p. 71-75.
16. Soderquist, T.J., et al., *Evaluation of the catalytic decomposition of $H_2O_2$ through use of organo-metallic complexes – A potential link to the luminol presumptive blood test.* Forensic Science International, 2012. **219**(1–3): p. 101-105.
17. Reip, A., *Luminescence and the quantification of iron in blood using Luminol*, in *Department of Chemistry*. 2007, University of Reading: University of Reading.
18. Dunlap, P.V., *Bioluminescence, Microbial*, in *Encyclopedia of Microbiology (Third Edition)*, M. Schaechter, Editor. 2009, Academic Press: Oxford. p. 45-61.
19. Moline, M.A., et al., *7 - Bioluminescence in the sea*, in *Subsea Optics and Imaging*, J. Watson and O. Zielinski, Editors. 2013, Woodhead Publishing. p. 134-170.
20. Blasse, G. and B.C. Grabmaier, *Luminescent Materials*. 1994.
21. Thomas, G.L., *The physics of fingerprints and their detection.* Journal of Physics E: Scientific Instruments, 1978. **11**(8): p. 722.
22. French, B.Y.a.M., *Latent Print Development*, in *Fingerprint Sourcebook*. 2010. p. 68.
23. Bond Obe, J.W. and E. Lieu, *Electrochemical behaviour of brass in chloride solution concentrations found in eccrine fingerprint sweat.* Applied Surface Science, 2014. **313**(0): p. 455-461.
24. Fish, J.T., et al., *Chapter 4 - Fingerprints and Palmprints*, in *Crime Scene Investigation (Third Edition)*, J.T. Fish, et al., Editors. 2014, Anderson Publishing, Ltd.: Boston. p. 85-110.
25. Frick, A.A., P. Fritz, and S.W. Lewis, *Chemistry of Print Residue*, in *Encyclopedia of Forensic Sciences*, J.A.S.J.S.M. Houck, Editor. 2013, Academic Press: Waltham. p. 92-97.
26. Jones, B.J., *Nano fingerprints.* Materials Today, 2011. **14**(11): p. 567.

27. Lennard, C., *FORENSIC SCIENCES | Fingerprint Techniques*, in *Reference Module in Chemistry, Molecular Sciences and Chemical Engineering*. 2013, Elsevier.
28. Ortiz-Bacon, D.L. and C.L. Swanson, *Fingerprint Sciences*, in *Encyclopedia of Forensic Sciences*, J.A.S.J.S.M. Houck, Editor. 2013, Academic Press: Waltham. p. 153-158.
29. Williams, D.K., C.J. Brown, and J. Bruker, *Characterization of children's latent fingerprint residues by infrared microspectroscopy: Forensic implications.* Forensic Science International, 2011. **206**(1–3): p. 161-165.
30. Girod, A. and C. Weyermann, *Lipid composition of fingermark residue and donor classification using GC/MS.* Forensic Science International, 2014. **238**(0): p. 68-82.
31. Archer, N.E., et al., *Changes in the lipid composition of latent fingerprint residue with time after deposition on a surface.* Forensic Science International, 2005. **154**(2-3): p. 224-239.
32. Croxton, R.S., et al., *Variation in amino acid and lipid composition of latent fingerprints.* Forensic Science International, 2010. **199**(1-3): p. 93-102.
33. Hong, S., et al., *A new method of artificial latent fingerprint creation using artificial sweat and inkjet printer.* Forensic Science International, 2015. **257**: p. 403-408.
34. Saferstein, R., *Criminalistics: An Introduction to Forensic Science*. 2004: Pearson Hall.
35. Králík, M. and L. Nejman, *Fingerprints on artifacts and historical items: examples and comments.* Journal of Ancient Fingerprints, 2007. **1**(1): p. 4-13.
36. Faulds, H., *On the Skin-furrows of the Hand.* Nature, 1888. **22**: p. 605.
37. Galton, F., *Personal identification and description.* Nature, 1888. **38**: p. 173-7.
38. Cummins, H. and R.W. Kennedy, *Purkinje's Observations (1823) on Finger Prints and Other Skin Features.* Journal of Criminal Law and Criminology (1931-1951), 1940. **31**(3): p. 343-356.

39. Purkyně, J.E., *Commentatio de examine physiologico organi visus et systematis cutanei.* 1823.
40. Andrzej Grzybowski, K.P., *Jan Evangelista Purkynje (1787–1869): First to describe fingerprints.* Clinics in Dermatology, 2015. **33**: p. 117-121.
41. Caplan, R.M., *How fingerprints came into use for personal identification.* Journal of the American Academy of Dermatology, 1990. **23**(1): p. 109-114.
42. Henry, E.R., *Classification and Uses of Fingerprints*. 1900, London: G Routledge & Sons.
43. *Trial of ALFRED STRATTON (22) ALBERT ERNEST STRATTON*, O.B.P. Online, Editor. May 1905: London.
44. *People v. Jennings*, J. Department, Editor. 1911: 252 Ill.
45. Getty, G.W.P., James, *Richard Speck and the eight slaughtered nurses*. Public Defender. 1974, New York: Grosset & Dunlap.
46. Carlo, P., *The Night Stalker: The Life and Crimes of Richard Ramirez*. 1996, New York: Kensington Publishing Corp.
47. Wilson, C., *The Mammoth Encyclopedia of the Unsolved*. 2000: Carroll & Graf Publishers.
48. MacDonell, H.L., *Bristless brush development of latent fingerprints.* Identification News, 1961. **11**: p. 7.
49. Bajorath, J., *Molecular crime scene investigation – dusting for fingerprints.* Drug Discovery Today: Technologies, 2013. **10**(4): p. e491-e498.
50. Kumari, H., R. Kaur, and R.K. Garg, *New visualizing agents for latent fingerprints: Synthetic food and festival colors.* Egyptian Journal of Forensic Sciences, 2011. **1**(3–4): p. 133-139.
51. Sodhi, G.S. and J. Kaur, *Powder method for detecting latent fingerprints: a review.* Forensic Science International, 2001. **120**(3): p. 172-176.
52. Daluz, H.M., *Fundamentals of Fingerprint Analysis*. 2014: CRC Press. 340.
53. Kobus, H.J., M. Stoilovic, and R.N. Warrener, *A simple luminescent post-ninhydrin treatment for the improved visualisation of fingerprints on documents in cases where ninhydrin alone gives poor results.* Forensic Science International, 1983. **22**(2–3): p. 161-170.

54. Lennard, C.J., et al., *Synthesis of Ninhydrin Analogues and Their Application to Fingerprint Development: Preliminary Results.* Journal of the Forensic Science Society, 1986. **26**(5): p. 323-328.
55. Lennard, C.J., et al., *Synthesis and evaluation of ninhydrin analogues as reagents for the development of latent fingerprints on paper surfaces.* Journal of the Forensic Science Society, 1988. **28**(1): p. 3-23.
56. Liberti, A., G. Calabrò, and M. Chiarotti, *Storage effects on ninhydrin-developed fingerprints enhanced by zinc complexation.* Forensic Science International, 1995. **72**(3): p. 161-169.
57. Schiltz, E., K.D. Schnackerz, and R.W. Gracy, *Comparison of ninhydrin, fluorescamine, and o-phthaldialdehyde for the detection of amino acids and peptides and their effects on the recovery and composition of peptides from thin-layer fingerprints.* Analytical Biochemistry, 1977. **79**(1–2): p. 33-41.
58. Schulz, M.M., et al., *Ninhydrin-dyed latent fingerprints as a DNA source in a murder case.* Journal of Clinical Forensic Medicine, 2004. **11**(4): p. 202-204.
59. Yang, R. and J. Lian, *Studies on the development of latent fingerprints by the method of solid–medium ninhydrin.* Forensic Science International, 2014. **242**(0): p. 123-126.
60. Aviv, O., et al., *Controlled iodine release from polyurethane sponges for water decontamination.* Journal of Controlled Release, 2013. **172**(3): p. 634-640.
61. Jasuja, O.P., A. Kaur, and P. Kumar, *Fixing latent fingermarks developed by iodine fuming: A new method.* Forensic Science International, 2012. **223**(1–3): p. e47-e52.
62. Jasuja, O.P. and G. Singh, *Development of latent fingermarks on thermal paper: Preliminary investigation into use of iodine fuming.* Forensic Science International, 2009. **192**(1-3): p. e11-e16.
63. Kelly, P.F., et al., *The recovery of latent text from thermal paper using a simple iodine treatment procedure.* Forensic Science International, 2012. **217**(1–3): p. e27-e30.
64. Lennard, C. *The Detection and Enhancement of Latent Fingerprints*. in *13th INTERPOL Forensic Science Symposium*. 2001. Lyon, France.

65. Wargacki, S.P., L.A. Lewis, and M.D. Dadmun, *Understanding the Chemistry of the Development of Latent Fingerprints by Superglue Fuming.* J Forensic Sci, 2007. **52**(5): p. 1057-1062.
66. Kalka, N.D. and R.A. Hicklin, *On relative distortion in fingerprint comparison.* Forensic Science International, 2014. **244**(0): p. 78-84.
67. Payne, G., et al., *A further study to investigate the detection and enhancement of latent fingerprints using visible absorption and luminescence chemical imaging.* Forensic Science International, 2005. **150**(1): p. 33-51.
68. Speir, J.A. and J. Hietpas, *Frequency filtering to suppress background noise in fingerprint evidence: Quantifying the fidelity of digitally enhanced fingerprint images.* Forensic Science International, 2014. **242**(0): p. 94-102.
69. UK, H.O. Manual of Fingerprint Techniques. 1986.
70. James, J.D., W.P. Lewis, and B. Wilshire, *Control of reflective properties of flake metal products.* Powder Metallurgy, 1993. **36**(1): p. 42-46.
71. James, J.D., C.A. Pounds, and B. Wilshire, *Obliteration of latent fingerprints.* Journal of Forensic Sciences, 1991. **36**(5): p. 1376-1386.
72. James, J.D., C.A. Pounds, and B. Wilshire, J. Forensic Ident., 1992. **42**: p. 531-542.
73. MacDonall, H.L., 1964.
74. Olsen, R.D., Scott's Fingerprint Mechanics, 1978.
75. Wilshire, B. and N. Hurley, J. Forensic Sci., 1995. **40**: p. 837.
76. Wilshire, B. and N.J. Hurley, Forensic Sci., 1996.
77. Jones, B.J., et al., *Nano-scale composition of commercial white powders for development of latent fingerprints on adhesives.* Science & justice : journal of the Forensic Science Society. **50**(3): p. 150-155.
78. Liu, J., et al., *Water-soluble multicolored fluorescent CdTe quantum dots: Synthesis and application for fingerprint developing.* Journal of Colloid and Interface Science. **342**(2): p. 278-282.
79. Liu, L., et al., *Exploration of the use of novel $SiO_2$ nanocomposites doped with fluorescent $Eu^{3+}$/sensitizer complex for latent fingerprint detection.* Forensic Science International, 2008. **176**(2-3): p. 163-172.

80. Liu, L., et al., *The effectiveness of strong afterglow phosphor powder in the detection of fingermarks.* Forensic Science International, 2009. **183**(1-3): p. 45-49.

81. Pitkethly, M., *Nanotechnology and forensics.* Materials Today, 2009. **12**(6): p. 6-6.

82. Rowell, F., K. Hudson, and J. Seviour, *Detection of drugs and their metabolites in dusted latent fingermarks by mass spectrometry.* Analyst, 2009. **134**(4): p. 701-707.

83. Trapecar, M. and M.K. Vinkovic, *Techniques for fingerprint recovery on vegetable and fruit surfaces used in Slovenia -- A preliminary study.* Science & Justice, 2008. **48**(4): p. 192-195.

84. Liu, W., et al., *Synthesis of $Y_2O_3:Eu^{3+}$ coated $Y_2O_3$ phosphors by urea-assisted homogeneous precipitation and its photoluminescence properties.* Materials Letters. **96**(0): p. 42-44.

85. Atabaev, T.S., H.-K. Kim, and Y.-H. Hwang, *Submicron $Y_2O_3$ particles codoped with Eu and Tb ions: Size controlled synthesis and tuning the luminescence emission.* Journal of Colloid and Interface Science. **373**(1): p. 14-19.

86. Hyppänen, I., et al., *Up-conversion luminescence properties of $Y_2O_2S:Yb^{3+},Er^{3+}$ nanophosphors.* Optical Materials.

87. Stober, W., A. Fink, and E. Bohn, *Controlled growth of monodisperse silica spheres in the micron size range.* Journal of Colloid and Interface Science, 1968. **26**(1): p. 62-69.

88. Liu, G. and G. Hong, *Synthesis of $SiO_2/Y_2O_3:Eu$ core-shell materials and hollow spheres.* Journal of Solid State Chemistry, 2005. **178**(5): p. 1647-1651.

89. Plumer, N., et al., *Stober silica particles as basis for redox modifications: Particle shape, size, polydispersity, and porosity.* Journal of Colloid and Interface Science. **368**(1): p. 208-219.

90. Theaker, B.J., K.E. Hudson, and F.J. Rowell, *Doped hydrophobic silica nano- and micro-particles as novel agents for developing latent fingerprints.* Forensic Science International, 2008. **174**(1): p. 26-34.

91. Cervantes-Vásquez, D., O.E. Contreras, and G.A. Hirata, *Quantum efficiency of silica-coated rare-earth doped yttrium silicate.* Journal of Luminescence, 2013. **143**(0): p. 226-232.

92. Gharazi, S., A. Ershad-Langroudi, and A. Rahimi, *The influence of silica synthesis on the morphology of hydrophilic nanocomposite coating.* Scientia Iranica, 2011. **18**(3): p. 785-789.

93. Kurt, İ., I. Acar, and G. Güçlü, *Preparation and characterization of water reducible alkyd resin/colloidal silica nanocomposite coatings.* Progress in Organic Coatings, 2014. **77**(5): p. 949-956.

94. Yoon, Y. and R.M. Lueptow, *Concentration of colloidal silica suspensions using fluorescence spectroscopy.* Colloids and Surfaces A: Physicochemical and Engineering Aspects, 2006. **277**(1–3): p. 107-110.

95. Jakša, G., B. Štefane, and J. Kovač, *Influence of different solvents on the morphology of APTMS-modified silicon surfaces.* Applied Surface Science, 2014. **315**(0): p. 516-522.

96. Yong, W.Y.D., et al., *One-pot synthesis of surface functionalized spherical silica particles.* Colloids and Surfaces A: Physicochemical and Engineering Aspects, 2014. **460**(0): p. 151-157.

97. Zhao, J., et al., *Surface modification of $TiO_2$ nanoparticles with silane coupling agents.* Colloids and Surfaces A: Physicochemical and Engineering Aspects, 2012. **413**(0): p. 273-279.

98. Zhang, Q., et al., *Permeable Silica Shell through Surface-Protected Etching.* Nano Letters, 2008. **8**(9): p. 2867-2871.

99. Withnall, R., et al. *A novel approach for the preparation of discrete phosphor nanoparticles*. 2010.

100. Shinde, K.N., et al., *Phosphate Phosphors for Solid-State Lighting*. 2012: Springer Berlin Heidelberg.

101. Plyler, E.K., *Infrared Spectra of Methanol, Ethanol, and n-Propanol* Journal of Research of the National Bureau of Standards, 1952. **48**(4): p. 281-286.

102. Rana, V., et al., *Surface-enhanced Raman Spectroscopy for Trace Identification of Controlled Substances: Morphine, Codeine, and Hydrocodone.* Journal of Forensic Sciences: p. no-no.

103. Connatser, R.M., et al., *Toward Surface-Enhanced Raman Imaging of Latent Fingerprints.* Journal of Forensic Sciences, 2010.
104. Burgio, L., et al., *Pigment analysis by Raman microscopy of the non-figurative illumination in 16th- to 18th-century Islamic manuscripts.* Journal of Raman Spectroscopy, 2008. **39**(10): p. 1482-1493.
105. Best, S.P., R.J.H. Clark, and R. Withnall, *Non-destructive pigment analysis of artefacts by Raman microscopy.* Endeavour, 1992. **16**(2): p. 66-73.
106. Withnall, R., et al., *Achieving structured colour in inorganic systems: Learning from the natural world.* Optics & Laser Technology, 2011. **43**(2): p. 401-409.
107. Edwards, H.G.M., et al., *An analytical Raman spectroscopic study of an important english oil painting of the 18th Century.* Spectrochimica Acta Part A: Molecular and Biomolecular Spectroscopy, 2014. **118**: p. 598-602.
108. Freitas, R.P., et al., *Analysis of a Brazilian baroque sculpture using Raman spectroscopy and FT-IR.* Spectrochimica Acta Part A: Molecular and Biomolecular Spectroscopy, 2016. **154**: p. 67-71.
109. Gutiérrez-Neira, P.C., et al., *Raman spectroscopy analysis of pigments on Diego Velázquez paintings.* Vibrational Spectroscopy, 2013. **69**: p. 13-20.
110. Lauridsen, C.B., J. Sanyova, and K.P. Simonsen, *Raman analysis of complex pigment mixtures in 20th century metal knight shields of the Order of the Elephant.* Spectrochimica Acta Part A: Molecular and Biomolecular Spectroscopy, 2015. **150**: p. 54-62.
111. Miguel, C., et al., *The alchemy of red mercury sulphide: The production of vermilion for medieval art.* Dyes and Pigments, 2014. **102**: p. 210-217.
112. Button, V., *The portrait drawings of Hans Holbein the Younger : function and use explored through materials and techniques*. 2013, Royal College of Art. p. 331.
113. Saitoh, H., et al., *Metal composition of $Y_2O_3$:Eu powder evaluated using particle analyzer.* Science and Technology of Advanced Materials, 2005. **6**(2): p. 205-209.
114. Martinez-Rubio, M.I., et al., *A synthetic method for the production of a range of particle sizes for Y2O3: Eu phosphors using a copolymer microgel of*

*NIPAM and AMPS.* Journal of the Electrochemical Society, 2002. **149**(2): p. H53-H58.

115. Newport, A., J. Silver, and A. Vecht, *The Synthesis of Fine Particle Yttrium Vanadate Phosphors from Spherical Powder Precursors Using Urea Precipitation.* Journal of the Electrochemical Society, 2000. **147**(10): p. 3944-3947.
116. Silver, J., *Metal Compounds as Phosphors*, in *Comprehensive Coordination Chemistry II*, J.A.M.J. Meyer, Editor. 2003, Pergamon: Oxford. p. 689-717.
117. Silver, J., et al., *Yttrium Oxide Upconverting Phosphors. 5. Upconversion Luminescent Emission from Holmium-Doped Yttrium Oxide under 632.8 nm Light Excitation.* J. Phys. Chem. B, 2003. **107**(35): p. 9236-9242.
118. Silver, J., et al., *Yttrium Oxide Upconverting Phosphors. 3. Upconversion Luminescent Emission from Europium-Doped Yttrium Oxide under 632.8 nm Light Excitation.* J. Phys. Chem. B, 2001. **105**(38): p. 9107-9112.
119. Silver, J., et al., *The Effect of Particle Morphology and Crystallite Size on the Upconversion Luminescence Properties of Erbium and Ytterbium Co-doped Yttrium Oxide Phosphors.* J. Phys. Chem. B, 2001. **105**(5): p. 948-953.
120. Silver, J., et al., *Yttrium Oxide Upconverting Phosphors. Part 4: Upconversion Luminescent Emission from Thulium-Doped Yttrium Oxide under 632.8-nm Light Excitation.* J. Phys. Chem. B, 2003. **107**(7): p. 1548-1553.
121. Silver, J., et al., *Yttrium Oxide Upconverting Phosphors. Part 2: Temperature Dependent Upconversion Luminescence Properties of Erbium in Yttrium Oxide.* J. Phys. Chem. B, 2001. **105**(30): p. 7200-7204.
122. Silver, J. and R. Withnall, *Probes of Structural and Electronic Environments of Phosphor Activators: Mössbauer and Raman Spectroscopy.* Chem. Rev, 2004. **104**(6): p. 2833-2856.
123. Tanner, P.A., X. Zhou, and F. Liu, *Assignment of Electronic Transitions and Electron-Phonon Coupling of $Er^{3+}$ Doped into $Y_2O_3$.* J. Phys. Chem. A, 2004. **108**(52): p. 11521-11525.
124. Anh, T.K., et al., *Nanomaterials containing rare-earth ions Tb, Eu, Er and Yb: preparation, optical properties and application potential.* Journal of Luminescence, 2003. **102-103**: p. 391-394.

125. Fu, Y.-P., *Preparation and characterization of $Y_2O_3$:Eu phosphors by combustion process.* Journal of Materials Science, 2007. **42**(13): p. 5165-5169.

126. Qin, X., et al., *Synthesis and upconversion luminescence of monodispersed, submicron-sized $Er^{3+}$:$Y_2O_3$ spherical phosphors.* Journal of Alloys and Compounds. **493**(2): p. 672-677.

127. Vu, N., et al., *Photoluminescence and cathodoluminescence properties of $Y_2O_3$:Eu nanophosphors prepared by combustion synthesis.* Journal of Luminescence, 2007. **122-123**: p. 776-779.

128. Wang, L., et al., *Photoluminescence properties of Y2O3:Tb3+ and YBO3:Tb3+ green phosphors synthesized by hydrothermal method.* Materials Chemistry and Physics.

129. Insu Cho, J.-G.K., and Youngku Sohn, *Photoluminescence Imaging of $SiO_2$@$Y_2O_3$:Eu(III) and $SiO_2$@$Y_2O_3$:Tb(III) Core-Shell Nanostructures.* Bull. Korean Chem. Soc., 2014. **35**(2): p. 575-580.

130. Muenchausen, R.E., et al., *Effects of Tb doping on the photoluminescence of $Y_2O_3$:Tb nanophosphors.* Journal of Luminescence, 2007. **126**(2): p. 838-842.

131. Xiu, Z., et al., *Uniform and well-dispersed $Y_2O_3$:Eu/$YVO_4$:Eu composite microspheres with high photoluminescence prepared by chemical corrosion approach.* Colloids and Surfaces A: Physicochemical and Engineering Aspects, 2012. **401**(0): p. 68-73.

132. Silver, J., et al., *P-80: A New Oxide/Oxysulfide Based Phosphor Triad and High-Efficiency Green-Emitting (Y, Gd)$_2O_2S$:Tb Phosphor for FED Applications.* SID Symposium Digest of Technical Papers, 2005. **36**(1): p. 594-597.

133. Giakoumakis, G.E., et al., *$Y_2O_2S$:Eu phosphor screens evaluation.* Med Phys, 1993. **20**(1): p. 79-83.

134. Yan, X., *Phosphors for Lighting Applications*, in *Wolfson Centre for Materials Processing*. 2012, Brunel University: Brunel University. p. 164.

135. Huang, P., et al., *Luminescence improvement of $Y_2O_2S$:$Tb^{3+}$, $Sr^{2+}$, $Zr^{4+}$ white-light long-lasting phosphor via $Eu^{3+}$ addition.* Ceramics International, 2013. **39**(5): p. 5615-5621.

136. Kaliakatsos, J.A., G.E. Giakoumakis, and G.J. Papaioannou, *Temperature dependence of $Y_2O_2S$:Tb cathodoluminescence.* Solid State Communications, 1988. **65**(1): p. 35-36.

137. Pengde, H., et al., *Three primary colors upconversion phosphors and combined white upconversion luminscence in $Y_2O_2S$ matrix.* Materials Research Bulletin, 2015. **70**: p. 658-662.

138. Peng-Fei Ai, Y.-L.L., Li-Yuan Xiao, Hou-Jin Wang and Jian-Xin Meng, *Synthesis of $Y_2O_2S : Eu^{3+}, Mg^{2+}, Ti^{4+}$ hollow microspheres via homogeneous precipitation route.* Sci. Technol. Adv. Mater., 2010. **11**: p. 5.

139. Sordelet, D. and M. Akinc, *Preparation of spherical, monosized $Y_2O_3$ precursor particles.* Journal of Colloid and Interface Science, 1988. **122**(1): p. 47-59.

140. Koutoku Ohmi, S.T., Hiroshi Kobayashi and Takashi Nire, *$Y_2O_2S$:Tb Phosphor Thin Films Grown by Multisource Deposition and Their Luminescent Properties.* Jpn. J. Appl. Phys, 1993. **32**: p. 487-489.

141. R Withnall, J.S., G R Fern, A L Lipman, S Zhang, I Marian, E Barrett, *Photoluminescence of Y2O2S:REE and Gd2O2S:REE phosphors under 257 nm excitation.* Central Laser Facility Annual Report 2004/2005, 2005: p. 147-148.

142. Ismail A.M. Ibrahim, A.A.F.Z., Mohamed A. Sharaf, *Preparation of spherical silica nanoparticles: Stober silica.* Journal of American Science, 2010. **6**(11): p. 985-989.

143. Lapresta-Fernández, A., et al., *Magnetic core–shell fluorescent pH ratiometric nanosensor using a Stöber coating method.* Analytica Chimica Acta, 2011. **707**(1–2): p. 164-170.

144. Lee, M.H., F.L. Beyer, and E.M. Furst, *Synthesis of monodisperse fluorescent core-shell silica particles using a modified Stöber method for imaging individual particles in dense colloidal suspensions.* Journal of Colloid and Interface Science, 2005. **288**(1): p. 114-123.

145. Plumeré, N., et al., *Stöber silica particles as basis for redox modifications: Particle shape, size, polydispersity, and porosity.* Journal of Colloid and Interface Science, 2012. **368**(1): p. 208-219.

146. Qiu, B., et al., *Stöber-like method to synthesize ultradispersed $Fe_3O_4$ nanoparticles on graphene with excellent Photo-Fenton reaction and high-performance lithium storage.* Applied Catalysis B: Environmental, 2016. **183**: p. 216-223.

147. Rutledge, H., et al., *Imbedding germanium quantum dots in silica by a modified Stöber method.* Materials Science in Semiconductor Processing, 2014. **17**: p. 7-12.

148. Abe, S., et al., *Photophysical properties and biocompatibility of Photoluminescent $Y_2O_3$:Eu nanoparticles in polymethylmetacrylate matrix.* J Nanosci Nanotechnol, 2014. **14**(4): p. 2891-4.

149. Chen, W.-H., H.-H. Lin, and F.C.-N. Hong, *Improvement of conversion efficiency of multi-crystalline silicon solar cells using reactive ion etching with surface Pre-etching.* Thin Solid Films.

150. Ghulinyan, M., et al., *Formation of Mach angle profiles during wet etching of silica and silicon nitride materials.* Applied Surface Science, 2015. **359**: p. 679-686.

151. Rad, M.A., K. Ibrahim, and K. Mohamed, *Formation of $SiO_2$ surface textures via $CHF_3$/Ar plasma etching process of poly methyl methacrylate self-formed masks.* Vacuum, 2014. **101**: p. 67-70.

152. Schurink, B., et al., *Highly uniform sieving structure by corner lithography and silicon wet etching.* Microelectronic Engineering, 2015. **144**: p. 12-18.

153. Seo, D., et al., *Selective wet etching of $Si_3N_4$/$SiO_2$ in phosphoric acid with the addition of fluoride and silicic compounds.* Microelectronic Engineering, 2014. **118**: p. 66-71.

154. Vlasukova, L.A., et al., *Threshold and criterion for ion track etching in $SiO_2$ layers grown on Si.* Vacuum, 2014. **105**: p. 107-110.

155. GREENBERG, S.A., *THE DEPOLYMERIZATION OF SILICA IN SODIUM HYDROXIDE SOLUTIONS.* J. Phys. Chem. **61**(7): p. 960-965.

156. Jakša, G., B. Štefane, and J. Kovač, *Influence of different solvents on the morphology of APTMS-modified silicon surfaces.* Applied Surface Science, 2014. **315**: p. 516-522.

157. Palimi, M.J., et al., *Surface modification of $Fe_2O_3$ nanoparticles with 3-aminopropyltrimethoxysilane (APTMS): An attempt to investigate surface treatment on surface chemistry and mechanical properties of polyurethane/$Fe_2O_3$ nanocomposites.* Applied Surface Science, 2014. **320**: p. 60-72.

158. Hughes, E. *Fingerprints on demand*. Chemistry World 2012 [cited 2012; Available from: http://www.rsc.org/chemistryworld/2012/11/artificial-fingerprints-forensic-tests.

159. Staymates, J.L., M.E. Staymates, and G. Gillen, *Evaluation of a drop-on-demand micro-dispensing system for development of artificial fingerprints.* Analytical Methods, 2013. **5**(1): p. 180-186.

160. Liu, Y., et al., *Internal structure, hygroscopic and reactive properties of mixed sodium methanesulfonate-sodium chloride particles.* Physical Chemistry Chemical Physics, 2011. **13**(25): p. 11846-11857.

161. Liu, F., D. Zhang, and L. Shen, *Study on novel Curvature Features for 3D fingerprint recognition.* Neurocomputing, 2015. **168**: p. 599-608.

162. Zhang, Q., Y. Yin, and G. Yang, *Unmatched minutiae: Useful information to boost fingerprint recognition.* Neurocomputing, 2016. **171**: p. 1401-1413.

163. Becue, A., et al., *Use of quantum dots in aqueous solution to detect blood fingermarks on non-porous surfaces.* Forensic Science International, 2009. **191**(1-3): p. 36-41.

164. Dilag, J., H. Kobus, and A.V. Ellis, *Cadmium sulfide quantum dot/chitosan nanocomposites for latent fingermark detection.* Forensic Science International, 2009. **187**(1-3): p. 97-102.

165. Moret, S., A. Bacue, and C. Champod, *Cadmium-free quantum dots in aqueous solution: Potential for fingermark detection, synthesis and an application to the detection of fingermarks in blood on non-porous surfaces.* Forensic Science International. **224**(1-3): p. 101-110.

166. Algarra, M., et al., *Fingerprint detection and using intercalated CdSe nanoparticles on non-porous surfaces.* Analytica Chimica Acta. **812**: p. 228-235.

167. Wang, Y.F., et al., *Application of CdSe nanoparticle suspension for developing latent fingermarks on the sticky side of adhesives.* Forensic Science International, 2009. **185**(1-3): p. 96-99.

168. Darshan, G.P., et al., *Effective fingerprint recognition technique using doped yttrium aluminate nano phosphor material.* Journal of Colloid and Interface Science.

169. Saif, M., et al., *Novel non-toxic and red luminescent sensor based on $Eu^{3+}$:$Y_2Ti_2O_7$/$SiO_2$ nano-powder for latent fingerprint detection.* Sensors and Actuators B: Chemical, 2015. **220**: p. 162-170.

# Published Papers

- Robert Withnall, Jack Silver, Alexander Reip (2011). Displaying Latent Fingerprints Using Phosphor Nanopowders. 18th International Display Workshop, Nagoya, Japan.

- Withnall, R., et al. Raman Spectroscopy Gains Currency. Infrared and Raman Spectroscopy in Forensic Science, John Wiley & Sons, Ltd: 185-204. Jan 2012

# Appendix A – Conference Participation

## 1: Technology World Conference, Excel Centre, London, 2009

# Improving the detection of latent fingerprints using phosphor nanopowders

**Alexander Reip, Jack Silver, Robert Withnall**

*Wolfson Centre, Brunel University, Uxbridge, UB8 3PH, UK*

alexander.reip@brunel.ac.uk 07765 902137

## 1. Introduction

Nanotechnology has been increasing employed in forensic science for the detection of latent fingerprints, using multiple techniques from new aluminium nanomaterials for dusting to quantum dot dispersions, to try increase and enhance areas where prints are likely to be found at scenes of crime. Many of these are not viable to use in conditions other than in a lab due to the harmful effects they can cause over long term use.

Past research[1] has shown the success of using europium doped yttria for increasing the detection of fingerprints and that work has been built upon to improve the powders ability to adhere to the fingerprint by modifying the surface of the phosphor while making sure the modifications do not hinder the fluorescent ability of the phosphor.

## 2. Experimental

The two phosphors $Y_2O_3$:Eu and $Y_2O_3$:Tb were used due to their excitation wavelength of 254nm and differing emission wavelengths (612nm for Europium and 543nm for Terbium). Both were synthesised using the homogeneous precipitation method and then fired in a furnace for six hours at 800ºC. The resulting phosphors were then coated with silica using a modified version of the Stöber method [2] and then from this stage the surface of the silica was etched to lower the coating width and finally modified using various techniques.

To ensure consistency in the results the prints were taken from one donor. The finger was washed with ethanol and allowed to dry in air for ten minutes without contact. These eccrine prints were then placed on cleaned glass slides. To create sebaceous prints the same method was used except after the drying period the finger was rubbed on the back of the neck and then between the fingers before being placed onto the glass slide. To observe the differences in the ageing of fingerprints some samples were left for two weeks in the dark in a slide tray.

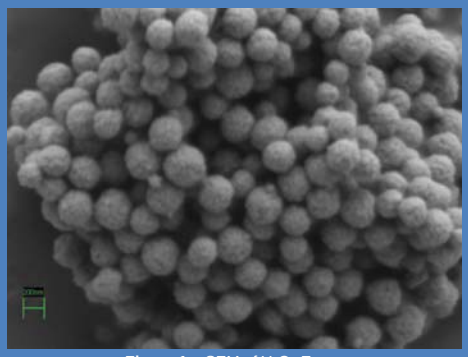

**Figure 1 –** SEM of $Y_2O_3$:Eu

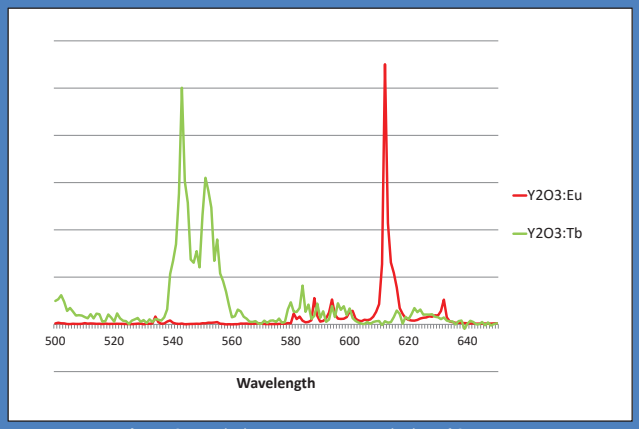


**Figure 2 –** Emission spectra at an excitation of 254nm

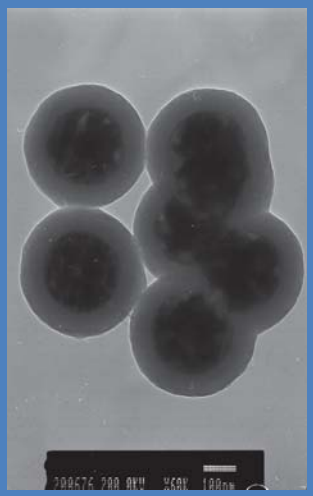

**Figure 3 –** TEM of silica coated $Y_2O_3$:Tb

## 3. Results and discussion

The silica coated $Y_2O_3$:Tb was modified with a triethoxy(octyl)silane (TMOS). This gave the phosphor a long chained hydrocarbon tail which was found to increase the attachment to the more oil based sebaceous fingerprints. The silica coated $Y_2O_3$:Eu was found to have a high attachment to the more aqueous based eccrine fingerprints and so this was used without modification. Using both phosphors on a 15 stage depletion series showed that they are able to adhere to even very dry fingerprints.

When tested on two week old and newly created fingerprints the purely silica coated phosphors adhered primarily to newer prints whereas the TMOS modified phosphor adhered to the more aged prints due to the lack of decomposition and lack of evaporation of the oils. The newer prints contained more aqueous salts and sweat so were a much better surface for the silica coated phosphors.

## 4. Future Work

The powders show great promise in enhancing the detection of latent fingerprints. The next work that will be carried out is to see whether more information can be developed from the fingerprint. These tests include modifying coated phosphors with drug antibodies so areas can be dusted for fingerprints that could have traces of drugs on them and also looking at the treated print under Raman spectroscopy to see whether other compounds can be detected such as explosive residues.

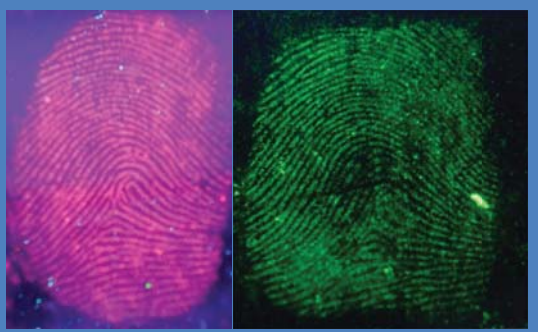

**Figure 4 –** Dusted prints $Y_2O_3$:Eu (left ) and $Y_2O_3$:Tb (right)

**References**

[1] Mi Jung Choi et al (2008). "Metal-containing nanoparticles and nano-structured particles in fingermark detection." Forensic Science International **179** (2-3): 87-97

[2] Stöber. W, Fink. A and Bohn E (1968) "Controlled growth of monodisperse silica spheres in the micron size range." *J. Colloid Interf. Sci.* **26**: 62-69

# Chapter 6 Conference Participation

## 2: Experimental Techniques Centre, Brunel University, London, 2010

# Improving the detection of latent fingerprints using phosphor nanopowders

**Alexander Reip, Jack Silver, Robert Withnall**

*Wolfson Centre, Brunel University, Uxbridge, UB8 3PH, UK*

alexander.reip@brunel.ac.uk 07765 902137

## 1. Introduction

Nanotechnology has been increasing employed in forensic science for the detection of latent fingerprints, using multiple techniques from new aluminium nanomaterials for dusting to quantum dot dispersions, to try increase and enhance areas where prints are likely to be found at scenes of crime. Many of these are not viable to use in conditions other than in a lab due to the harmful effects they can cause.

Past research[1] has shown the success of using europium doped yttria for increasing the detection of fingerprints and that work has been built upon to improve the powders ability to attach to the fingerprint by modifying the surface of the phosphor while making sure the modifications do not hinder the fluorescent ability of the phosphor.

## 2. Experimental

The two phosphors $Y_2O_3$:Eu and $Y_2O_3$:Tb were used due to their excitation wavelength of 254nm and differing emission wavelengths (612nm for Eu and 543nm for Tb). Both were synthesised using the homogeneous precipitation method and then fired in a furnace for six hours at 800ºC. The resulting phosphors were then coated with silica using a modified version of the Stöber method [2] and then from this stage the surface of the silica was modified using various techniques.

To ensure consistency in the results the prints were taken from one donor. The finger was washed with ethanol and allowed to dry in air for ten minutes without contact. These eccrine prints were then placed on cleaned glass slides. To create sebaceous prints the same method was used except after the drying period the finger was rubbed on the back of the neck and then between the fingers before being placed onto the glass slide. To observe the differences in the ageing of fingerprints some samples were left for two weeks in the dark in a slide tray.

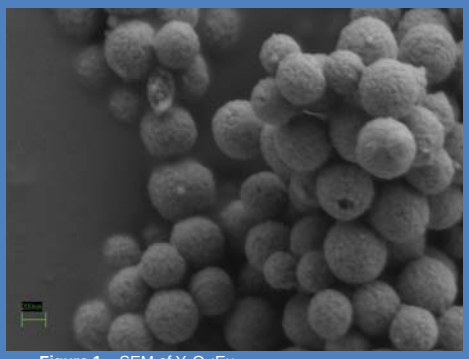

**Figure 1 –** SEM of $Y_2O_3$:Eu

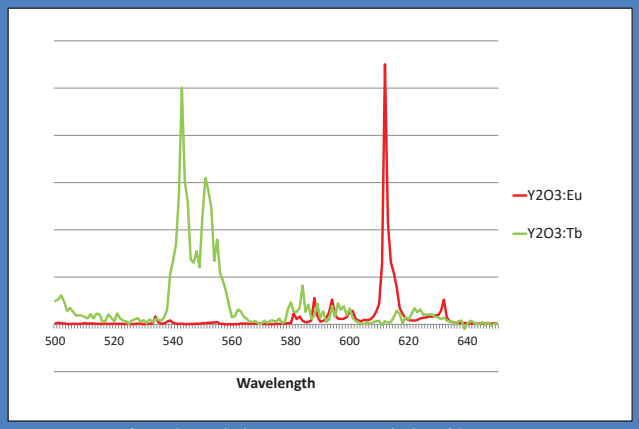


**Figure 2 –** Emission spectra at an excitation of 254nm

**Figure 3 –** TEM of silica coated $Y_2O_3$:Tb

## 3. Results and discussion

The silica coated phosphors were modified with different silanes which would help the adhesion to the fingerprint. Each phosphor was then tested on prints that had been left for different lengths of time. Of all the silanes tested the best results came from a APTES modified silane which had been reacted with succinic anhydride to give a carboxylic end and a long chain hydrocarbon silane (TMOS).

The carboxylate adhered primarily to newer prints whereas the TMOS modified phosphor adhered to the more aged and sebaceous prints. As the older prints will have had more time in the air there would be more evaporation and decomposition of the ions and metabolites and more hydrocarbons and oil residue would be left which the TMOS phosphor would preferably adhere to. Whereas the newer eccrine prints gave a much better result for the carboxylate due to the ions that are deposited in the print.

**Figure 4 –** $Y_2O_3$:Eu print taken on glass slide and enhanced image

## 4. Future Work

The powders show great promise in enhancing the detection of latent fingerprints. The next work that will be carried out is to see whether more information can be developed from the print after it has been located with the powder. These tests include drug particle detection using Raman spectroscopy, more tests on much older fingerprints and also the testing of fingerprints placed on different substrates.

**References**

[1] Mi Jung Choi et al (2008). "Metal-containing nanoparticles and nano-structured particles in fingermark detection." Forensic Science International **179** (2-3): 87-97

[2] Stöber. W, Fink. A and Bohn E (1968) "Controlled growth of monodisperse silica spheres in the micron size range." *J. Colloid Interf. Sci.* **26**: 62-69

ETCbrunel
www.ETCbrunel.co.uk

# Chapter 6 Conference Participation

## 3: XXII International Conference on Raman Spectroscopy, Boston, USA, 2010

# A Study of Silica Coated Phosphors for Latent Fingerprint Visualisation

A. Reip, R. Withnall, and J. Silver

*Centre for Phosphors and Display Materials, Wolfson Centre for Materials Processing, Brunel University, Kingston Lane, Uxbridge, Middlesex UB8 3PH, UK; Email Robert.Withnall@brunel.ac.uk*

## INTRODUCTION

Nanotechnology is being increasingly employed in forensic science for the detection of latent fingerprints, using multiple techniques from new aluminium nanomaterials for dusting to quantum dot dispersions, to try to increase and enhance areas where prints are likely to be found at scenes of crime. Many of these are not viable to use in conditions other than in a laboratory due to the harmful effects they can cause.

Past research has shown the success of using europium doped yttria for increasing the detection of fingerprints [1] and that work has been built upon by us to improve the powders' affinities for fingerprints by modifying the surfaces of the phosphors while making sure the modifications do not hinder the luminescent properties of the phosphors (see Figure 1).

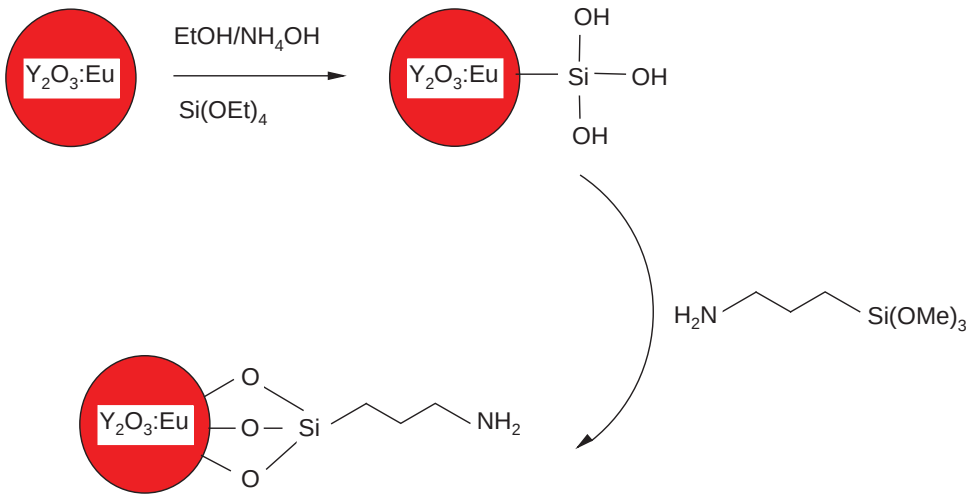


**FIGURE 1.** Reaction scheme for coating the phosphor particles with silica and then functionalizing the silica coatings with (3-aminopropyl)trimethoxysilane (APTMS) in order to make the particles hydrophilic.

## RESULTS AND DISCUSSION

As can be seen from the Raman spectra of the phosphor and APTMS modified silica coated phosphor shown in Figures 2a and 2b, respectively, a strong Raman band at 377 $cm^{-1}$ appears due to the cubic phase of $Y_2O_3$:Eu, along with emission bands due to $Eu^{3+}$ in the 600-2500 $cm^{-1}$ region. The APTMS modified silica coated phosphor exhibits a broad Raman band due to C-H stretching vibrations in the 2800-3000 $cm^{-1}$ region that is not evident in the phosphor which is not coated with silica.

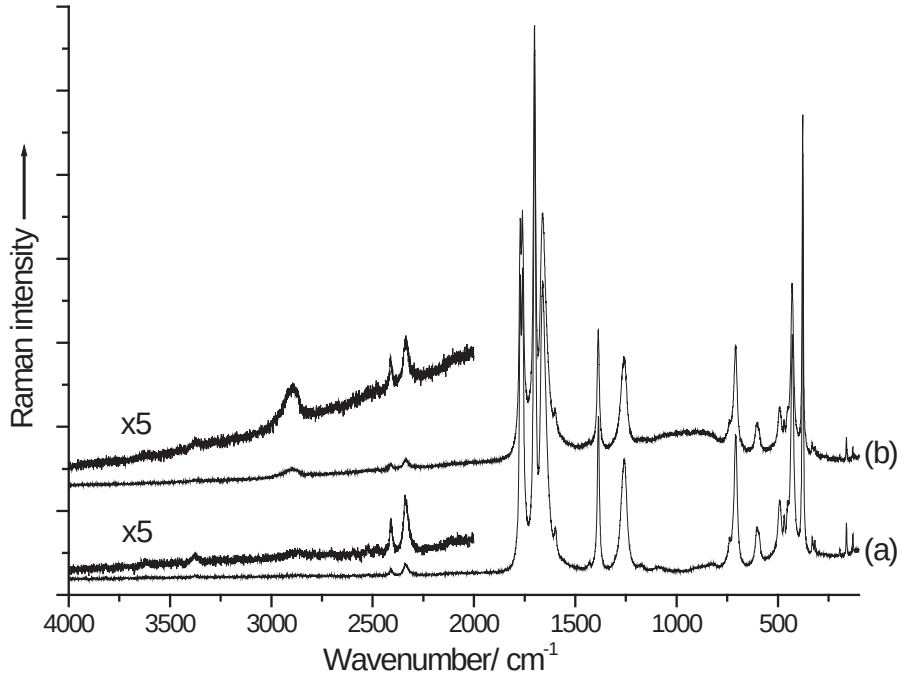


**FIGURE 2.** Raman and emission spectra of:- (a) $Y_2O_3$:Eu phosphor, and (b) $Y_2O_3$:Eu phosphor coated with silica and functionalized with APTMS. The exciting wavelength was equal to 632.8 nm.

## REFERENCES

1. M. Choi, A. McDonagh, P. Maynard and C. Roux, "Metal-containing nanoparticles and nano-structured particles in fingermark detection." *Forensic Science International* **179** (2-3): 87-97 (2008).

# A Study of Silica Coated Phosphors for Latent Fingerprint Visualisation

**Alexander Reip[1], Jack Silver[1], Robert Withnall[1], Ben Jones[2]**

[1]*Wolfson Centre, Brunel University, Uxbridge, UB8 3PH, UK*
[2]*ETC Brunel, Brunel University, Uxbridge, UB8 3PH, UK*

alexander.reip@brunel.ac.uk 07765 902137

## 1. Introduction

Nanotechnology has been increasingly employed in forensic science for the detection of latent fingerprints, using multiple techniques from new aluminium nanomaterials for dusting to quantum dot dispersions, to try to increase and enhance areas where prints are likely to be found at scenes of crime. Many of these are not viable to use in conditions other than in a lab due to the harmful effects they can cause.

Past research has shown the success of using europium doped yttria for increasing the detection of fingerprints [1] and that work has been built upon by us to improve the powders' affinities for fingerprints by modifying the surfaces of the phosphors while making sure the modifications do not hinder the luminescent properties of the phosphors. The use of RAMAN spectroscopy has been used to examine whether the modifications on the surface of the phosphor hinder the luminescent properties of the phosphor has.

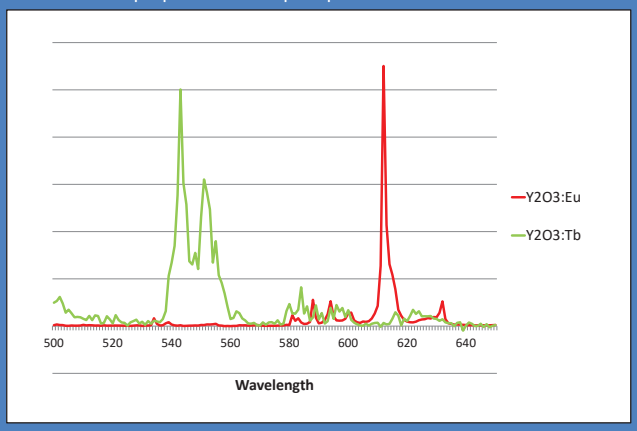


**Figure 1 –** Emission spectra of $Y_2O_3$:Eu and $Y_2O_3$:Tb using an exciting wavelength of 254 nm

## 2. Experimental

The two phosphors $Y_2O_3$:Eu and $Y_2O_3$:Tb were used due to their excitation wavelength of 254 nm and differing emission wavelengths (in the red for $Y_2O_3$:Eu and in the green for $Y_2O_3$:Tb, as shown in Figure 1). Both were synthesised using the urea homogeneous precipitation method [2] and then fired in a furnace for six hours at 800°C (SEM of fired powders shown in figure 4) . The resulting phosphors were then coated with silica using a modified version of the Stöber method [3] (see TEM of silica coated $Y_2O_3$:Eu in Figure 2) and then from this stage the surface of the silica was modified using various techniques.

The powders were then analysed using a Horiba Jobin Yvon LabRAM HR Raman Confocal Microscope under a 633nm laser.

**Figure 2 –** TEM of silica coated $Y_2O_3$:Tb

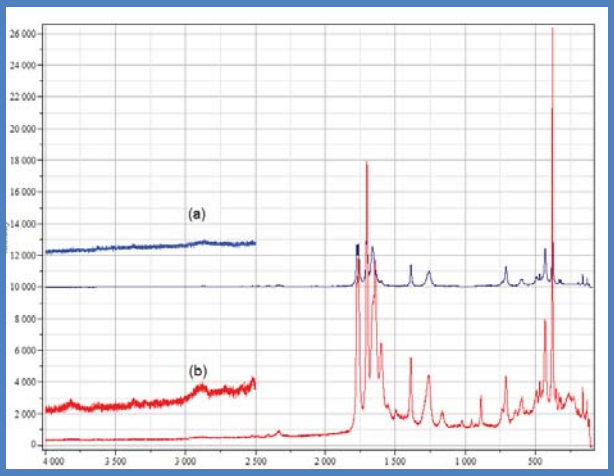


**Figure 3** – Raman of $Y_2O_3$:Eu (a) and $Y_2O_3$:Eu modified with APTES (b)

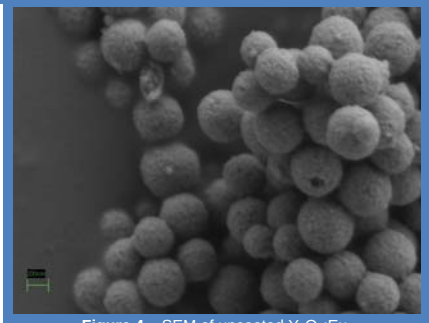

**Figure 4** – SEM of uncoated $Y_2O_3$:Eu

**Figure 5 –** $Y_2O_3$:Eu print taken on glass slide (left hand side) and enhanced image (right hand side)

## 3. Results and discussion

The silica coated phosphors were modified with different silanes which would help the adhesion to the fingerprint. Each phosphor was then tested on prints (as shown in Figure 5) that had been left for different lengths of time. Of all the silanes tested the best results came from an aminopropyl triethyl silane (APTES) modified particle which had been reacted with succinic anhydride to give a carboxylic end and a long chain hydrocarbon silane (TMOS).

The RAMAN spectra (as shown in figure 3) show the strong Raman band at 377 $cm^{-1}$ appears due to the cubic phase of $Y_2O_3$:Eu, along with emission bands due to $Eu^{3+}$ in the 600-2500 $cm^{-1}$ region. The APTES modified silica coated phosphor exhibits a broad Raman band due to C-H stretching vibrations in the 2800-3000 $cm^{-1}$ region that is not evident in the phosphor which is not coated with silica.

## 4. Future Work

The powders show great promise in enhancing the detection of latent fingerprints. The next work that will be carried out is to see whether more information can be developed from the print after it has been located with the powder. These tests include drug particle detection using Raman spectroscopy, more tests on much older fingerprints and also the testing of fingerprints placed on different substrates.

**References**

[1] Mi Jung Choi et al (2008). "Metal-containing nanoparticles and nano-structured particles in fingermark detection." Forensic Science International 179 (2-3): 87-97

[2] Silver, J.; Martinez-Rubio, M.I.; Ireland, T.G.; Fern, G.; Withnall, (2001 ) R. J. Phys. Chem. B., 105, 9107-9112.

[3] Stöber. W, Fink. A and Bohn E (1968) "Controlled growth of monodisperse silica spheres in the micron size range." J. Colloid Interf. Sci. 26: 62-69

# Chapter 6 Conference Participation

4: TechWorld Conference, Excel Centre, London, 2010

Awarded: Poster Commendation

# Improving the detection of latent fingerprints using phosphor nanopowders

**Alexander Reip, Jack Silver and Robert Withnall**

*Wolfson Centre for Materials Processing, Brunel University, Uxbridge UB8 3PH, Middlesex, UK*

**E-mail:** alexander.reip@brunel.ac.uk; **Tel. no:** 07765 902137

## 1. Introduction

Nanotechnology has been increasingly employed in forensic science for the detection of latent fingerprints, using multiple techniques from new aluminium nanomaterials for dusting to quantum dot dispersions, to try to increase and enhance areas where prints are likely to be found at scenes of crime. It is not viable to use many of these in conditions other than in a lab due to the harmful effects they can cause over long term use.

Past research has shown the success of using europium doped yttria for increasing the detection of fingerprints and that work has been built upon to improve the powders ability to adhere to the fingerprint by modifying the surface of the phosphor while making sure the modifications do not hinder the fluorescent ability of the phosphor [1].

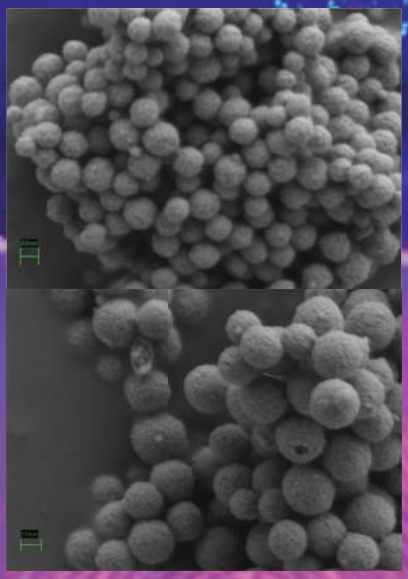

**Figure 1 –** SEM of $Y_2O_3$:Eu (top) $Y_2O_3$:Tb (bottom)

## 2. Experimental

The two phosphors $Y_2O_3$:Eu and $Y_2O_3$:Tb were used due to their excitation wavelength of 254nm and differing emission wavelengths (611 nm for Europium and 543 nm for Terbium). Both were synthesised using the homogeneous precipitation method and then fired in a furnace for six hours at 800°C. The resulting phosphors (see SEMs in Fig. 1) were then coated with silica (see TEMs in Fig. 2) using a modified version of the Stöber method and then from this stage the surface of the silica was etched to lower the coating width and finally modified using various techniques (see Fig 3.) [2].

To ensure consistency in the results the prints were taken from one donor. The finger was washed with ethanol and allowed to dry in air for ten minutes without contact. These eccrine prints were then placed on cleaned glass slides. To create sebaceous prints the same method was used except after the drying period the finger was rubbed on the back of the neck and then between the fingers before being placed onto the glass slide. To observe the differences in the ageing of fingerprints some samples were left for two weeks in the dark in a slide tray.

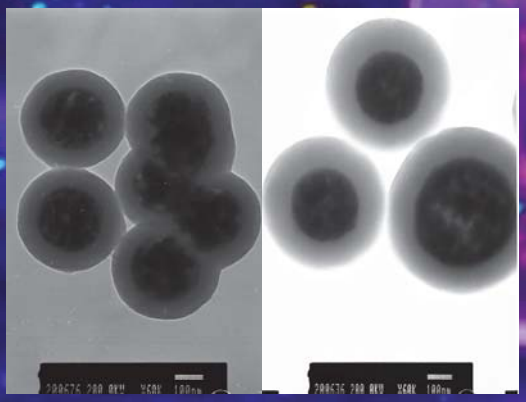

**Figure 2 –** TEM of silica coated $Y_2O_3$:Tb (left) $Y_2O_3$:Eu (right)

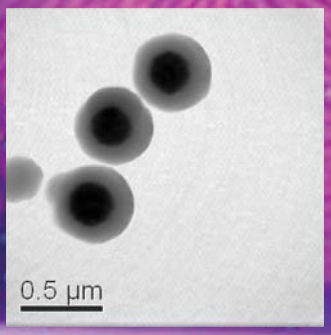


**Figure 3 –** TEM of modified silica coated $Y_2O_3$:Tb

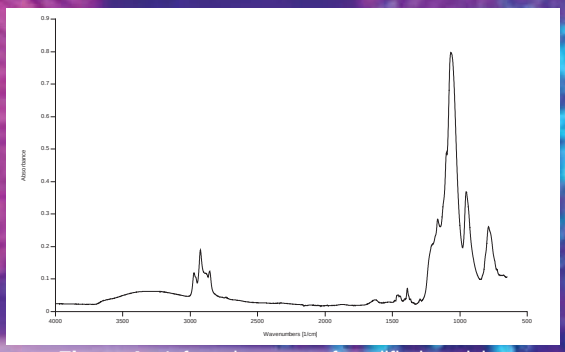

**Figure 4 –** Infrared spectra of modified particles

## 3. Results and discussion

The silica coated $Y_2O_3$:Tb was modified with a triethoxy(octyl)silane (TMOS). This gave the coated phosphor a long chained hydrocarbon tail which was found to increase the attachment to the more oil based sebaceous fingerprints. Figure 4 shows the modification at around 3000cm$^{-1}$ of the CH stretches. The silica coated $Y_2O_3$:Eu was found to have a high attachment to the more aqueous based eccrine fingerprints and so this was used without modification. Using both phosphors on a 15 stage depletion series showed that they are able to adhere to even very dry fingerprints.

When tested on two year old and newly created fingerprints the purely silica coated phosphors adhered primarily to newer prints whereas the TMOS modified phosphor adhered to the more aged prints due to the lack of decomposition and lack of evaporation of the oils. The newer prints contained more aqueous salts and sweat so were a much better surface for the silica coated phosphors.

## 4. Future Work

The phosphor powders show great promise in enhancing the detection of latent fingerprints compared to traditional powders (see Fig. 5). The next work that will be carried out is to see whether more information can be developed from the fingerprint. These tests include modifying coated phosphors with drug antibodies so areas can be dusted for fingerprints that could have traces of drugs on them and also looking at the treated print using Raman spectroscopy to see whether other compounds can be detected such as explosive residues.

**Figure 5 –** Comparison between (left to right) bichromate, graphite, $Y_2O_3$:Eu and $Y_2O_3$:Tb

**References**

[1] Mi Jung Choi et al (2008). "Metal-containing nanoparticles and nano-structured particles in fingermark detection." Forensic Science International **179** (2-3): 87-97

[2] Stöber. W, Fink. A and Bohn E (1968) "Controlled growth of monodisperse silica spheres in the micron size range." *J. Colloid Interf. Sci.* **26**: 62-69

# Chapter 6 Conference Participation

5: Graduate School Conference, Brunel University, 2011

Awarded: Vice Chancellors Prize for Research Student

# Improving the detection of latent fingerprints using phosphor nanopowders

**Alexander Reip, Jack Silver and Robert Withnall**

*Wolfson Centre for Materials Processing, Brunel University, Uxbridge UB8 3PH, Middlesex, UK*

**E-mail:** alexander.reip@brunel.ac.uk; **Tel. no:** 07765 902137

## 1. Introduction

Nanotechnology has been increasingly employed in forensic science for the detection of latent fingerprints, using multiple techniques from new aluminium nanomaterials for dusting to quantum dot dispersions, to try to increase and enhance areas where prints are likely to be found at scenes of crime. It is not viable to use many of these in conditions other than in a lab due to the harmful effects they can cause over long term use.

Past research has shown the success of using europium doped yttria for increasing the detection of fingerprints and that work has been built upon to improve the powders ability to adhere to the fingerprint by modifying the surface of the phosphor while making sure the modifications do not hinder the fluorescent ability of the phosphor [1].

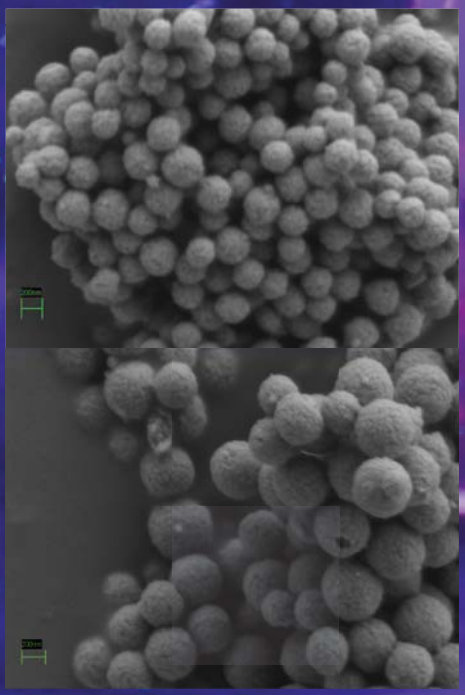

**Figure 1 –** SEM of $Y_2O_3$:Eu (top) $Y_2O_3$:Tb (bottom)

## 3. Results and discussion

The silica coated $Y_2O_3$:Tb was modified with a triethoxy(octyl)silane (TMOS). This gave the coated phosphor a long chained hydrocarbon tail which was found to increase the attachment to the more oil based sebaceous fingerprints. The silica coated $Y_2O_3$:Eu was found to have a high attachment to the more aqueous based eccrine fingerprints and so this was used without modification. Using both phosphors on a 15 stage depletion series showed that they are able to adhere to even very dry fingerprints.

When tested on two week old and newly created fingerprints the purely silica coated phosphors adhered primarily to newer prints whereas the TMOS modified phosphor adhered to the more aged prints due to the lack of decomposition and lack of evaporation of the oils. The newer prints contained more aqueous salts and sweat so were a much better surface for the silica coated phosphors.

## 2. Experimental

The two phosphors $Y_2O_3$:Eu and $Y_2O_3$:Tb were used due to their excitation wavelength of 254nm and differing emission wavelengths (611 nm for Europium and 543 nm for Terbium). Both were synthesised using the homogeneous precipitation method and then fired in a furnace for six hours at 800°C. The resulting phosphors (see SEMs in Fig. 1) were then coated with silica (see TEMs in Fig. 2) using a modified version of the Stöber method and then from this stage the surface of the silica was etched to lower the coating width and finally modified using various techniques [2].

To ensure consistency in the results the prints were taken from one donor. The finger was washed with ethanol and allowed to dry in air for ten minutes without contact. These eccrine prints were then placed on cleaned glass slides. To create sebaceous prints the same method was used except after the drying period the finger was rubbed on the back of the neck and then between the fingers before being placed onto the glass slide. To observe the differences in the ageing of fingerprints some samples were left for two weeks in the dark in a slide tray.

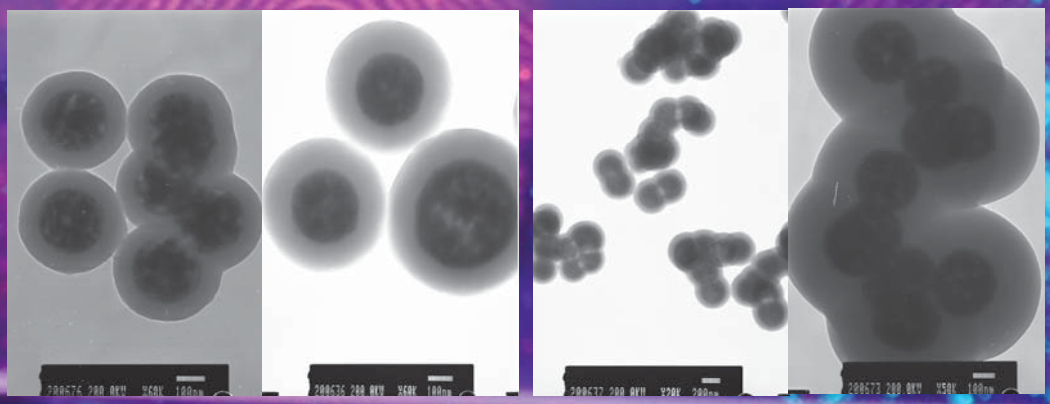

**Figure 2 –** TEM of silica coated $Y_2O_3$:Tb (left and second left) ) and $Y_2O_3$:Eu (right and second right)

## 4. Future Work

The phosphor powders show great promise in enhancing the detection of latent fingerprints compared to traditional powders (see Fig. 3). The next work that will be carried out is to see whether more information can be developed from the fingerprint. These tests include modifying coated phosphors with drug antibodies so areas can be dusted for fingerprints that could have traces of drugs on them and also looking at the treated print using Raman spectroscopy to see whether other compounds can be detected such as explosive residues.

**Figure 3 –** Comparison between (left to right) bichromate, graphite, $Y_2O_3$:Eu and $Y_2O_3$:Tb

**References**

[1] Mi Jung Choi et al (2008). "Metal-containing nanoparticles and nano-structured particles in fingermark detection." Forensic Science International **179** (2-3): 87-97

[2] Stöber. W, Fink. A and Bohn E (1968) "Controlled growth of monodisperse silica spheres in the micron size range." *J. Colloid Interf. Sci.* **26**: 62-69

# Chapter 6 Conference Participation

6: SED Research Conference, Brunel University, 2011

Awarded: Poster Prize

SED Research Conference 2011
Brunel University
20th – 22nd June 2011

# Improving the detection of latent fingerprints using phosphor nanopowders

Alexander Reip, Jack Silver and Robert Withnall
*Wolfson Centre for Materials Processing, Brunel University, Uxbridge UB8 3PH, Middlesex, UK*
alexander.reip@brunel.ac.uk

## Introduction

Nanotechnology has been increasingly employed in forensic science for the detection of latent fingerprints, using multiple techniques from new aluminium nanomaterials for dusting to quantum dot dispersions, to try to increase and enhance areas where prints are likely to be found at scenes of crime. Different substrates use a diverse range of methods to develop prints when they are found and each method has its own drawbacks. It is not viable to use many of these in conditions other than in a lab due to the harmful effects they can cause over long term use. With this in mind a new easier to use technique that can be used on any substrate from wood to glass to paper was looked into.

Past research has shown the success of using europium doped yttria for increasing the detection of fingerprints and that work has been built upon to improve the powders ability to adhere to the fingerprint by modifying the surface of the phosphor while making sure the modifications do not hinder the fluorescent ability of the phosphor [1].

## Methodology/Approach

The europium doped yttria was used as well as a terbium doped yttria due to both having an high intensity when excited at 254 nm but each having a different emission (europium at 612 nm and terbium at 543 nm.) (See fig 1) Having synthesised two different phosphors modifications can be examined to see whether these give better adherence or resolution.

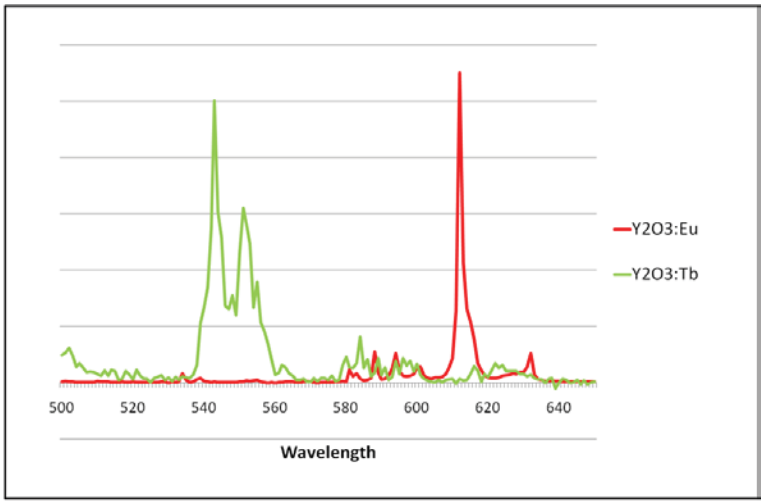


Fig 1 – Emission spectra of $Y_2O_3$:Eu and $Y_2O_3$:Tb using an exciting wavelength of 254 nm

$Y_2O_3$:RE (RE = Eu, Tb) was synthesized using the homogeneous precipitation method. Molar ratios of $Y(NO_3)_3$ and $RE(NO_3)_3$ were mixed, diluted with distilled water to 500mL and the resulting solution heated to 90$^oC$ whilst stirred. Once at temperature urea (35g) was added and the solution left at temperature for 2 hours. After this time the precursor was filtered and dried at 50$^oC$. This was then coated with silica using a modified version of the Stöber method [2]. 1g of the precursor was dispersed in 400mL of ethanol to which 20mL distilled water and 25mL tetraethoxyorthosilane was added. This solution was stirred and 8mL ammonia added. The solution was left stirring for 1 hour and then the coated precursor was separated by centrifuge and washed with ethanol. This was then dried at 60$^oC$ in an oven followed by sintering in a furnace at 1000$^oC$ for 6 hours. 1g of one of the silica coated phosphors was dispersed in 100mL ethanol. The solution was stirred and 20mL tetraethyloctylsilane was added. This was left stirring for 48 hours before being separated by centrifuge, washed with ethanol and dried.

To ensure consistency in the results the fingerprints were taken from one donor. The finger was washed with ethanol and allowed to dry in air for ten minutes without contact. These eccrine prints were then placed on cleaned glass slides. To create sebaceous prints the same method was used except after the drying period the finger was rubbed on the back of the neck and then between the fingers before being placed onto the glass slide. To observe the differences in the ageing of fingerprints some samples were left for two weeks in the dark in a slide tray. A depletion series was made using three fingers cleaned as before and set down fifteen times in a row on a sheet of glass to test how far along each of the powders could detect. The particle sizes and morphology were determined by SEM using an Oxford Supra 35 and TEM using a JEOL JEM 2000 FX. Fluorescence spectra were taken on a Bentham Spectrometer and infrared spectroscopy was taken using a Perkin Elmer Spectrum One FTIR Spectrometer with an ATR attachment.

## Results and Discussion

The silica coated $Y_2O_3$:Tb was modified with a trimethoxy(octyl)silane to give the coated phosphor a long chained hydrocarbon tail which was found to increase the adherence to the more oil based sebaceous fingerprints. The silica coated $Y_2O_3$:Eu was found to have a high attachment to the more aqueous based eccrine fingerprints and so this was used without modification. The particles were found to be approx 200nm when imaged with a SEM (fig 2.) and after coating and modification the size was 300nm seen using a TEM (See fig 3.)

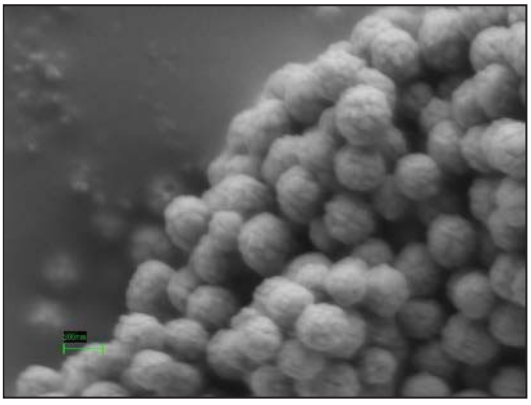

Fig 2 – SEM of $Y_2O_3$:Eu particles

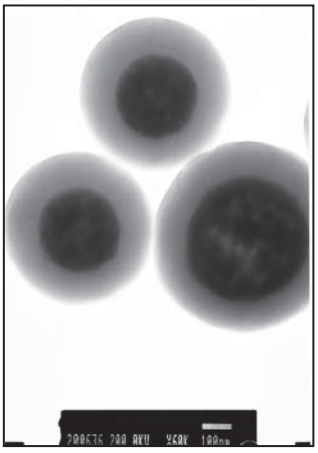

Fig 3 – TEM of $Y_2O_3$:Tb particles coated with silica and modified with TMOS

Using infra red spectroscopy the modification was found to have attached to the surface of the silica and when tested on two week old and newly created fingerprints the purely silica coated phosphors adhered primarily to newer prints whereas the TMOS modified phosphor adhered to the more aged prints due to the lack of decomposition and lack of evaporation of the oils. The newer prints contained more aqueous salts and sweat so were a much better surface for the silica coated phosphors (see fig 4.)

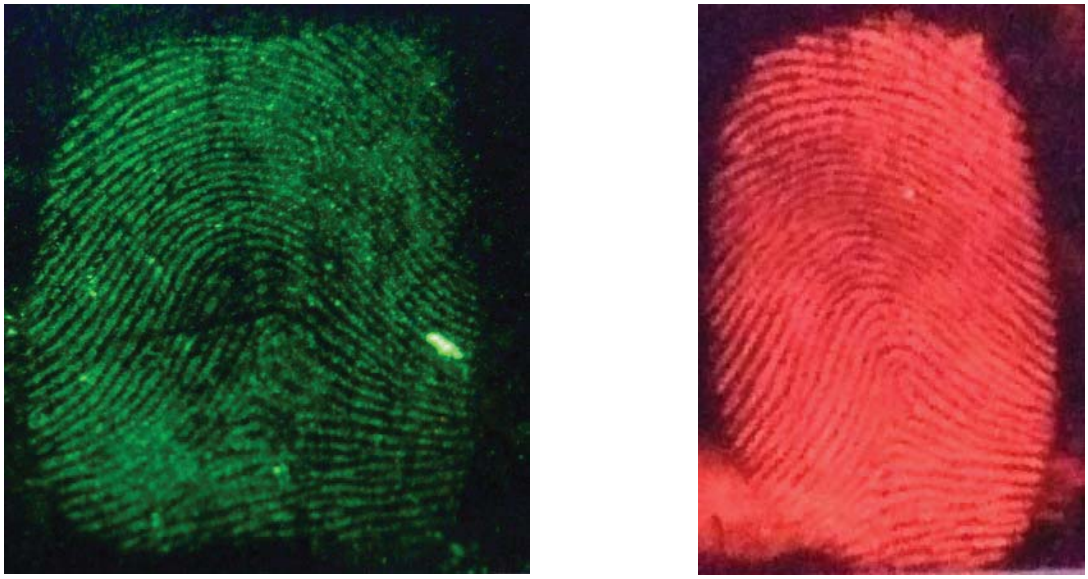

Fig 4 – TMOS coated then modified $Y_2O_3$:Tb dusted print (left) and $Y_2O_3$:Eu coated with silica dusted print (right)

## Conclusion

The phosphor powders show great promise in enhancing the detection of latent fingerprints compared to traditional powders. The next work that will be carried out is to see whether more information can be developed from the fingerprint. These tests include modifying coated phosphors with drug antibodies so areas can be dusted for fingerprints that could have traces of drugs on them and also looking at the treated print using Raman spectroscopy to see whether other compounds can be detected such as explosive residues.

## References

[1] Mi Jung Choi et al (2008). “Metal-containing nanoparticles and nano-structured particles in fingermark detection.” Forensic Science International 179 (2-3): 87-97

[2] Stöber. W, Fink. A and Bohn E (1968) “Controlled growth of monodisperse silica spheres in the micron size range.” *J. Colloid Interf. Sci.* 26: 62-69

**Keywords: fingerprint, detection, phosphor, nanoparticle and forensic**

# Chapter 6 Conference Participation

## 7: IDW ’11 The 18th International Display Workshops, Nagoya, Japan, 2011

# Improving the detection of latent fingerprints using phosphor nanopowders

Jack Silver, Robert Withnall and Alexander Reip

Centre for Phosphor and Display Materials, Wolfson Centre for Materials Processing,
Brunel University, Uxbridge, Middlesex, UB8 3PH, UK.

## Abstract

Past research has shown the success of using europium doped yttria for increasing the detection of fingerprints and that work has been built upon to improve the powders ability to adhere to the fingerprint by modifying the surface of the phosphor while making sure the modifications do not hinder the fluorescent ability of the phosphor

## Presentation Style

Prefer oral presentation but will accept poster

## Workshop / Topical Session

## 1. Objectives and Background

The discovery of latent fingerprints at any crime scenes are a major part of making a case and then getting a conviction in court. Since the first statistical analysis model showing the rarity of false positives was 64 billion to 1[1] they were the most significant factor in police cases till the adoption of DNA profiling in 1984 [2].

The techniques that are used for detecting latent prints have vastly changed in recent years. The main two powders that have been used since its discovery were charcoal and chalk powder depending on the colour of the surface being dusted. Over time superior powders were needed as the original two were very basic and did not always give a good result. From this two main factors were identified for powders to be used. The size of the particles are a major issue because the finer the powder the better detail can been seen on a fingerprint but once particles get too small then they will overwhelm the fingerprint and give a much worse image. The other major factor is the adherence of the powder to the fingerprint. The powder needs to be able to stick to the print and then be removed through methods such as tape lifting but not to come off during the dusting process. There are two types of fingerprint which are found, each depending on the individual. The most well known type is eccrine prints which occur with the sweat glands on the fingertips and which are mainly aqueous based containing mainly water and salts [3]. The other is sebaceous which occurs when a person rubs the back of their neck or face. These are mainly oil based prints [4] and normally last longer as the main components take longer to evaporate unlike the eccrine prints. This is a factor which will be investigated to see whether a powder can be developed to see one type better than another. A smaller factor to consider is also colour. The surfaces that need to be checked for prints could be so varied in colour that some powders would not show up.

Nanomaterials are becoming increasingly employed in forensic science to detect latent fingerprints because the particle sizes can be carefully monitored. A lot of work has been carried out using multiple techniques from new aluminium nanomaterials [5] for dusting to quantum dot dispersions [6] to try to increase and enhance areas where prints are likely to be found at scenes of crime. It is not viable to use many of these in conditions other than in a lab due to the harmful effects they can cause over long term use. The aim of this work was to use $Y_2O_3$ nanophosphors to not only increase the adherence of particles to the latent fingerprints but to also to use the fluorescent effects of the phosphors to give a good detailed print lift on surfaces of any colour.

Therefore from the above issues phosphors doped with different rare earth metals were synthesized using a homogeneous precipitation method to regulate the particle size and then coated with silica which was then modified to increase the adherence to prints.

## 2. Results

Europium and terbium were used as the activators in this study as both are excited at 254nm but have different emissions ($Eu^{3+}$ at 612nm and $Tb^{3+}$ at 543nm). Both were doped into $Y_2O_3$ at 5 mol% which has been shown to give a high intensity. An SEM of $Y_2O_3$:Eu and $Y_2O_3$:Tb shows discrete particles with an average size of 200nm after annealing at 1000$^o$c. (see Figure 1) This shows the particles are around the same size as the commercial bichromate powders which are used with particle sizes shown to be also around 200nm (Figure 2) A modified version of the Stöber method [7] was used to coat the particles with silica which was optimized to give a coating width of approximately 50nm (Figure 3).

The $Y_2O_3$:Eu coated particles were then modified with triethoxy(octyl)silane (TEOS) to increase the adherence to older more oil based fingerprints, which again increased the particle size slightly (Figure 4). FTIR showed the modification of the coating adhered to the coated phosphor with the long chain $CH_2$ group shown at 2920cm$^{-1}$ (Figure 5)

and luminescence tests of the precoated and coated particles showed little change in the relative luminescence intensity. Both phosphors were then tested on fingerprints taken from one donor.

To ensure consistency in the results the prints the finger of the donor was washed with ethanol and allowed to dry in air for ten minutes without contact. These eccrine prints were then placed on cleaned glass slides. To create sebaceous prints the same method was used except after the drying period the finger was rubbed on the back of the neck and then between the fingers before being placed onto the glass slide. To observe the differences in the ageing of fingerprints some samples were left for two weeks in the dark in a slide tray. The prints were then dusted with each type of phosphor and the residue tape lifted and photographed under 254nm UV light. (Figure 6) The results of the tests show good adherence to the fingerprint residue both with the modified and unmodified prints.

## 3. Originality and Prior Publications

This work is original since we have not previously reported the

## 4. Impacts

- The luminescent properties of modified phosphors were shown to not reduce the intensity compared to the uncoated phosphors.
- The modification was shown by FTIR to have reacted and be present on the surface of the particles.
- The modified particles show great adherence to the fingerprint residue even after a two week period

## Acknowledgement

The authors are grateful to the EPSRC

## 5. References

[1] Galton F, (1892) *Fingerprints.* New York: Macmillan and Co

[2] Jeffreys A, Wilson V, Thein S. (1985) "Individual-specific 'fingerprints' of human DNA". *Nature* 316 (6023) 76–9

[3] Archer, N. E., Y. Charles, et al. (2005). "Changes in the lipid composition of latent fingerprint residue with time after deposition on a surface." *Forensic Science International* 154(2-3): 224-239.

[4] Knowles A M (1978) “Aspects of physicochemical methods for the detection of latent fingerprints” *J. Phys. E: Sci. Instrum.*, 11, 713-721

[5]

[6] Dilag, J., H. Kobus, et al. (2009). "Cadmium sulfide quantum dot/chitosan nanocomposites for latent fingermark detection." *Forensic Science International* 187(1-3): 97-102.

[7] Stöber. W, Fink. A and Bohn E (1968) “Controlled growth of monodisperse silica spheres in the micron size range.” *J. Colloid Interf. Sci.* **26**: 62-69

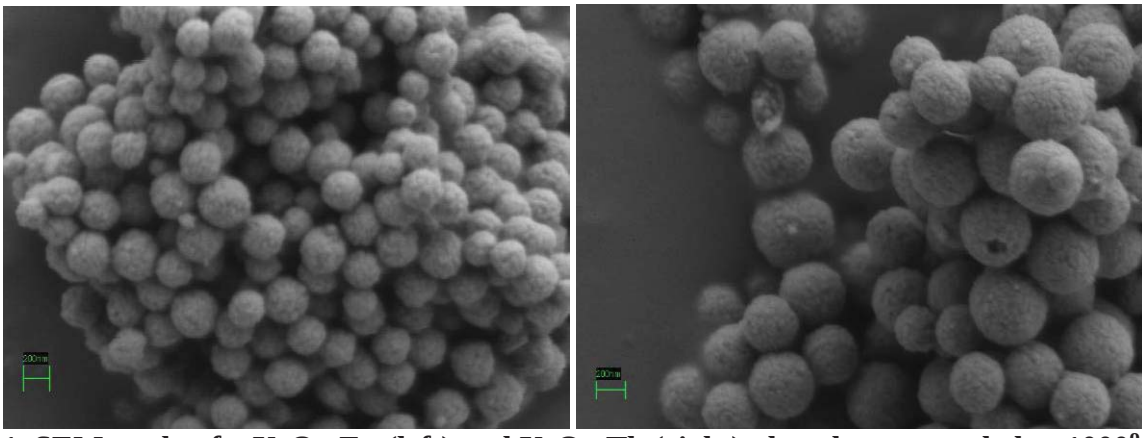

**Fig. 1 SEM study of a $Y_2O_3$:Eu (left) and $Y_2O_3$:Tb (right) phosphors annealed at 1000$^o$C**

**Fig. 2 TEM image of $Y_2O_3$:Eu phosphor particles annealed at 1000°C**

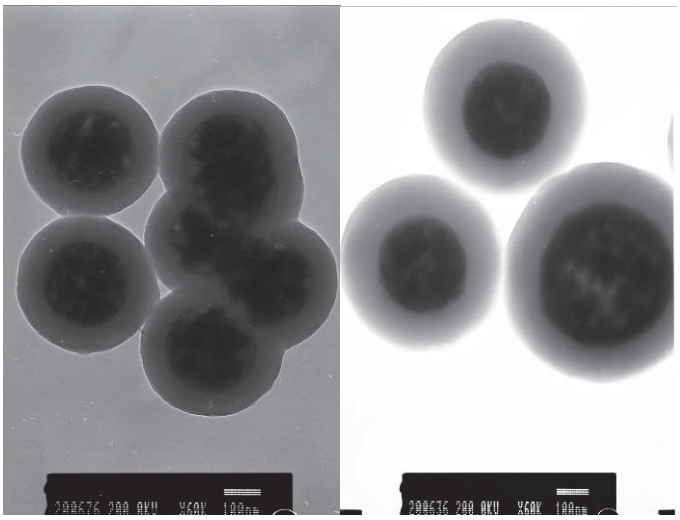

**Fig. 3 TEM image of $Y_2O_3$:Eu (left) and $Y_2O_3$:Tb (right) phosphor particles coated with $SiO_2$**

**Fig. 4 TEM image of $Y_2O_3$:Eu particles coated with $SiO_2$ and modified with TEOS**

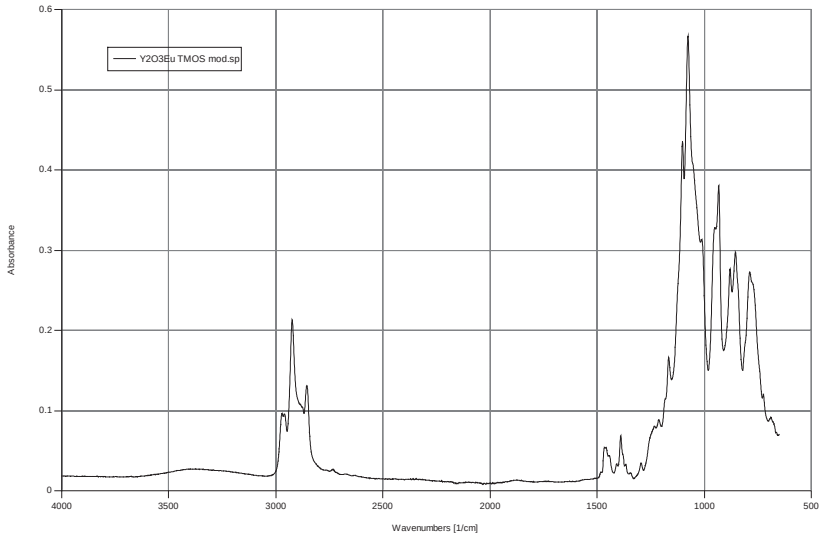


**Fig. 5 FTIR of $Y_2O_3$:Eu particles coated with $SiO_2$ and modified with TEOS**

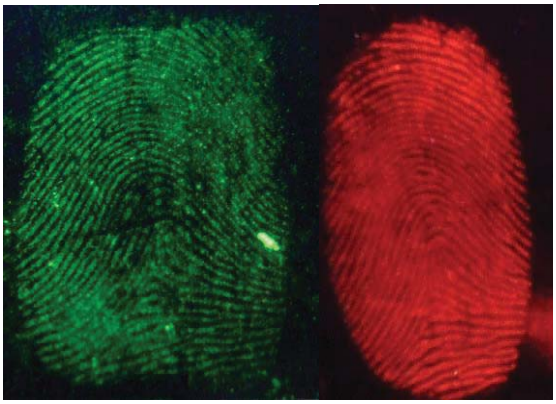

**Fig. 6 Tape lifted fingerprints using $Y_2O_3$:Tb (Left) and modified $Y_2O_3$:Eu (right)**